HIGH PERFORMANCE BIODEGRADABLE STARCH/LDPE NANOCOMPOSITES PREPARED VIA TWIN SCREW EXTRUDER

by

FUNDA İNCEOĞLU

Submitted to the Graduate School of Engineering and Natural Sciences
in partial fulfillment of
the requirements for the degree of
Doctor of Philosophy

Sabancı University

August 2007

HIGH PERFORMANCE BIODEGRADABLE STARCH/LDPE NANOCOMPOSITES PREPARED VIA TWIN SCREW EXTRUDER

APPROVED BY:

Assoc. Prof. Dr. Yusuf Z. Menceloğlu (Thesis Supervisor)	……
Prof. Dr. Atilla Güngör	……
Asst. Prof. Melih Papila	……
Prof. Dr. Canan Atılgan	……
Assoc. Prof. Hikmet Budak	……

DATE OF APPROVAL: ……

HIGH PERFORMANCE BIODEGRADABLE STARCH/LDPE NANOCOMPOSITES PREPARED VIA TWIN SCREW EXTRUDER

Funda İNCEOĞLU

MAT, PhD Thesis, 2007

Thesis Supervisor: Assoc. Prof. Yusuf Z. MENCELOĞLU

Keywords: Biodegradable, nanocomposite, starch, polyethylene, twin screw extruder

ABSTRACT

Developing biodegradable films with an optimum combination of desirable mechanical properties and biodegradation performance is the main objective of the present study. For this purpose, low density polyethylene (LDPE)/Starch blends reinforced with layered clays were prepared using twin screw extruder. The effect of compatibilizer, starch form and its content, clay type and processing methods on the physico-mechanical properties of blend was investigated and discussed in a comprehensive manner. The results have shown that in order to achieve good biopolymer dispersion with strong interfacial adhesion, starch should be converted into thermoplastic starch (TPS) and suitable compatibilizer should be employed. Maleic anhydride grafted polyethylene (MAgPE) as compatibilizer worked best between LDPE and TPS. The highest amount of TPS that can be used in the blend formulations was found to be 40 wt%. Beyond that, the fracture mechanism changed from ductile to brittle fracture. The presence of clay, in general, enhanced the mechanical as well as barrier properties and biodegradation rate of the blends. The degree of enhancement influenced by the clay type and the phase where it was mainly dispersed. The presence of organoclay in LDPE matrix mainly improved the mechanical, tear and heat seal strength of the films, while the intercalation of Na^{+}-montmorillonite clay with starch molecules was found to be more effective in enhancing the moisture barrier properties. In biodegradation test, starch was degraded in the presence of enzyme and resulted in porous structure of LDPE films that is more susceptible to oxidative and hence biotic reactions.

ÇİFT BURGULU EKSTRUDER İLE HAZIRLANAN YÜKSEK PERFORMANSLI BİYOBOZUNUR NİŞASTA/AYPE NANOKOMPOZİTLERİ

Funda İNCEOĞLU

MAT, Doktora Tezi, 2007

Tez Danışmanı: Doç.Dr.Yusuf Z. MENCELOĞLU

Anahtar Kelimeler: Biyobozunur, nanokompozit, nişasta, polietilen, çift burgulu ekstruder

ÖZET

Bu çalışmada yüksek mekanik performansın yanında biyo-bozunur özelliğe sahip filmlerin geliştirilmesi amaçlanmıştır. Bu hedef doğrultusunda alçak yoğunluklu polietilen (AYPE)/Nişasta karışımları tabakalı yapıya sahip kil ile de güçlendirilerek çift burgulu ekstrüder kullanılarak hazırlanmıştır. Çalışma boyunca kullanılan bağlayıcının, nişastanın formunun ve miktarının, kil tipinin ve değişik işleme şekillerinin ürünün fiziko-mekanik özelliklerine olan etkisi incelenmiştir. Yapılan çalışmalar ışığında iyi bir dağılım ve yüksek uyum için kullanılan nişastanın ilk önce termoplastik nişasta haline getirilmesi ve daha sonra polietilen ile karışım esnasında uygun bağlayıcının kullanılması gerektiği ortaya çıkmıştır. Alçak yoğunluklu polietilen ve nişasta arasında bağlayıcı olarak en iyi performansı maleik-anhidrid modifiye polietilen göstermiştir. Polietilenin içerisine eklenebilecek en yüksek termoplastik nişasta miktarı %40 olarak bulunmuştur. Bu noktadan sonra kırılma mekanizması, esneyerek kopmadan daha kırılgan bir kopmaya doğru gitmiştir. Geliştirilen sistemin içerisine kil eklenmesi mekanik özellikleri arttırmanın yanısıra bariyer özellikleri iyileştirmiş ve biyo-bozunma hızını arttırmıştır. Bu iyileşmenin miktarı kil tipi ve kilin dağıtıldığı faz ile bağlantılıdır. Alçak yoğunluklu polietilen içerisinde dağıtılan organokil daha çok üretilen filmin mekanik, yırtılma ve yapışma kuvvetini iyileştirmiş olup, Na^+-montmorillonit kilinin nişasta içerisinde dağıtılması ise sistemin nem bariyer özelliklerini daha fazla oranda artırmıştır. Biyo-bozunma testleri enzim ortamında yapılmış olup inkübasyon sonucunda nişastanın enzimler tarafından parçalandığı ve oksidatif/biotik bozunma reaksiyonlarına daha kolay maruz kalabilecek çok gözenekli polietilen yapısının ortaya çıktığı görülmüştür.

Sevgili eşim Baran İnceoğlu'na…

ACKNOWLEDGEMENTS

I would like express my special thanks to my thesis supervisor, Assoc. Prof. Yusuf Z. Menceloğlu, for his valuable advice and guidance of this work. I am grateful to him not only for his acedemic contributions, but also for his unlimited support and trust.

I am also grateful to my thesis committee members Prof. Dr. Canan Atılgan, Asst. Prof. Melih Papila, Prof. Dr. Atila Güngör and Assoc. Prof. Hikmet Budak for their valuable review and comments on the dissertation.

My sincere thanks are for Cahit Dalgıçdır and Cem M. İnan for their precious contributions to this study. They worked very hard with me with much interest to the subject of this thesis.

I would like to acknowledge my dear friends İbrahim İnanç, Eren Şimşek, İlhan Özen, Yasemin Kaya, Filiz Çetin, Günseli Bayram and Burak Birkan for their valuable helps and contributions to this study. Special thanks to Haluk Konyalı and Özge Malay for their great friendships.

I would like to extend my special thanks to Ferruh Kulak and Selin Nursal from Alcan Rotopak A.Ş., for their helps on evaluating mechanical and barrier properties of my film samples. Thanks to Dr. George Wagner for his valuable supports throughout the study. I am also grateful to Dr. Füsun Güner from PETKİM for allowing us to use fim-blowing line.

I express my thanks and appreciation to my family for their understanding, motivation and their respect to my academic life.

Finally, I am particularly grateful to my husband, Baran İnceoğlu, not only for his endless love and encouragement but also for his valuable assistance and contributions to this study. He was always with me with his full support and love in every stage of my life. Therefore, this study is dedicated to him.

TABLE OF CONTENTS

LIST OF FIGURES

LIST OF TABLES

LIST OF ABBREVIATIONS

ABS	Acrylonitrile Butadiene Styrene
ASA	Acrylonitrile Styrene Acrylate
BDP	Biodegradable Polymer
CA	Cellulose Acetate
CAB	Cellulose Acetate Butyrate
CAP	Cellulose Acetate Propionate
CEC	Cation Exchange Capacity
CO	Carbon Monoxide
CS	Casein
CZ	Corn Zein
DBM-g-LDPE	Dibutyl Maleate Ester Grafted Polyethylene
DSC	Differential Scanning Calorimeter
EAA	Ethylene– acrylic Acid Copolymer
EVOH	Ethylene Vinyl Alcohol
FT-IR	Fourier Transform Infrared
GHG	Greenhouse Gas
GS	Gelatinized Starch
HDPE	High Density Polyethylene
LDPE	Low Density Polyethylene
LLDPE	Linear Low Density Polyethylene
MAgPE	Maleic Anhydride Grafted Polyethylene
MAH	Maleic Anhydride
OMLS	Organically Modified Layered Silicate
OP	Oxygen Permission
PA	Polyamide
PC	Polycarbonate
PCL	Polycaprolactone
PE	Polyethylene

PE-g-GMA	Glycidyl Methacrylate Grafted Polyethylene
PEO	Poly(ethylene oxide)
PET	Poly(ethylene terephthalate)
PHB	Poly(3-hydroxybutyrate)
PHBV	Poly(3-hydroxybutyrate-co-3-hydroxyvalerate)
PHV	Poly-3-hydroxyvalerate
PLA	Poly(lactic acid)
PLS	Polymer Layered Silicate
PMMA	Poly(methylmethacrylate)
PMMA	Polymethymethacrylate
PP	Polypropylene
PS	Polystyrene
PTFE	Polytetrafluoroethylene
PU	Polyurethane
PVA	Polyvinyl alcohol
PVA	Polyvinyl Alcohol
PVC	Poly(vinyl chloride)
PVOH	Polyvinyl alcohol
PVOH	Polyvinyl Alcohol
PVOH	Polyvinyl Alcohol
QAC	Quaternary Ammonium Compound
RH	Relative Humidity
SAN	Styrene Acrylonitrile
SEM	Scanning Electron Microscope
SPI	Soy Protein Isolate
TEM	Transmission electron Microscopy
T_g	Glass Transition Temperature
TPS	Thermoplastic Starch
WG	Wheat Gluten
WPI	Whey Protein Isolate
WVP	Large Water Vapour Permission
XRD	X-ray Diffraction

CHAPTER 1

1. INTRODUCTION

Synthetic polymers have become one of the most important materials all over the world due to their excellent properties and their ability to be chemically manipulated to have a wide range of strengths and shapes. However, their increasing usage leads to the environmental pollution that becomes serious, particularly from package materials, disposable containers, and agricultural mulch films due to their huge consumption in our daily life. According to an estimate, forty percent of the 100 million tons of plastics produced every year is discarded into landfills. Several hundred thousand tonnes of plastics are discarded into marine environments and accumulate in oceanic regions [1]. There are some proposed solutions to this problem and one of them is the polymer recycling. Yet, it has not been successful over worldwide scale, because it is expensive and the synthetic waste is difficult to sort according to origin, color and contained additives. Therefore, there is an increasing need for more environmentally friendly polymeric materials to replace the synthetic polymers, at least partly by introduction of biodegradable material. Therefore, it is inevitable for us to develop a method of production of these polymeric materials with adequate properties so that we do not add much material waste in the landfills.

Pollution due to plastics is a result of the slow rate of disappearance of the synthetic polymers from the environment because of their production via chemical synthesis so that enzymes or microorganisms that degrade or utilize them have not evolved yet. Whereas, the biological polymers, due to their synthesis via the enzymatic route, degrade rapidly in the biological medium. Polymers differ in the rate or form of degradation, which is determined by the energy required to break the bond, and the location of the bond. Polymers with strong covalent bonds in the backbone (like C-C)

and with no hydrolyzable groups require long times and/or catalysts for degradation. These catalysts could be heat, electromagnetic radiation (visible light, UV, g-radiation), chemicals (water, oxygen, ozone, halogenated compounds), or any combination of the above. The molecules with such hydrolyzable groups (e.g. C-O-C, C-N-C) are degraded much more efficiently and rapidly [2].

The currently available biodegradable polymers can be divided into three general classes: aliphatic polyesters, polymers based on natural polymers, and biodegradable vinyl polymers. Some commercially available synthetic biodegradable polymers include polycaprolactone (PCL), polyhydroxyalkanotes, poly(3-hydroxybutyrate) (PHB), poly(3-hydroxybutyrate-co-3-hydroxyvalerate) (PHBV), poly(lactic acid) (PLA), poly(butylene succinate), poly(butylene succinate-co-adipate), and poly(vinyl alcohol). Although many of these polymers possess excellent properties, they are not widely used because of their high cost and production using nonrenewable petroleum resources. Among the natural biodegradable polymers, starch obtained from various botanical sources, is the most abundant, renewable, and inexpensive biopolymer. Starch is a natural carbohydrate storage material accumulated by green plants in the form of granules. It is composed of linear polysaccharide molecules (amylose) and branched molecules (amylopectin) and it can be added to synthetic polymers to lower the cost of the final product. However, starch by itself is not suitable for production of materials due to moisture susceptibility, brittleness, and processing difficulties. Therefore it is often blended with hydrophobic polymers, mostly with polyethylene (PE) , to improve the properties of processibility.

Addition of starch to polyolefins not only provide biodegradability but also increase the printability and ink adhesion of polyolefins thereby eliminating the physical or chemical treatments such as corona discharge, chemical etching, and so forth. One major problem with granular starch composites, on the other hand, is their limited processibility, due to large particle size (5–100 micrometer) which make it difficult to produce blown thin film out of it. Numerous studies have shown that the addition of dry starch granules to polyethylene follows the general trend for filler effects on polymer properties [3-8]. The modulus increases due to the stiffening effect of the starch granules and the elongation decreases as the starch content is increased. In general, the addition of granular starch to polyolefin results in a severe reduction of tensile strength

and elongation at break. The main problem associated with the use of starch as filler is its hydrophilic nature and consequent incompatibility with the hydrophobic polymers. One of the alternative approaches to bring compatibility between starch and the polymer matrix is by modification of the starch. Native starch granules swell when they absorb water through hydrogen bonding with their free hydroxyl groups, but they still retain their order and crystallinity. However, when these swollen starch granules are heated, hydrogen bonding between adjacent glucose units is disrupted and the crystallinity is progressively destroyed. This process is called gelatinization. The processing of starch and water in a heated extruder is an efficient way to obtain gelatinized starch (GS) since the high shear that can be generated in the extruder disrupts the starch granules. Further study has been devoted to the development of materials containing GS. Otey et al. developed GS/EAA (ethylene– acrylic acid copolymer) cast films that demonstrated good transparency, flexibility and mechanical properties [9]. Blends of GS with other polymers were prepared by first mixing starch, ethylene– acrylic acid copolymer (EAA) and other additives in a long initial process. However, the addition of LDPE led to the reduction of both tensile strength and elongation at break. Detailed studies on this polymeric system have shown that amylose and amylopectin parts of starch form complexes with EAA. The hydrophobic segment of EAA molecules is trapped in the hydrophobic core of the starch helix [6]. These findings led to the proposal that compatibilizers other than EAA should be employed to improve interfacial adhesion with polyolefin and reduce the GS particle size, without promoting the formation of starch complexes.

Addition of a plasticizer such as glycerol or sorbitol can further improve the ductility of GS [10]. Plasticized GS is known as thermoplastic starch (TPS) and is capable of flow. However, poor water resistance and low strength are limiting factors for the materials prepared only from TPS, thus it is often blended with other polymers. Therefore, many researchers studied the effect of plasticizers on starch with the aim of producing thermoplastic materials. The melt blending of TPS has been studied with polyethylene and biodegradable polyesters such as polycaprolactone, polylactic acid and results indicated that addition of such plasticizers considerably improves mechanical properties when compared with native starch [11-16]. Even so, starch films have poorer mechanical properties than synthetic polymers and the tensile properties of these blends decreased significantly as TPS content increased. The elongation at break

is the property most adversely affected by the presence of TPS particles and typically ductile polymers, such as polyethylene and polycaprolactone, became fragile with the addition of 20–30 wt% TPS which was attributed to the poor interaction between these polymers and TPS. Recent research has indicated that the addition of small amounts of inorganic fillers such as organically modified clay particles increased the mechanical properties of TPS due to the intercalation of plasticizer part of the TPS into the organophilic clay platelets, yet the tensile strength and elongation at break values were too low to be used in many applications [17,18]. Another approach was to use poly(ethylene- co-acrylic acid), poly(ethylene-co-vinyl alcohol), or oxidized PE as a compatibilizer in PE-starch composites, but the composites also exhibited unsatisfactory mechanical properties because of the limited opportunities for compatibilizer to interact with polyethylene [3]. Recently, increased interest has focused on the use of starch together with polymers containing reactive groups (e.g., maleic anhydride, glycidyl methacrylate) as compatibilizers due to the better dispersion of starch in the polymer blend containing functional group [3,12,19-23]. However, the deterioration in many of the properties of synthetic polymers such as tensile strength, flexibility, tear strength, and moisture barrier properties could not be overcome totally by using these reactive groups, especially for high TPS contents.

The main purpose of the present study is to increase the rate of degradation of polyethylene without loosing much from its good mechanical and optical properties. For this purpose, low density polyethylene (LDPE)/Starch blends reinforced with layered clays were prepared using twin screw extruder. The effect of compatibilizer, starch form and its content, clay type and processing methods on the physico-mechanical properties of the blend was investigated and discussed. The most critical question here is: What will happen to the degradation mechanism of synthetic polymers after the addition of a biopolymer? Recent studies have shown that when a natural polymer is mixed with a synthetic one, the degradation rate of the synthetic polymer increases [1,24-29]. It was suggested that microorganisms first create pores by consumption of biopolymer and thereby increase the surface area of the composite. This in turn enhances oxygen-based reactions, which could increase synthetic polymer chain oxidation. Since this is the slowest step in the degradation mechanism of synthetic polymers, any factor which increases the oxidation tendency of polymers also controls the degradation of plastics.

Hence, creating oxidized polymer chain ends in a degraded composite will make a synthetic polymer susceptible to biotic reactions.

CHAPTER 2

2. BACKGROUND

2.1 World Plastic Consumption

Plastics have become an integral part of our everyday life, and have been used for a multitude of purposes. They are now utilized in almost every manufacturing industry ranging from automobiles to medicine because of their numerous advantages over other materials like metals, glass and papers. They are not only less expensive than alternative materials, but they are often better in performance and they can be manipulated to have a wide range of strengths and shapes.

Synthetic polymers developed in the early 1900's included Bakelite, rayon, and cellophane. One of the earliest of the synthetic polymers made from petroleum products was nylon, invented in 1939. Nylon could be spun into fibers, and woven into fabrics. Nylon had many of the same properties as silk, and during World War 2 became a substitute for parachutes. The success of nylon products led to the invention of rayon,dacron, orion, and polyester.

The world's annual consumption of plastic materials was around 5 million tonnes in 1950s. It has increased to 86 million tonnes in 1990 and became 176 million tonnes, with the average of 28 kg per person, in 2003. Demand for the plastics is forecast to expand nearly to 250 million tonnes (37 kg per person) in 2010. North America, western Europe and the south Asia are the regions where plastic consumption is very high [30].

Table 2.1 World plastic consumption according to regions [30].

	1990	*2003*	*2010*
Million Tonnes	86	176	250
Regional Plastic Consumptions (%)			
Africa- Middle East	4.0	6.0	5.5
Middle Europe	6.0	3.5	4.0
Latin America	4.0	5.5	5.5
Japan	12.0	6.0	5.5
South Asia (excluding Japan)	16.5	32.0	36.0
North America	29.0	25.0	24.0
Western Europe	28.5	22.0	19.5
Total	100.0	100.0	100.0

There are about 50 different groups of plastics, with hundreds of different varieties. The most commonly used plastics include polyethylene, polypropylene, poly(vinyl chloride), polystyrene, poly(ethylene terephthalate) and polyurethane. Their annual consumptions are given in Table 2.2. Approximately 80% of the worldwide consumption is due to polyethylene (PE), polypropylene (PP), polyvinyl chloride (PVC) and polystyrene (PS). Low density polyethylene (LDPE) is used to make food packaging, grocery bags, trash bags, agricultural covers, bottles and pipes. High density polyethylene (HDPE) is used to make milk jugs, laundry detergent jugs, and lids. It is also used in nonpackaging articles such as sporting goods, pipes, electrical insulation, and toys. Polypropylene is used for packaging film, bottles, wire coatings, molded parts of automobiles, housewares, pipes, child car seats, etc. Poly(vinyl chloride) is produced in both rigid and flexible forms. Rigid PVC is used to produce building materials such as window frames, pipes, credit cards, etc. Flexible one is used for floor and wall coverings, rainwear, electrical insulation and clear film in packaging applications. Polystyrene has also wide application in packaging industry. Nonpackaging applications include housewares, such as furniture, dishes, tray, shower doors, toys, flower pots, etc. The majority of the world's Poly(ethylene terephthalate) (PET) production is for synthetic fibers (in excess of 60%) with bottle production accounting for around 30% of global demand. Polyurethane (PU) has a wide range of application due to their chemical

structure that can be manipulated to products with different strength from soft elastomers to rigid foam. It is widely used for coatings , insulation , mattresses, automobile seats and glue.

There are many other synthetic polymers that are manufactured in a variety of products, but in a smaller scales than the plastics mentioned previously. These are characterized as an engineering plastics having excellent mechanical or optical properties, high temperature stability, or excellent chemical resistance. They are often used in automotive and electronics industry. Acrylonitrile-butadiene-styrene (ABS), polycarbonate (PC) and polyamide (PA) are the examples for common engineering plastics.

Table 2.2 World plastic consumption according to plastic types [30].

Plastic Type	***Million Tonnes***		***Anual Increase Rate (%)***
	2003	***2010***	
LDPE	31.7	43.5	4.6
HDPE	25.7	37.5	5.5
PP	35.4	53.4	6.0
PVC	28.6	38.0	4.2
PS	14.6	19.8	4.4
ABS/SAN/ASA	6.2	9.3	6.0
PA	2.2	3.4	6.5
PC	2.2	3.8	8.0
PET	9.1	17.5	10.0
PU	10.0	14.5	5.5

Packaging represents the largest single sector of plastics. The sector accounts for 29% of total plastics consumption. Around one-half of the plastic used in packaging is for containers, such as soft-drink bottles, laundry detergent, and bleach. One-third is in the form of plastic sheet or film. The remainder is for closures like caps, coatings, etc. Plastics are used on a large scale for trash bags, that might be called packaging for trash.

Approximately a billion pounds of plastics per year are manufactured for that purpose alone. A typical type of plastics that is consumed in packaging is shown in Table 2.3.

Table 2.3 Polymer types used in packagings [31].

Plastic	***Total Usage (%)***
LDPE	33
HDPE	31
PP	10
PET	7
PS	5
PVC	5

The second biggest market in plastic sector is the construction materials. Nearly 20 billion pounds of plastic are manufactured in the United States to be used as a building materials in place of metal and wood.

Plastics have been extensively used in automotive industry for the last 20 years. Aproximately 105 kg of each otomobile produced in 2000 was made of plastics. The use of plastic not only provided lightness but also enabled the production of more sophisticated systems including security systems in automobiles. Electirical components, including electric socket, television-radio-computer frames, wiring insulation, etc. are mainly produced from plastics. Furniture and houseware acount for %12 of total plastic consumption.

Agricultural uses of plastics are also very important in increasing the yield of crop as much as 200 or 300 percent. These covers are useful in raising the soil temperature, maintaining the moisture, preventing nutrient loss and growing of insects. Plant containers, watering products, netting to prevent crops from birds are some other examples for the uses of plastics in agricultural industry.

Other uses of plastics include biomedical applications (wound-closure products, drug delivery systems, gloves, plastic wraps, some implants, etc), sport and hoby

industry (bicycle body, golf stick, child toys, etc), coatings, scientific research equipments and military equipments [31].

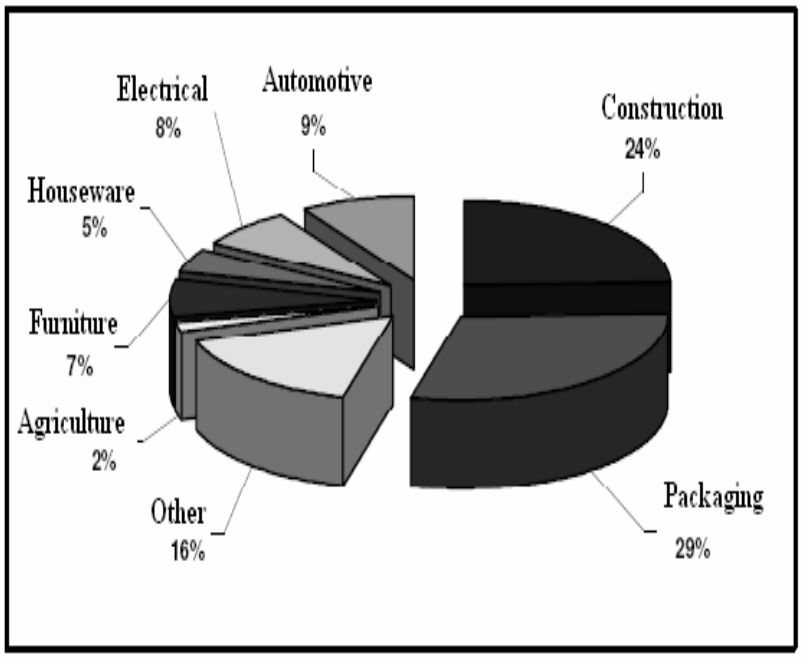

Figure 2.1 Uses of plastics in different sectors [30].

2.2 Plastics and the Environment

The first major problem related with the huge consumption of polymers in plastic production is the raw materials from which they are produced. Virtually all plastics are made from petroleum (crude-oil), natural gas and coal. They are natural resources that have taken millions of years to be formed, and are nonrenewable. It is estimated that 4% of the world's annual oil production is used as a feedstock for plastics production and an additional 3-4% during manufacture. Thus, the use of limited and nonrenewable supply of fossil resources for the large-scale manufacture of plastics becomes an important environmental concern all over the world.

The large uses of fossil fuels over a relatively short period of time have also raised concerns as to whether the natural mechanisms for maintaining carbon dioxide balance have been strained. By one estimate, the carbon dioxide flow from land into the atmosphere has been increasing at an annual rate of approximately 10% of the baseline

reindustrialize flow. The increase has contributed to a buildup of atmospheric carbon dioxide of approximately 0.4 % a year. Carbon dioxide accounts for about half the greenhouse effect by which some atmospheric gases absorb and reradiate long wavelength (infrared) radiation. A natural greenhouse effect is responsible for increasing the annual global temperature of Earth's atmosphere and surface from a rather chilly -18^{o}C to 15^{o}C. Today, whether an enhanced greenhouse effect due to the buildup of greenhouse gases is leading to a significant warming of the planet is of crucial environmental concern.

The second environmental concern is the pollution due to the generation of by-products during manufacturing process of polymers. By the development of new manufacturing procedures (for examples, using new catalysts systems) and recycling technology, the amount of polluting waste products is significantly reduced but not eliminated. Environmental pollution caused by the manufacturing of polyolefin is given in Table 2.4 [32].

Table 2.4 Pollution per ton of polyolefin product (PE,PP) [32].

Year / ***Pollution (kg)***	***1972***	***1985***	***1995***
Air	20.9	6.1	2.8
Water	36.7	2.6	1.3
Waste	11.7	37.7	5.8
Total	69.3	46.4	9.9

Accumulation of plastic waste in the landfills is also a big problem. Because most plastics are non-degradable, they take a long time to break down, possibly up to hundreds of years. With more and more plastics products, the landfill space required by plastics waste is a growing concern. Between 1988 and 1998, the number of landfills in the United states dropped from 8,000 to 2,314. In New York State there were 550 landfills in the mid-1980s, but many of the smaller landfills have been closed without replacement, leaving around 30. One analysist estimates that all of the garbage that will be produced in the United States for the next thousand years would fit into one-tenth of 1 percent of the land area.

In the United States over 60 billion pounds of plastic are discarded into the waste stream each year (In 1970, the plastics waste stream was only 4 billion pounds). In Western Europe over 35 billion pounds of plastics waste are generated each year. Well over half the plastics waste stream is in municipal solid waste which includes common garbage or trash generated by homes businesses, institutions, and industries.

Plastics account for around 18 percent of the volume of municipal solid waste and represent the fastest growing component. Excluding organic waste-paper, yard waste, food waste and wood- plastics make up 30 percent of the remaining weight and as much as one-half of the remaining volume [31].

Worldwide about one-half of all discarded plastic comes from packaging. Almost one-third comes from packaging that is discarded soon after use. Heavy-duty plastic construction materials have a longer life span, which means that much of the plastic that was put into use decades ago, when plastics use began in earnest, will start showing up in increasing amounts in the near future.

2.3 Managing Plastics Waste

2.3.1 Replace, Reduce, Reuse

There are some proposed techniques to reduce the environmental pollution caused by plastics. Reduction of the plastic consumption by replacing plastics with other conventional materials seems to be the most basic solution but it is not easy to limit the usage of plastics by as long as they are so useful, inexpensive and versatile. Indeed, today it is the plastic materials that have replaced many conventional materials like paper, glass and metals due to their excellent properties such as low weight, low cost, safety, easy processibility and versatility. Comparing the energy required to produce plastic to that of paper, glass or metals, the production of plastics is both economical and ecological choice. For example, 0.1 KHW energy is required for production of plastic container as compared to 3 KWH for aluminum and 2.4 KWH for glass containers [33]. Comparing one of the most common polymer, polyethylene (PE) used

for grocery bags as compared to kraft paper reveals that, PE use less energy than the paper, create less solid waste by volume and have less atmospheric emissions as shown in Table 2.5 [34]. Both PE and PS resin production processes emit fewer particulates and less NO_x, SO_2 and CO than the paper processes. Moreover, in order to replace plastic with paper, more trees have to be cut and this is not good for the environment. Therefore, it is clear that overall environmental damage due to use of plastics is less detrimental than for other conventional materials.

Table 2.5 Energy Used and Pollution Generated during the Manufacture of 50,000 Carrier Bags [34].

Environmental Burden	***Polyethylene***	***Paper***
Energy (GJ) During Manufacture	29.0	67.0
Air Pollution (kg)		
SO_2	9.9	28.1
NO_x	6.8	10.8
CH_x	3.8	1.5
CO	1.0	6.4
Dust	0.5	3.8
Water Burden (kg)		
Chemical oxygen demand	0.5	107.8
Biological oxygen demand	0.02	43.1

Reduction of plastics waste by "source reduction" is possible to some extent. For example, it may be possible to produce much thinner products without loosing the desired properties with the replacement of one plastic material by another type exhibiting better mechanical performance. Modifications in product design can also lead to size reduction and the amount of disposable material is decreased.

The "reuse" strategy is an alternative approach to the pollution problem. However, it is also limited due to the impurities coming from the original use. Waste bags, agricultural bags, food packages, and disposable diapers cannot be reused and they account for millions of tones of plastics that are discarded into the landfills each year.

2.3.2 Recycling and Energy Recovery

There are various modes of recycling like primary recycling, secondary recycling, tertiary recycling via chemical treatment and recovery of energy.

Primary recycling means reuse of off-grade and scrap materials directly by the converter plant. However, recycled plastics are always inferior to original ones because during processing, they may be contaminated or lose some useful properties. In some cases, they undergo thermal history. Therefore, they are often reground and added as a blend to virgin raw material in an amount of between 10% and 25%.

Secondary recycling means that used plastics are collected, cleaned, separated according to their origin, and finally grinding and reused either as separate species or in a blend. The first step is the separation of domestic waste into several groups such as plastics, metal, glass, paper and organics. The next steps include industrial collection and separation by using modern equipment of sorting and cleaning that leads to final individual products. This is a complex and expensive operation, as each species must be further subdivided into various metals, glass of different colors, and plastics of different families and grades. The secondary recycling is preferable when used plastic is unblended one. PET bottle for soft drinks is a good example although the separation of HDPE cups from bottle causes difficulty in recycling process. PC may also serve as multiple-use bottles that can be sterilized and refilled, thus decreasing the amount of waste. Today, the most recycled and reprocessed plastics are PET, HDPE and LDPE.

Tertiary recycling is the chemical treatment of the scrap plastics in order to obtain some useful materials like monomers, oligomers, chemicals or fuels. Controlled depolymerization (as in pyrolysis) renders selectively pure monomers. For acrylics, such as PMMA, the method is successfully commercialized. The pure monomer may replace the virgin raw material. PET, polyamides and polyurethane are also suitable plastics for depolymerization. The main advantage of tertiary recycling over the secondary one is to end up with pure monomer which can further be converted to first quality resins. For example, monomer obtained from depolymerization of PET can be used safely in food packaging which is not allowable for the product of secondary recycling process. Pyrolysis is also possible for thermoset polymers as well as blended

plastics. The mixed plastic in blends can be depolymerized at high temperature into monomers that can be easily separated and repolymerized. In the case of thermoset, since the product includes fuel, that is used for energy. Whereas, some polymers (like PE, PS, etc.) degrade during pyrolysis and the presence of impurities makes the process harder.

Recovery of the caloric value of plastics may be useful whenever there is no market for the recycled plastic or the process is not feasible. The energy content of the commodity polymers is more than twice that of coal or paper and four times that of general waste. However, it is not accepted everywhere as the environmentally hazardous materials (toxic gases, chlorine chemicals, dioxins, heavy metals, nitrogen oxides, etc.) are evolved during combustion of plastics. Plastics are usually combusted in the form of total waste which reduces the energy recovery and leads to more ash formation. Japan leads in the use of incineration of solid waste at about 50% (including 67% of plastic wastes), compared to 30% in Europe and about 15% in the United States. The success of incineration depends on modern design in particular for high efficiency and good control of pollution emission (which can cost about 20% to 30% of the whole process). PVC is known as the major contributor of the toxic emissions due to the emission of hydrochloric acid and plasticizers. Therefore its consumption in the production of disposable packaging has been diminished. However, it is an attractive solution when there is not enough landfill for solid waste as it is the case in Japan and many populated places of western world. [33].

In spite of these proposed solutions for waste management, according to a 2001 Environment Agency report, only 8% of post-consumer plastic waste is incinerated, 7% is recycled and 80% is still sent to landfill.

2.3.3 Photo-, Oxidative and Hydrolytic Degradations

The main problem related with the managing plastic waste is the stability of the current plastics to degradation. Therefore, the subject of making plastics degradable is a challenging idea to reduce the plastic waste disposal into the landfills.

It is known that many environmental factors effect the degradation of polymeric materials, such as exposure to sunlight, high temperature, high-energy radiation, oxidation, hydrolization, microorganisms, rain, chemicals including ozone, mechanical stress, etc. Within the various factors, the ultraviolet light plays an important role in the degradation of the polymers. Therefore, the study on photo-oxidative degradation of polymeric materials is an attractive field in rendering plastics into photodegradable materials. The strategy is to attach a photosensitizing group to the polymer chain so as to promote photodegradation. The idea is that, when the photosensitive group is exposed to the sunlight, it will absorb radiation and causes the formation of smaller segments by chain scission. As photodegradation proceeds, the chains are broken in more and more places leaving the plastic brittle. Finally, erosion by various environmental conditions like wind and rain completes the breakdown of the fragile plastic into a friable powder.

Resins of nondegradable commodity plastics like polyethylene, polypropylene, and polystyrene can be modified and made photosensitive. Some chromophoric species, such as carbonyl groups, hydroperoxides, metallic impurities, polynuclear aromatics, oxygen-polymer charge transfer complexes, etc., have been used for polyolefins to initiate photodegradation. These sensitizing groups, such as a ketone group, is introduced into the polymer chain by copolymerization with an appropriate ketone monomer. Carbon monoxide (CO) is an another common example to produce a photodegradable polymer. The copolymerization of ethylene and carbon monoxide is mainly used for the large scale manufacture of photodegradable six-pack holders for beverage containers. Composition containing 1% CO will photodegrade after about three weeks' exposure to outdoor sunlight and break up into small particles. Sometimes, a photosensitizing group can be incorporated after polymerization. Metallic salts, of

nickel, cobalt, iron or some other metal, are incorporated as a photosensitive additives during processing. [31].

There are some obstacles, on the other hand, for the success of photodegradation mechanism in reducing the plastic paste. The thickness of the plastic, for example, plays an important role in that UV-light should reach deep inside the plastic material. In this aspect, most of the commonly used plastic items such as bottles, containers, housewares, etc. will be degraded very slowly. Moreover, the photodegradation mechanism will not be initiated for the plastics buried in the soil.

Newer technologies have been developed that do not rely on photo degradation, so that exposure to sunlight is not necessary. There are now additives that, when compounded with a polyolefin, promote environmental degradation through the chemical processes of oxidation and hydrolysis. Oxidation is a chemical reaction in which electrons are lost by an atom or molecule. It can be carried out either by direct combination with oxygen or by reaction with oxidizing agents. In reactions of organic molecules, oxidation is reflected in the addition of oxygen atoms to a molecule or the removal of hydrogen atoms. The oxidation of ethanol, for example, to acetaldehyde, then to acetic acid provides for the elimination of alcohol by the human body.

$$CH_3CH_2OH + \text{oxidizing agent} \longrightarrow CH_3CHO$$

$$CH_3CHO + \text{oxidizing agent} \longrightarrow CH_3COOH$$

The newer polyolefin additive formulations allow oxidative degradation to be initiated either by natural daylight, or by heat, or even by mechanical stress. The fragments formed by oxidative degradation are wettable, leading to increased interactions with water and promoting hydrolysis. Hydrolysis is a chemical reaction in which a compound is converted into another compound by taking up the elements of water. Esters, for example, undergo hydrolysis to produce the corresponding carboxylic acid and alcohols and the reaction is:

$$RCO_2R' + H_2O \longrightarrow RCO_2H + R'OH$$

Through oxidative and hydrolytic degradation the polyolefin chains undergo progressive chain scission. In time, embrittlement occurs and eventually turns into a

friable powder, perhaps even invisible to the naked eye. The possible applications for this formulation are plastic products where disposal might include soil burial, as with compost bags and agricultural mulch covers.

There are two dangers of using self-degradable plastics; first, the collapse of plastic might occur during useful lifetime and the recycled products of such compounds would have reduced properties.

In order to eliminate the collapse of the material during lifetime, the idea of programmed or controlled degradation has been developed. The aim is to prevent significant decrease in performance properties of the material during processing and the planned useful lifetime and provide degradation after the period of use. This type of specific behavior can be achived, for example, by adding metal ion complexes. The complexes act as stabilizers during processing but then decompose, after an induction period, in a controllable manner to form products that are photoactivators. By a careful choice of the right combination of stabilizer and activator concentrations, the length of the induction period and the rate of the degradation that follows can be controlled.

2.3.4 Biodegradation

The idea of biodegradation of wastes is considered as the best approach for reducing the environmental pollution. For these reason, throughout the world today, the development of biodegradable materials with useful properties during their lifetime has been a subject of great research challenge to the community of materials scientists, ecologist and engineers.

Biodegradation, or biotic degradation, is chemical degradation brought about by the action of naturally occurring microorganisms such as bacteria, fungi, and algae. As biodegradation proceeds it produces carbon dioxide and/or methane. In the present of oxygen, the degradation that occurs is aerobic degradation, and carbon dioxide evolves. If there is no oxygen in the environment, the degradation is anaerobic degradation, and methane is produced.

The rate of biodegradation in soil is affected from the soil conditions like temperature, moisture, oxygen concentration, acidity, and the amount of microorganisms. Low temperature strongly inhibits degradation process. In very cold climates, the organic matter can remain well preserved for a thousand of years in a soil. Moisture is also important parameter since it supports hydrolytic degradation. The concentration of oxygen determines whether aerobic or anaerobic degradation will occur. Although there are many bacteria that live in an oxygen-free environment, there are many more that use oxygen. Degradation also requires microbial activity in a degradation environment. Degradation rate is nearly zero in a sterile soil.

Regardless of the environment, the rate of plastics degradation also depends on the chemical composition of the plastic. The chemical structure of the most common commodity plastics such as polyethylene, polypropylene, poly (vinyl chloride), and polystyrene contain C-C single bonds in their backbones. That feature makes them resistant to hydrolytic degradation. They can be degraded through oxidative mechanism but not very readily. The oxidative degradation is initiated by the action of heat or light. The first step of peroxidation is the slowest step in the reaction hence it is the rate determining step and leads to very long lifetime for many of synthetic polymers, as long as 200 years for some polymer grades like polyethylene. The degree of oxidation strongly depends on the morphology of the polymer. The crystalline regions are impermeable to oxygen, thus oxidation of these synthetic polymers occurs mainly in the amorphous regions. Once oxidative degradation has been initiated, the polymer chains start to fragmentation to much smaller and biodegradable products such as carboxylic acids, alcohols, hydroxyl carboxylic acid, etc.

Poly (vinyl alcohol) is one of the rare polymers having a backbone of C-C single bonds that is nevertheless biodegradable. It has a hydroxyl side groups which make it strongly hydrophilic, and thus soluble in water. This property helps to promote degradation through hydrolysis mechanisms.

Hydrolytic degradation of many of the synthetic polymeric materials takes place when polymers containing hydrolyzable groups, such as esters, amides, carbonates, or urethanes, are exposed to moisture. The degree of crystallinity is also important in these polymers because the crystalline regions are less permeable to water than the

amorphous regions, making highly crystalline polymers particularly resistant to hydrolytic degradation. The hydrolysis reaction leads to the generation of biodegradable organic matters such as carboxylic acids, alcohols, carbohydrates, etc. The organic material is degraded to the point that it becomes humus by microorganisms in soil. Bacteria start the process of decaying organic matter, but are soon joined by fungi and protozoa. Microorganisms also contribute to the degradation process. In soil, insects and invertebrates (such as snails and slugs) feed on microorganisms and plant residues to produce humus. Through natural decomposing, carbon atoms are returned to the ecosystem and once again made available for living plants to recapture them through the process of photosynthesis. Under some conditions, microorganisms can also contribute to the degradation of plastics through ingestion, mastication, and excretion.

The two alternate mechanisms for synthetic polymer biodegradation are summarized in Figure 2.2.

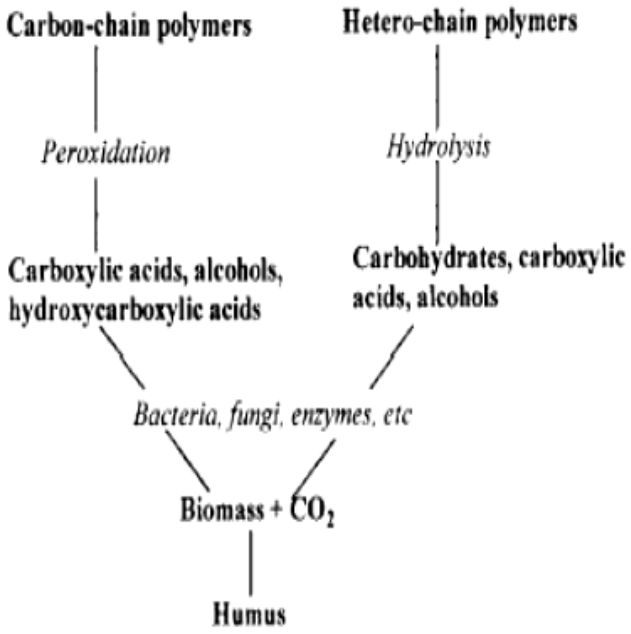

Figure 2.2 Biodegradation mechanisms for synthetic polymers [34].

Natural polymers or biopolymers are inherently biodegradable, as they must be in order to take part in nature's cycles of renewal. The chemical structure of various types of biopolymers such as starch, protein, chitosan, cellulose, etc. are different from those

of the synthetic polymers. They have many oxygen and nitrogen atoms in their polymer backbones and thus they are readily biodegradable.

The use of biodegradable polymers from natural sources in place of synthetic ones is not feasible, on the other hand, due to the inferior properties and processing difficulties of natural polymers. It is now possible to produce completely biodegradable plastics, such as polylactic acid (PLA), poly(vinyl alcohol) (PVOH), polycaprolactone (PCL), polyhydroxyalkanotes (PHA),poly(3-hydroxybutyrate) (PHB), poly(3-hydroxybutyrate-co-3-hydroxyvalerate) (PHBV), poly(butylene succinate), and poly(butylene succinate-co-adipate), synthetically but they are expensive products and their production is based on the use of more fossil fuels than that for the many commercial synthetic polymers.

Therefore, it is generally accepted that the most suitable way of producing satisfactory biodegradable polymers is to preparation of blends or composites using synthetic polymers and natural ones. Recent studies on the biodegradability of synthetic-natural polymer blends or composite materials have shown that the degradation rate of the synthetic polymers increases with the incorporation of natural biopolymer [1,24-29]. It was suggested that microbes first create pores by consumption of biopolymer and thereby increase the surface area of the composite. Increased surface area enhances oxygen-based reactions, which could increase synthetic polymer chain oxidation. Since this is the slowest step in the degradation mechanism of synthetic polymers, any factor which increases the oxidation tendency of polymers also controls the degradation of plastics. Hence, creating oxidized polymer chain ends in a degraded composite will make a synthetic polymer susceptible to biotic reactions.

2.4 Global Market For Biodegradable Polymers

According to technical market research report RP-175R Biodegradable Polymers from Business Communications Co. Inc., the global market for biodegradable polymers is currently estimated at 114 million lbs. There have been technology advances, lower pricing, new products, and markets for biodegradable polymers. Average annual growth

rates are very high, with forecasts for the market well over 200 million lbs by the end of the decade.

US degradable plastic demand is expected to grow 16.8 percent annually through 2010 as these products become more price competitive and continue to benefit from various sustainable resource initiatives. In terms of applications, packaging constitutes nearly 47% of total polymers market in 2005. However, compost packaging will overtake the market, representing nearly 50% of the market by 2010. Other products such as medical/hygiene, agricultural, and paper coatings play a smaller but no less important role in the total market size, representing 11% of the total applications in 2005 [35].

Table 2.6 Global Biodegradable Polymer Market by Application (million lbs)

Application	***2000***	***2005***	***2010***	***Ave. Annual Growth Rate, 2005-10***
Packaging[1]	33	53	83	9.4
Compost Bags	23	48	95	14.6
Other[2]	5	13	28	16.6
Total	61	114	206	12.6

[1]Includes loose-fill packaging, which constitutes about two-thirds of the total.
[2]Includes medical/hygiene products, agricultural, paper coatings, etc.

2.5 Biodegradable Polymers

Biodegradable polymers are classified as the polymeric materials that are capable of decomposing when given an appropriate environment and a sufficient amount of time. Some biodegradable polymers occur in nature and they are usually called as biopolymers or natural polymers. They are produced by living organisms such as plants, animals, and microorganisms through biochemical reactions. Polysaccharides, such as starch and cellulose, and proteins are biopolymers present in the biomass in great abundance. Polyesters, produced by microorganisms, are another type of biopolymers. Biodegradable polymers can also be produced synthetically from natural sources. These

are called as “sythetic biopolymers”. Lactic acid, various amino acids and triacylglycerols are example of biomolecules that are polymerized into biodegradable polymer. Other biodegradable polymers can be derived from the petroleum sources or may be obtained from mixed sources of natural and petroleum.

The current researches have been mostly focused on cellulose, protein, poly(3-hydroxybutyrate) (PHB), PLA and starch based biodegradable polymers.

2.5.1 Cellulose

Cellulose is the most plentiful type of polysaccharide that is present in plant cell walls. It forms the structural fibers of plants, keeping the cell wall intact and giving it strength. It constitutes 90% of dry cotto and 50% of wood. Figure 2.3 represents the molecular structure of cellulose.

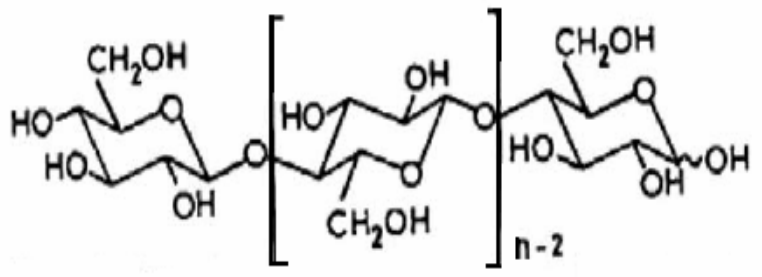

Figure 2.3 Molecular structure of cellulose.

Approximatelly, 150 billion tons of cellulose are produced commercially each year, mainly from wood, but also from cotton [31]. Much of it is used in the production of paper and paper products. Many cellulosic products, such as wood shavings, have long been used as a filler in polymers, in order to decrease their cost without degrading their mechanical properties. For the last 30 years, cellulose fibers such as wood fibers or cotton have been studied as reinforcement agents in composites. They combine good mechanical properties, that is, a strength and a modulus of the same order of those of mineral fillers, with the advantages of cellulose, which is biodegradable and renewable. The main problem is the formation of fiber aggregates during the processing due to the high viscosity of the matrix fiber. The fibers are generally long and entangled but the

application of a strong mechanical dispersion process can lead to a decrease in their length below the critical fiber length and, therefore, in their reinforcing properties. The second problem is the wettability of the polar cellulose with usually nonpolar synthetic polymer, leading to an agglomeration of the fibers in the composite. There are some proposed solutions to these problems by different researchers, one being the grafting process of polymer on the fiber surfaces, which causes a better affinity with the matrix and a better dispersion [36]. Another approach proposed is to use an aqueous medium for both fillers and polymer matrix. By this method, it is suggested that if the fibers are sufficiently well dispersed in the aqueous medium, the formation of fiber aggregates can be avoided after the evaporation of water [37].

In a latter time, cellulose plastics have been developed and their use in place of petroleum-based polymers has gained great attraction because they are biodegradable polymer and have excellent optical clarity as well as high toughness. Cellulose plastics like cellulose acetate (CA), cellulose acetate propionate (CAP), and cellulose acetate butyrate (CAB) are thermoplastic materials produced through esterification of cellulose. The biodegradation is dependent on the degree of modification. Usually, chemical modifications reduce the biodegradability of the polymer [31]. Modified cellulose are used in the manufacture of paint, plaster, adhesives, ceramics, cosmetics, pharmaceutical film coatings, etc. The main drawback of cellulose acetate plastic is that its melting range is close to its decomposition temperature. Therefore, they are extruded in the presence of different plasticizers and additives to produce various grades of commercial cellulose plastics in pelletized form. The phthalate plasticizer, normally used in commercial cellulose ester plastic, is now under scrutiny for its potential health and environmental impact. Therefore, eco-friendly plasticizers such as citrate, and/or blends of citrate, and derivatized vegetable oil have been suggested to use in recent studies in order to avoid the use of phthalate plasticizer [38,39].

The water vapour and oxygen transmission rates of cellulose acetate films are high but the film is considered excellent for fresh produce and pastries because it breathes and does not fog up. Cellulose acetate resin cost is $1.60-2.10 per pound and finished film price is approximately $4.00 per pound.

2.5.2 Protein

Proteins are natural polymers which are fully biodegradable like cellulose and starch. Proteins do not have the regular repeating units of other polymers, due to the different side groups on the amino acid residues which make up the protein chain. Nonetheless, considerable effort has gone into exploring and developing protein-based films.

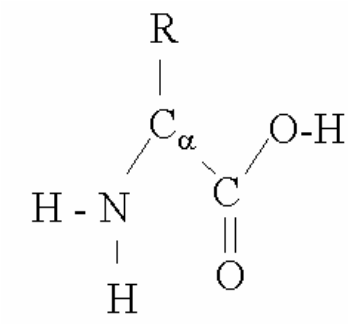

Figure 2.4 Structure of α-amino acid (R group determines the chemical properties of the α-amino acid and may be any one of the 20 different side chains).

The most successful films based on a protein are collagen films used commercially as edible casings and wraps for meat products. Collagen is a fibrous, structural protein in animal tissue, with common repeating unit: glycine, proline and hydroxyproline. Unfortunately, collagen is not thermoplastic; thus, collagen film must be made by extruding a viscous colloidal acidic dispersion into a neutralizing bath, washing and then drying. The mechanical properties of collagen film depend on composition (e.g., plasticizer content) and whether longitudinal or transverse sections are tested. The tensile strength of collagen is considerably lower. Lowering the plasticizer content would increase film strength but with the cost of decreased modulus. Achievement of mechanical properties similar to polystyrene is possible. However, mechanical properties of collagen film are inferior to LDPE and HDPE.

The other proteins which have been studied for film formation include corn zein (CZ), wheat gluten (WG), soy protein isolate (SPI) and whey protein isolate (WPI), which are globular in nature, and casein (CS), which has an open, extended structure. Films from these proteins are generally formed out of ethanolic solution (CZ and WG) or aqueous solution (CZ latex, SPI, WPI and CS). However, some or all of these proteins may exhibit thermoplastic behaviour under the right conditions.

All of these proteins have fairly large water vapour permission (WVP). Composite films which include wax have considerably lower WVP. The oxygen permission (OP) of films made from CZ, WG and SPI are quite low at 0% relative humidity (RH). As with collagen film, RH has a large effect on OP for films from these materials. Nonetheless, at low to intermediate RHs, protein films have OPs significantly lower than the PEs and PPs, and comparable to polyester.

As with permeability properties, mechanical properties are strongly affected by plasticizer content (and RH). On the basis of limited data, it appears that plasticized films made from the globular proteins have a combination of tensile strength and modulus similar to collagen film. Among the globular proteins, CZ and WG films made from ethanolic solutions appear to possess superior mechanical properties compared to SPI and WPI films made from aqueous solution. The limited mechanical property data for protein films makes it difficult to foresee applications, but edible food coatings or paper coatings are possibilities.

Soy protein isolate and corn zein have been shown to have properties resembling thermoset plastics and can be compression molded into shapes which have mechanical properties similar to polystyrene. Formaldehyde cross-linked starch-zein gave molded shapes with significantly greater water resistance than starch, zein or soy protein alone. Thus, crosslinked starch-zein has potential for molding into utensils and containers usually fabricated from polystyrene. Mixtures of soy protein and native corn starch have thermoplastic properties which are suitable for extrusion and injection molding [40].

2.5.3 Microbial Polyesters

Other naturally-occurring polymers being considered for biodegradable products are the microbial polyesters (polyhydroxyalkanoates). Polyhydroxyalkanoates (PHA)s serve as energy and carbon storage materials in bacteria. They accumulate when carbon is in excess but some other nutrient limits growth. They are consumed when no external carbon source is available. The most abundant PHA in nature is poly-3-hydroxybutyrate

(PHB). Other PHAs include those containing hydroxyvalerate units, as in poly-3-hydroxyvalerate (PHV) and poly-4-hydroxybutyrate.

PHAs are now produced commercially from microorganisms through fermentation. In bioreactors, microorganisms are fed a carbon source substrate, such as glucose or sucrose for PHB, or propionic acid for PHV. Propionic acid can be produced by the fermentation of wood pulp waste or from petroleum. PHAs are produced in a two-stage fermentation process consisting of cell growth followed by polymer accumulation, which proceeds to as much as 80 or 90 percent of the cell's dry weight. The polymer material, in the form of granules, is removed from the cells by aqueous extraction, resulting in a white powder [41].

Polyhydroxybutyrate (PHB) plastic by itself is very brittle, but copolymers of hydroxybutyrate and hydroxyvalerate (PHBV) display a range of brittleness, strength, and other properties according to the copolymer composition. PHBV can exhibit physical properties and processing behaviour resembling polyethylene at high hydroxyvalerate content or polypropylene at low hydroxyvalerate content [31].

PHBV is reported to possess good oxygen, moisture and aroma barrier properties. Good moisture barrier properties are consistent with the fact that PHBV is relatively more hydrophobic than polysaccharides and proteins. Furthermore, while the oxygen barrier may not be as good as that for polysaccharides and proteins at low relative humidity (RH), it should not be as sensitive to increasing RH. PHBV can be processed by injection molding, extrusion blow molding, film and fiber forming, and a variety of coating and lamination techniques. It has been processed into a wide range of packaging materials, including bottles, coated paperboard milk cartons, dishes, cup, credit cards, golf tees, motor oil containers, etc. An early commercial application (in 1990) was in the manufacture of a blow-molded bottle for the shampoo industry.

Production of PHAs has reached approximately a million pounds a year. The main limitation, however, is the cost of PHBV. Current price for PHBV resin is $8-10 per pound, but projected price is lower [40].

2.5.4 Polylactic Acid (PLA)

Polylactic Acid (PLA) is not a natural polymer, but it is based on lactic acid which can be produced by fermentation of simple sugars.

Lactic acid, $CH_3CHOHCOOH$, is found in many natural foods and in fermented foods, such as yogurt, buttermilk, sourdough breads, and others. It can be produced commercially by chemical synthesis or by fermentation; fermentation is now the major route. In the fermentation process sugar feedstock, such as dextrose (glucose), are obtained either directly from sources such as sugar beets or sugar cane, or through the conversion of starch from corn, corn steep liquor, potato peels, wheat, rice, or some other starch source. After lactic acid is recovered from the fermentation process, it is purified in a multistep process, which represents a major part of the production cost.

Poly(lactic acid) (PLA) is the polyester synthesized from lactic acid; its structure is shown in Figure 2.5. Condensation polymerization of lactic acid generally produces a low molecular weight polymer, which is then treated with coupling reagents that act as chain extenders to give high molecular weight PLA. Recently a condensation polymerization has been found to give high molecular weight PLA when carried out in a high boiling point solvent at reduced pressure and with added catalyst.

Alternatively, the low molecular weight prepolymer is depolymerised under reduced pressure to produce lactide, the cyclic dimer of lactic acid. Metal-catalyzed ring-opening polymerization of lactide produces a high molecular weight polymer with good mechanical properties. The name polylactide refers to the product of ring opening polymerization [31].

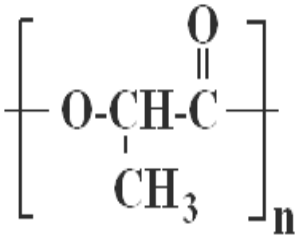

Figure 2.5 Structural formula of poly(lactic acid), a synthetic biopolymer.

PLA is thermoplastìc, insoluble in water, has good moisture and grease resistance and fully biodegradable when composted at temperatures above 60^{o}C or in seawater with microorganisms present. It degrades by hydrolysis and therefore can be recycled back to its monomer, lactic acid.

PLA has mechanical properties similar to PS. By its nature, the film produced from PLA is quite stiff. As it has a glass transition temperature (Tg) greater than room temperature, it is stiff and glassy compared to a olefin material which has a Tg less than room temperature. In addition, the elongation of a PLA film is very low as it is in its glassy state compared to a LDPE film that has elongations of 200 – 300%. These two facts make it very difficult to collapse a bubble of PLA film without creating a significant amount of wrinkles in the web. As PLA has excellent dead fold properties, these wrinkles will remain in the film and make further downstream converting difficult. However, mechanical properties of PLA can be modified by varying molecular weight and crystallinity, copolymerization and other modifications, with resulting properties which also mimic PE, PP or PVC. By plasticizing PLA with its lactide monomer, mechanical properties are modified to more closely resemble those of PE. Product targets for PLA include food service containers, yard waste and grocery bags, compost bags, and agricultural films. Its clarity, high gloss, and stiffness also make it useful for recyclable and biodegradable packaging, such as bottles, yogurt cups, and candy wrappers. One of the major drawbacks of its widespread uses is its cost which is $1-3 per pound [42].

Fossil energy requirements for selected petroleum-based polymers and PLA are shown in Figure 2.6. It is appearing that petro-chemical plastics can have equivalent or better eco-profiles than PLA. The main factors influencing this are energy for polymer manufacture and the effects of number of recycling loop [43].

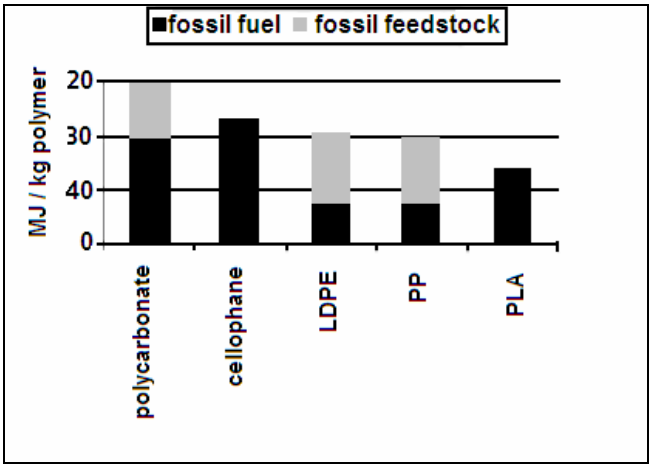

Figure 2.6 Fossil energy requirements for selected petroleum-based polymers and PLA [43].

2.5.5 Starch

In the family of renewable sources based biodegradable polymeric materials, starch has been considered as one of the most promising materials for the future because it is readily available and may form cost effective end products. Annual world production of starch is over 70 billion pounds. It is found in corn (maize), potatoes, wheat, tapioca (casava), peas, barley, rice, sorghum, and some other plants. Starch serves as energy storage function in plants. When it is metobolized by plants, energy is released and that energy is used for plant growth. Starch is a combination of amylose, which is a linear polymer and has a molecular weight of 2 to 6 x 10^5 [g/mol], and amylopectin (molecular weight ~10^6 [g/mol]). Both forms of starch are polymers of a-D-Glucose. Natural starches contain 10–20% amylose and 80–90% amylopectin. Amylose molecules consist typically of 200–20,000 glucose units which form a helix as a result of the bond angles between the glucose units (Figure 2.7a). On the other hand, amylopectin molecule has a highly branched structure (Figure 2.7b). Short side chains of about 30 glucose units are attached approximately every 20–30 glucose units along the chain. Amylopectin molecules may contain up to two million glucose units. Aqueous solutions of amylopectin are characterized by high viscosity, clarity, stability, and resistance to gelling. The level of amylopectin varies between different starch types.

Corn starch, for example, is typically made up of about 28 % amylose and 72 percent amylopectin.

In the native form of starch these two types of polymer are organized in granules as alternating semicrystalline and amorphous layers. The semicrystalline layers consist of ordered regions composed of double helices formed by short amylopectin branches, most of which are further ordered into crystalline structures. The amorphous regions of the semicrystalline layers and the amorphous layers are composed of amylose and non-ordered amylopectin branches. There is an additional complexity relating to the nature of the crystalline structures. The double helices comprising the crystallites may be densely packed in an orthogonal pattern, as in cereal tarches or less densely packed in a hexagonal pattern, as in potato starches. Starches are generally labeled according to the type of crystallite present in the granules.

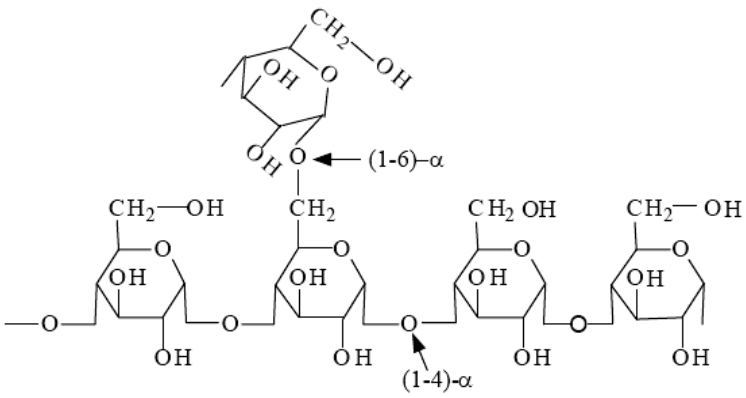

(a)

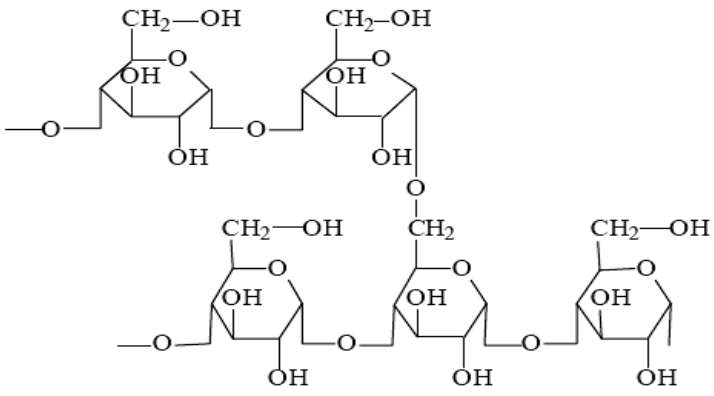

(b)

Figure 2.7 Molecular structures of (a) amylose and (b) amylopectin.

Even though starches are low-cost, abundant and fully-biodegradable polymers, it is not suitable for production of materials due to moisture susceptibility, brittleness, and processing difficulties. Articles made from starch will swell and deform upon exposure to moisture. Moreover, its melting temperature is higher than the degradation temperature due to the presence of long range H-bonds between its chains. Therefore, it cannot be shaped or molded into the articles. One of the approaches to overcome this problem is the modification of starch. Native starch granules swell when they absorb water through hydrogen bonding with their free hydroxyl groups, but they still retain their order and crystallinity. However, when these swollen starch granules are heated, hydrogen bonding between adjacent glucose units is disrupted and the crystallinity is progressively destroyed. This process is called gelatinization. The processing of starch and water in a heated extruder is an efficient way to obtain gelatinized starch (GS) since the high shear that can be generated in the extruder disrupts the starch granules. Addition of a plasticizer such as glycerol or sorbitol can further improve the ductility of GS. Plasticized GS is known as thermoplastic starch (TPS) and is capable of flow. However, poor water resistance and low strength are limiting factors for the materials prepared only from TPS. The prior art concerning biodegradable plastics from TPS was exemplified by European Patent (EP) No. 304,401 in the name of Warner-Lambert Co [44]. This patent discloses a processing technique that when starch containing a certain amount of moisture is kneaded with a plasticizer at a high temperature of 150^{o} C or higher in a closed system such as an extruder, the vapor pressure increases to break the hydrogen bond between starch molecules thus producing starch having thermoplasticity. This technique is mainly devoted to the production of molded parts. However, it is not suitable for film production. A high melting strength is required in processing film, and high elongation and tensile strength are necessary after production. Another crucial disadvantage of TPS is its high water vapor permeability which limits its applications, especially in packaging industry.

Table 2.7 illustrates the energy and greenhouse gas savings by selected biodegradable polymers relative to petrochemical polymers. It is important to note that thermoplastic starch is more eco-efficient than PLA [43].

Table 2.7 Energy and greenhouse gas (GHG) savings by selected BDPs relative to petrochemical polymers.

Biodegradable Polymer	***Energy Savings* (MJ/kg BDP)***	***GHG Savings* ($kgCO_2$ eq/kg BDP)***
Thermoplastic Starch (TPS)	51	3.7
TPS plus 60%Polycaprolactone	24	1.2
Polylactic acid (PLA)	19	1.0

* max. +/- 15% depending on whether relative to LDPE or LLDPE.

The modification of native starch can also be achieved by the replacement of hydroxyl groups with hydrophobic ester groups or direct grafting of polymeric chains onto the starch backbone. Starch-g-poly(methyl acrylate), starch-g-poly(methacrylic acid) and starch-g-polystyrene are some examples to the later approach. A saponified starch-gacrylonitrile copolymer is commercially known as Super Slurper. This material is capable of retaining several hundred times of its own weight in water and it is used in absorbent products such as disposable diapers, bandages, hospital bed pads, etc [45].

2.6 Starch and Synthetic Polymer Blends

2.6.1 Starch and Synthetic Biodegradable Polymer Blends

Synthetic biodegradable polymers have been available since 1990. They usually exhibit better physico-mechanical characteristics, as well as processing properties, compared to natural polymers. However, these synthetic polymers are more expensive than petroleum polymers and also has a slow degradability. Blending starch with these degradable synthetic polymers was one of the first approach to decrease the cost of the final products. For example, starch and polyvinyl alcohol (PVOH) have been blended to yield biodegradable, thermoplastic materials. Otey et al. developed a biodegradable agricultural mulch film from starch, polyvinyl alcohol and glycerol [46]. The film was covered with a water-resistant resin coating since both starch-PVA films are greatly affected by moisture. The water-resistant resin coating is prepared from a water-

resistant resin, such as plasticized polyvinyl chloride, and a polyol-toluene diisocyanate prepolymer bonding agent. Mayer et al. advanced the research results obtained by Otey et al. by blending of starch with polyvinyl alcohol and ethylene vinyl alcohol for degradable films [47]. This invention disclosed a method of extruding raw starch with biodegradable copolymers such as polyvinyl alcohol (PVOH), or ethylene vinyl alcohol (EVOH), a nucleating agent, and a plasticizer. The method described in the invention alleviated pre-preparation steps, reduced the cost and time required to prepare and extrude starch-based biodegradable materials and resulted in a substantially completely biodegradable product. Tudorachi et al. studied the mechanical properties and biodegradation behaviour of blends based on starch in mixture with PVOH [48]. They found that the tensile strength increased with increasing PVOH amount, as well as starch amount and decreased with increasing plasticizer amount in the blends. The elongation at break decreased with increasing starch content, while the PVOH concentration had little effect on this parameter. The highest values of weight loss were obtained for the samples with a high content of starch. During biodegradation, plasticisers (glycerine and urea) and starch were consumed together with some amorphous structures from polyvinyl alcohol. The preparation of cellulose acetate and starch based biodegradable injection molded plastics was disclosed in U.S. Pat. No. 5,288,318 [49]. The solid ingredients were combined and fed to an extruder used to make pellets or to feed injection molding equipment. The resulting plastic parts were water resistant, high strength and biodegradable.

Kotnis et al. (1995) prepared biodegradable plastic substitutes by blending up to 25% of starch with degradable polyhydroxybutyrate-valerate (PHBV) [50]. The cost of the product was still high due to the high percentage of PHBV. Moreover, the mechanical strength properties of the blends were greatly reduced. Krishnan and Narayan prepared a new degradable polymer by blending up to 45% starch with degradable polycaprolactone (PCL) [51]. However, this new material was not strong enough because the melting temperature of PCL is only 60^{o}C. Also, PCL gets soft when temperature is above 40^{o}C . These drawbacks greatly limited the applications of the starch-PCL blends. For example, it is impossible for them to be processed into blown films, because the crystallization temperature is so low that bubbles of the films can not be sufficiently cooled under atmospheric air condition. The influence of water on the stability of starch-based materials is another factor limiting their usefulness. This is

perhaps the greatest problem with all biologically-based polymers, because of their inherent hydrophilic nature.

2.6.2 Starch and Non-biodegradable Polymer Blends

Starch has been combined in a number of ways with nonbiodegradable synthetic polymers in an attempt to improve the film properties of the former and increase the degradability of the latter. Catia et al. introduced a technique by which, when a synthetic resin compatible with starch, such as ethylene-vinyl alcohol copolymer and ethylene-acrylic acid copolymer, is mixed with starch containing a certain amount of water in the presence of a plasticizer at a high temperature in an extruder, intermolecular bonds of starch are destructurized and the starch chemically and physically binds to the resin [52]. However, the synthetic resins such as ethylene-vinyl alcohol copolymer and ethylene-ethylacrylic acid copolymer, display no biodegradability and are very expensive, so that it is quite difficult to substitute the films prepared from these synthetic resins for plastic films for general uses.

Therefore, starch has been blended with much economic petroleum-based commodity polymers by a number of researcher to increase the degradation rate of synthetic part, reduce the usage of petroleum products and decrease the moisture sensitivity of starch. One of the most appropriate candidate for these purposes is polyethyle as it is the most commonly used packaging material.

2.6.2.1 Starch-Polyethylene Blends

The generally observed behavior of polyethylenes, as well as the growing interesting in finding biodegradable plastic materials, led to a demand for a “biodegradable polythylene” and many different products of this type appeared during the beginning of the 1970s. Griffin introduced the idea of increasing degradability of polyethylene by adding a biodegradable additive [24,25]. He mixed granular starch with polyethylene and observed that the degradation rate of LDPE in compost is accelerated. Peroxides were generated and consequently autooxidation was started. This means that

the chemical effect of biotic environment may nonenzymatically increase the degradative autooxidation of polyethylene that is generally described as “aging” [53].

However, previous studies have also shown that the addition of starch granules into these polymers follows the general trend for filler effects on polymer properties [3-8]. The modulus increased due to the stiffening effect of the granules and the elongation decreased as the starch content increases. The main problem associated with the use of starch as filler was its hydrophilic nature and consequent incompatibility with the hydrophobic polymers. Yoo et al. have shown the lack of adhesion between starch and LLDPE by SEM pictures in their study [54]. The removal of many dispersed starch granules from the fracture surface was assigned the weak interfacial adhesion between the matrix and biopolmer phases (Figure 2.8(a)). For most of the starch particles still remaining at the fracture surface, the presence of voids between the starch phases and LLDPE matrix further confirmed the need for the reactive compatibilizer between the two distinct phases as seen in Figure 2.8(b) and Figure 2.8(c).

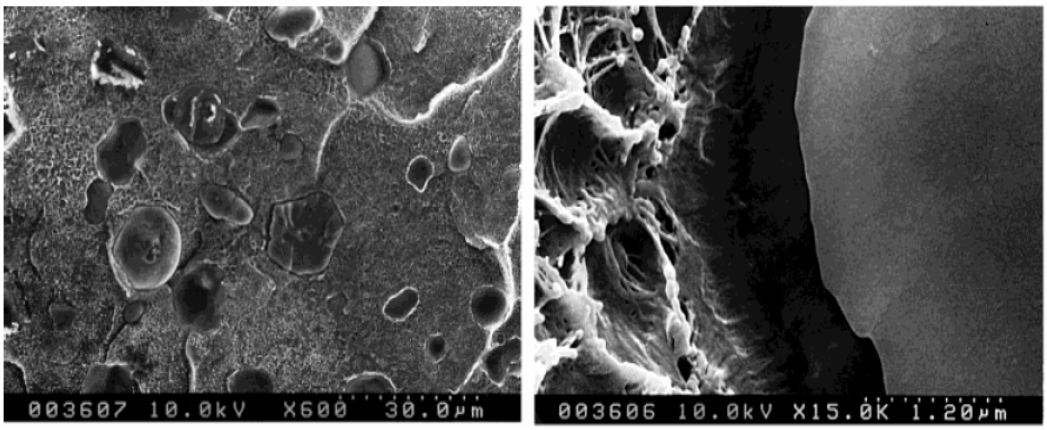

(a) **(b)**

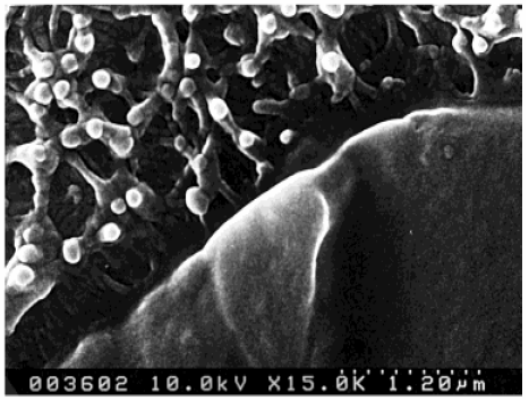

(c)

Figure 2.8 SEM micrographs of fracture surface of LLDPE/starch blends: (a) LLDPE (80 %)/starch (20%), (b) LLDPE(90 %)/starch (10%), (c) LLDPE (60%)/Compatibilizer (maleated polyethylene) (30%)/ starch(10%) [54].

Eventhough some enhanced mechanical properties were achieved with the use of maleated PE in synthetic polymer-starch blends, it was observed that the mechanical properties were still much lower than the mechanical properties of synthetic polymer itself. The most drastic decrease occurred in tensile strenght and the elongation properties. The transparency of the composite material was also effected negatively, due to the presence of unmelted starch granules that are several microns in size. The similar results were observed by using glycidyl methacrylate grafted polyethylene (PE-g-GMA) as a compatibilizer between ldpe and starch, as reported in the studies of Pedroso et. al. [22].

Many other compatibilizer systems with more hydrophilic structure, such as poly(ethylene- co-acrylic acid), poly(ethylene-co-vinyl alcohol), and oxidized PE, have been studied for PE-starch composites in the privous studies, but the products again exhibited unsatisfactory mechanical properties due to the limited opportunities of these compatibilizers to interact with polyethylene [3].

U.S. Pat. No.4,021,388 by G. J. L. Griffin disclosed a process for preparing biodegradable film improved by treating the surface of starch with silane coupling agent to be hydrophobic, but it only increased physical interacting strength a little between matrix resin and starch so that it had difficulty to solve the decrease of physical properties of films on incorporating starch [55].

The melt blending of TPS has also been studied with polyethylene and results indicated that addition of such plasticizers considerably improves mechanical properties when compared with native starch [11-16]. Even so, starch films had poorer mechanical properties than synthetic polymers and the tensile properties of these blends decreased significantly as TPS content increased. The elongation at break is the property most adversely affected by the presence of TPS particles and typically ductile polymers, such as polyethylene and polycaprolactone, became fragile with the addition of 20–30 wt% TPS which was attributed to the poor interaction between these polymers and TPS.

Many different compatibilizer systems have been studied so far for the blends containing polyolefin and GS or TPS. Otey et al. developed GS/EAA (ethylene– acrylic acid copolymer) cast films that demonstrated good transparency, flexibility and mechanical properties. Blends of GS with other polymers were prepared by first mixing starch, ethylene– acrylic acid copolymer (EAA) and other additives in a long initial process. However, the addition of LDPE led to the reduction of both tensile strength and elongation at break. Detailed studies on this polymeric system have shown that amylose and amylopectin parts of starch form complexes with EAA. The hydrophobic segment of EAA molecules is trapped in the hydrophobic core of the starch helix. In this case, it was also observed that EAA inhibits the rate of starch biodegradation [9]. These findings led to the proposal that compatibilizers other than EAA should be employed to improve interfacial adhesion with polyolefin and reduce the GS particle size, without promoting the formation of starch complexes. Complexes similar to EAA can also be formed with hydroxyl groups of the polyethylene–vinyl alcohol (EVOH) copolymer. As a result, materials with high amounts of starch can be produced. Also, the addition of EVOH can increase the processing ability and injection moldability of plasticized starch [56]. Poly(vinyl alcohol), however, is water soluble, thus limiting the use of such materials in aquatic environments.

Recently, increased interest has focused on the use of TPS together with polymers containing reactive groups (e.g., maleic anhydride, glycidyl methacrylate) as compatibilizers due to the better dispersion of starch in the polymer blend containing functional group[3,12,19-23].

Bikiaris et al. investigated the effect of maleic anhydride content in maleic anhydrede-g-polyethylene (MA-g-PE) used as a compatibilizer between LDPE and TPS [57]. They found that the compatibilization capacity of MA-g-PE with 0.8 mol% anhydride was better than that of MA-g-PE having 0.4mol% anhydride group, as observed in SEM pictures of blends (Figure 2.9). The same tensile strength as that of pure LDPE was achieved in 30 wt% TPS containing blend by using MA-g-PE with 0.8 mol% anhydride. Another important finding was that the presence of compatibilizer did not affect significantly the biodegradation rate of the material. However, the elongation at break values were found to be reduced drastically even at %20 TPS containing blends. This observation showed that it was not possible to produce blown films from such blends.

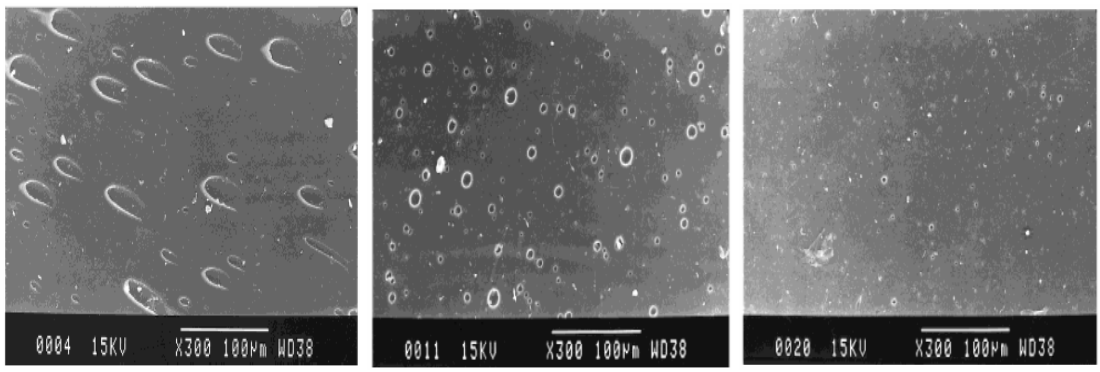

(a) **(b)** **(c)**

Figure 2.9 SEM micrographs of LLDPE/TPS blends: (a) uncompatibilized, (b) compatibilized with 0.4 mol% anhydride containing MA-g-PE, (c) compatibilized with 0.8 mol% anhydride containing MA-g-PE [57].

Wang et al. add maleic anhydride (MAH) monomer during the extrusion process of LLDPE and starch with plasticizer. The resulted blends had good interfacial adhesion and finely dispersed TPS and LLDPE phases. The average size of starch particles decreased from 15 µm in native corn starch to 10µm in LLDPE/TPS(50 wt%) blend and further decreased to 5 µm in blend having MAH as compatibilizer. The blends with MAH exhibited higher tensile strength, elongation at break, and thermal stability than those of the blends without the compatibilizer. However, the relative tensile strenght and the relative elongation at break were found to be reduced with the increase in TPS (50-90 wt%) and MAH (0.1-2 wt%) content. In all the blend contents, the tensile properties were inferior as compared to neat LLDPE [58].

The use of dibutyl maleate ester grafted polyethylene (DBM-g-LDPE) as a compatibilizer in LDPE/TPS blend was studied by Girija, et al. [59]. They observed the improvement in the relative impact strength (relative to LDPE) in compatibilized blends. For 20 and 30% loading, the tensile was found to be same as that of the unfilled LDPE. For higher loadings, 40 and 50%, it dropped to around 75% of that of neat LDPE. The tensile modulus values for 20–50% TPS loaded blends were the same as that of unfilled LDPE with 9–12% DBM-g-LDPE content. For 50% TPS loading, the relative elongation at break values were 53% of that of pure LDPE for the compatibilized blends. DSC studies revealed a loss of %crystallinity of LDPE as the TPS loading was increased. This behavior was attributed to the inhibition of close packing of the LDPE chains with TPS particles. For compatibilized blends, the crystallinity was still reduced compared to that of the uncompatibilized blends. The thermal stability of the blends was found to be decreased with increased TPS loading.

2.7 Polymer Nanocomposite Technology

Polymer nanocomposites consists of a polymeric material and reinforcing nanoscale materials (nanoparticles). The nanoparticle has at least one dimension on the nanometer scale. Nanoclays (layered silicates), carbon nanofibers, nanosilica, nanotitanium oxide, and carbon nanotubes are the most commonly used nanoparticles in the literature. Table 2.8 shows several benefits and disadvantages when nanoparticles are incorporated into the polymer matrix. In general, polymer nanocomposites exhibit remarkable improvements in mechanical properties, gas barrier properties, thermal stabilities, fire retardancy, abrasion resistant properties and structural stabilities. All of these benefits are achieved without increasing the density of the material. Dispersion difficulties and optical effects are the most common disadvantages in nanocomposite systems.

Table 2.8 Properties of nanoparticles in polymer matrix

Improved Properties	Disadvantages
• Mechanical properties(tensile strength, modulus) • Gas barrier • Synergistic flame retardant additive • Dimensional stability • Thermal stability • Chemical resistance	• Viscosity increase (limits processability) • Dispersion difficulties • Optical issues • Sedimentation • Black color when different carbon containing nanoparticles are used

Polymer nanocomposites were developed in the late 1980s by both commercial research organizations and academic laboratories. Toyota was the first company to commercialize these nanocomposites, and it used nanocomposite parts in one of its popular models for several years. Following Toyota's lead, a number of other companies also began investigating nanocomposites. Since 1980s, the patent and literature activity has also been astonishing. From 1992 to 2004, the number of citations for polymer nanocomposites has doubled every two years. Since 2001, polymer nanocomposites represent about 43% of the broader nanocomposite field, which includes metal, ceramic, and thin films. Nanocomposites having layered silicates and carbon nanotubes represent almost 50% of the ongoing investigation [60].

2.7.1 Polymer/Layered Silicate (PLS) Nanocomposites

2.7.1.1 Structure of layered silicates

Figure 2.10 illustrates the structure of the layered silicates commonly used in nanocomposites. Layered silicates are known as the 2:1 phyllosilicates. Montmorillonite, hectorite and saponite are the most commonly used layered silicates. Their chemial formula are shown in Table 2.9. They have a crystal lattice consisting of two-dimensional layers containing the two tetrahedral silicate layers and one octahedral alumina layer. The sheet of silicate tetrahedra consists of two layers of oxygen atoms and silicon in four-fold (tetrahedral) co-ordination. The alumina layer consists of two sheets of closely packed oxygen or hyroxyls, between which octahedrally coordinated

aluminum, magnesium or iron atoms are imbedded. The two tetrahedral layers sandwich the octahedral layer, sharing their apex oxygens with the latter. These three layers form one clay sheet with a thickness of around 1 nm. The lateral dimensions of these layers may vary from 300 Å to several microns and even larger depending on the particular silicate. These layers organize themselves to form stacks with a regular van der Walls gap in between them called the interlayer or the gallery. Many clay minerals present a partial substitution of tetrahedral Si^{+4} by Al^{+3}, or of octahedral Al^{+3} or Fe^{+3} by Fe^{+2} or Mg^{+2}. Such a substitution of tetravalent cations by trivalent ones, or of trivalent cations by bivalent ones, determines a deficit of postive charge and an excess of negative charge within the layers. The excess of layer negative charge can be counterbalanced by alkali or alkaline earth cations (like Na, K, Ca, Mg) situated in the interlayer. Sodium cation, for example, resides on the montmorillonite type clay. This type of layered silicate is characterized by a moderate surface charge known as the cation exchange capacity (CEC), and generally expressed as mequiv/100 g. Except under extremely acidic conditions, the layer charge is predominantly negative, which means that clays tend to sorb cations, and are said to have a certain CEC. This charge is not locally constant, but varies from layer to layer, and must be considered as an average value over the whole crystal. Montmorillonite contain excessive isomorphous substitution and usually have CEC values > 100 mequiv/100 g. [61].

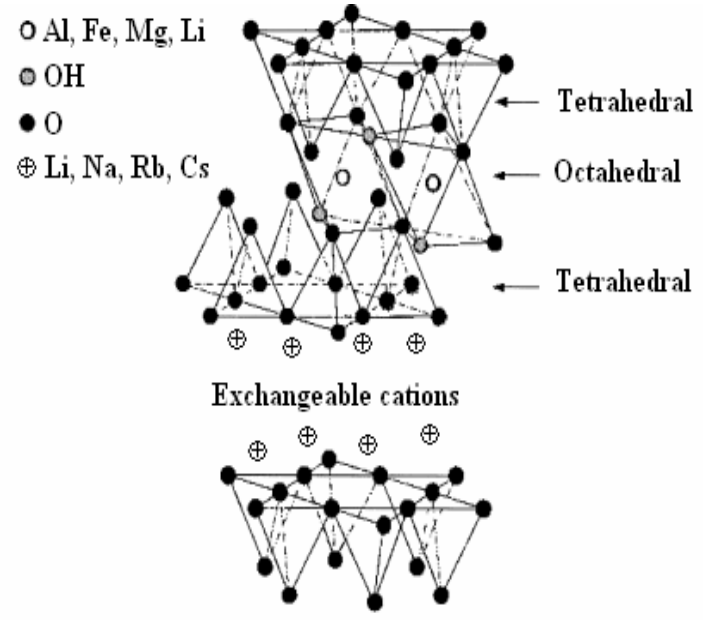

Figure 2.10 Structure of 2:1 phyllosilicates [61].

Table 2.9 Chemical formula and characteristic parameter of commonly used 2:1 phyllosilicates.

2:1 phyllosilicates	Chemical Formula	CEC (mequiv/100g)
Montmorillonite	$M_x(Al_{4-x}Mg_x)Si_8O_{20}(OH)_4$	110
Hectorite	$M_x(Mg_{6-x}Li_x)Si_8O_{20}(OH)_4$	120
Saponite	$M_xMg_6(Si_{8-x}Al_x)Si_8O_{20}(OH)_4$	86.6

* M, monovalent cation; x, degree of isomorphous substitution (between 0.5 and 1.3).

Layered silicates, in their pristine state, are extremely hydrophilic and therefore they are only miscible with hydrophilic polymers, such as poly(ethylene oxide) (PEO), poly(vinyl alcohol) (PVA), cellulose, etc. In order to make these layered silicates miscible with other polymer matrices such as nonpolar polyolefin systems and to render these hydrophilic phyllosilicates more organophilic, the hydrated cations of the interlayer should be exchanged with cationic surfactants such as quaternary alkylammonium or alkylphosphonium salts (quat), as shown in Figure 2.11. The modified clay (or organoclay) being organophilic, its surface energy is lowered and is more compatible with organic polymers. These polymers may be able to intercalate within the galleries, under well defined experimental conditions. Another function of the quat chemistry is to weaken the inherent Van Der Waals forces attacting adjacent sheets of layered silicate to facilitate delamination. Altough the increase of d-spacing between the clay layers is desirable, improving compatibility between the polymer and silicate surface is more important. Therefore, the compatibilizer system such as copolymer or grafted polymer is often used for the preparation of nanocomposite material from nonpolar matrix and layered silicate.

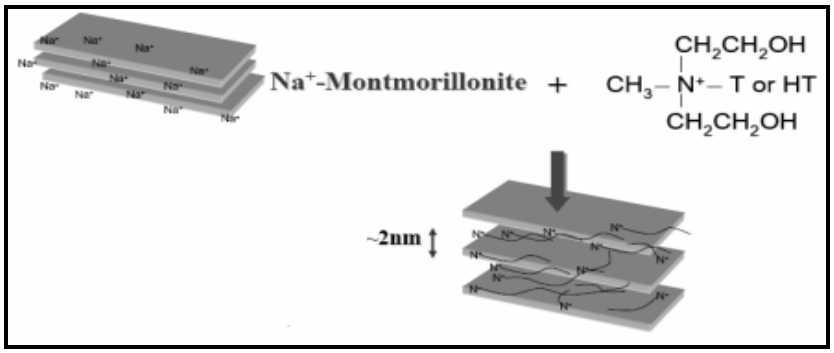

Figure 2.11 Modification of clay with alkyl ammonium cation, where T is Tallow (~65% C18, ~30% C16, ~5% C14).

2.7.1.2 Structure and Properties of PLS Nanocomposites

In recent years polymer/layered silicate (PLS) nanocomposites have attracted great interest, both in industry and in academia, because the starting clay minerals are easily available and they usually exhibit remarkable improvement in materials properties when compared with virgin polymer or conventional micro and macro-composites. These improvements include high moduli, increased strength and heat resistance, decreased gas permeability and flammability, and increased thermal stability. The main reason for these improvements in PLS nanocomposites arise from the processing challenges of layered silicates, such as the ability of transforming particles with several microns into > 1 million platelets as shown in Figure 2.12.

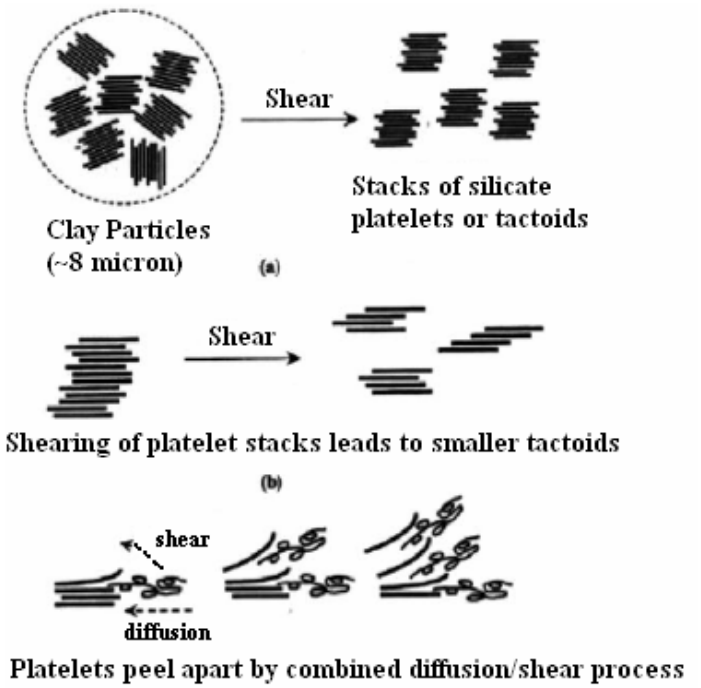

Figure 2.12 Processing challenge of layered silicates [61].

Layered silicates generally have layer thickness on the order of about 1 nm and very high aspect ratios (e.g. 10–1000) compared to many other conventional fillers. Therefore, when they are properly dispersed throughout the matrix, a few weight percent of layered silicates create a much higher surface area for polymer filler interactions than do conventional composites as schematically shown in Figure 2.13. For example, when the same volume fraction is considered, the microcomposite includes 1 filler particle whereas there are 10^9 nanoparticles in nanocomposite material.

In other words, less than 10% of the polmer is at the interface in microcomposites while it is more than 90% in nanocomposites.

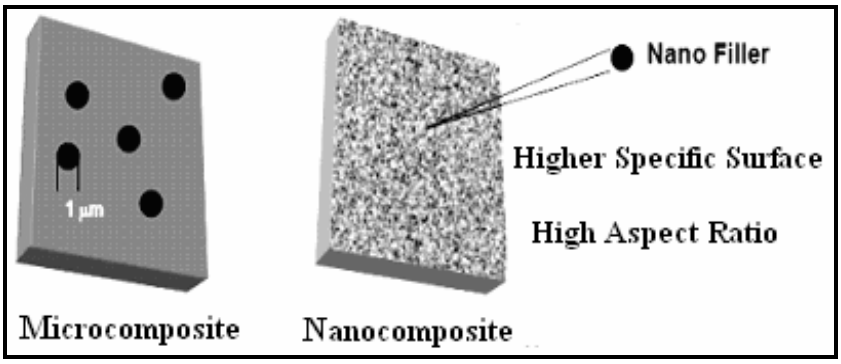

Figure 2.13 Schematic representation of microcomposite and nanocomposite interphases [62].

Depending on the strength of interfacial interactions between the polymer matrix and layered silicate (modified or not), the resulting nanocomposites can be classified morphologically into three categories: (a) Intercalated, (b) flocculated and (c) exfoliated (delaminated) states, as shown in Figure 2.14. In intercalated nanocomposites, one or more extended polymer chains interact with silicates and ordered multilayer nanocomposites are generated with alternative polymer and clay layers. Flocculated nanocomposite is conceptually same as intercalated nanocomposite. However, silicate layers are sometimes flocculated due to hydroxylated edge–edge interaction of the silicate layers. In an exfoliated nanocomposite, the individual clay layers are separated in a continuous polymer matrix by an average distance that depends on clay loading. Usually, the clay content of an exfoliated nanocomposite is much lower than that of an intercalated nanocomposite.

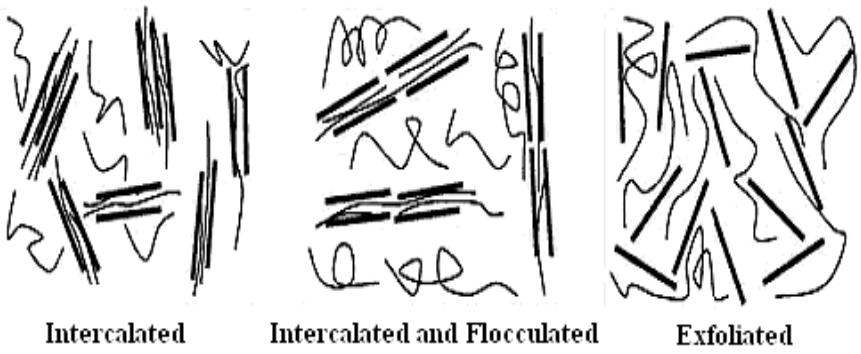

Figure 2.14 Schematically illustration of three different types of polymer/layered silicate nanocomposites [61].

The most commonly used techniques that are used to characterize those nanocomposite structures are X-ray diffraction (XRD) and transmission electron microscopy (TEM). By monitoring the position, shape, and intensity of the basal reflections for the distributed silicate layers from XRD diffractogram, the nanocomposite structure (intercalated or exfoliated) may be identified. In intercalated nanocomposite, the repetitive multilayer structure is preserved, allowing the interlayer spacing to be determined. The intercalation of the polymer chains increases the interlayer spacing, leading to a shift of the diffraction peak towards lower angle. As far as exfoliated structure is concerned, no more diffraction peaks are visible in the XRD diffractograms either because of a much too large spacing between the layers (i.e. exceeding 8 nm in the case of ordered exfoliated structure) or because the nanocomposite does not present ordering anymore. In the latter case, transmission electronic microscopy (TEM) is used as a complementary method to characterize the nanocomposite morphology. However, special care must be exercised to guarantee a representative cross-section of the sample for TEM analysis. The XRD patterns and corresponding TEM images of different types of nanocomposites are presented in Figure 2.15.

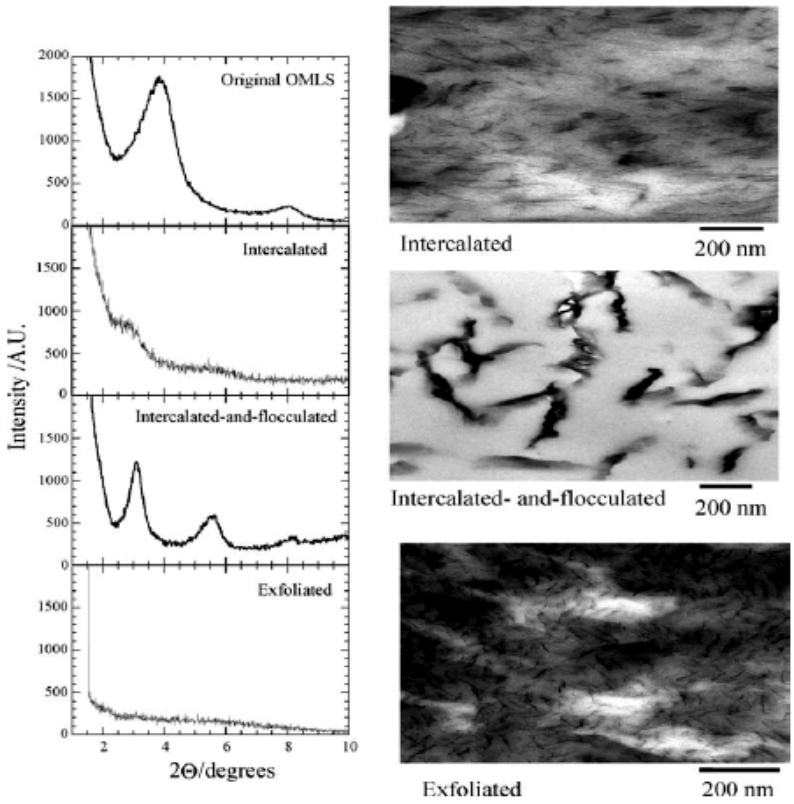

Figure 2.15 XRD patterns and TEM images of three different types of polymer/layered silicate nanocomposites [61].

2.7.1.3 Preparative Methods for PLS Nanocomposites

The preparative methods for PLS nanocomposites are divided into three main categories according to the starting materials and processing techniques:

a) In situ intercalative polymerization method

In this method, the layered silicate is first swollen with the liquid monomer or monomer/prepolymer solution. The polymer is than formed between the intercalated layers. Polymerization can be initiated either by heat or radiation, by the diffusion of a suitable initiator, or by an organic initiator or catalyst fixed through cation exchange inside the interlayer before the swelling step [63].

Although many of the researches related to the interlamellar polymerization reactions were started in the 1960s and the 1970s [64,65], the studies were initiated by the research of Toyota research team [66,67]. They studied the ring opening polymerization of ε-caprolactom monomer in which Na-montmorillonite organically modified by protonated a,o-aminoacid was swollen as shown schematically in Figure 2.16. They obtained nylon-6-based nanocomposites with different degree of delamination depending on the amount of organoclay used. They also indicated that the introduction of very small amounts of layered silicate led to the significant improvements in thermal and mechanical properties.

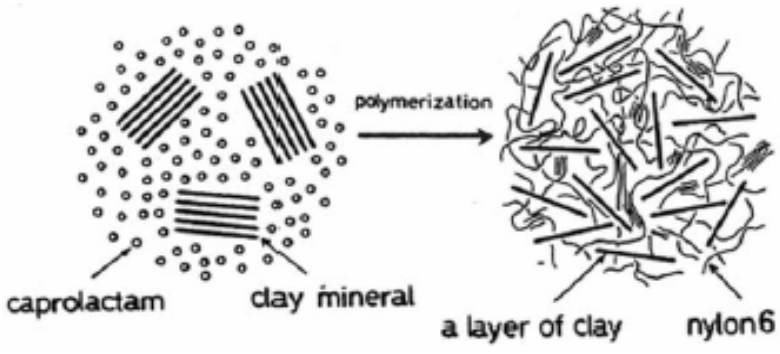

Figure 2.16 Schematic illustration for synthesis of Nylon-6/clay nanocomposite [67].

Chen et al. used this technique for the preparation of novel segmented polyurethane/clay nanocomposites. They reported that the nanoclay acted as a

multifunctional chain extender, inducing the formation of a star-shaped segmented polyurethane [68]. Wang and Pinnavaia reported the preparation of polyurethane–MMT nanocomposites using a direct in situ intercalative polymerization technique and they observed the formation of intercalated nanocomposite structure [69].

In situ intercalative polymerization has also been studied for producing poly(styrene) nanocomposites. Akelah and Moet modified Na-montmorillonite and Ca-montmorillonite with (vinylbenzyl)trimethyl ammonium chloride and increased the interlayer separation by 5.4 Å . These modified clays were then dispersed and swollen in various solvent and cosolvent mixtures such as acetonitrile, acetonitrile/toluene and acetonitrile/THF. Styrene polymerizations were carried out in presence of N,N'-azobis(isobutyronitrile) (AIBN). The intercalated morphology were obtained with interlayer spacings varying between 17.2 and 24.5 Å depending on the nature of he solvent used [70].

Doh and Cho studied several organonic modifier for Na-mmt and compared their ability to promote the intercalation of poly(styrene) through the free radical polymerization of styrene initiated by AIBN. Three tetraalkylammonium cations were tested, all based on the following formula: $(CH_3)2N$.(hydrogenated tallow alkyl)R where R may be either another hydrogenated tallow alkyl (Ta), 2- ethyl hexyl (Eh) or benzyl (Bz) group. They found that the best intercalation occurred for Bz-MMT. This behavior was attributed to a better affinity between styrene and benzyl groups. Even though this technique allows an extensive intercalation of PS chains through an adequate choice of the alkylammonium cation neither exfoliation nor control over the molecular parameter of the polymer (PS) produced have been observed [71].

Inceoglu et al. [72] used a new approach to prepare PS-based nanocomposite. They modified Na-mmt with ditallow dimethyl ammonium chloride and water soluble initiator which is 2,2'-Azobis(2-amidinopropane) dihydrochlorid in an aqueous medium. XRD results showed that the distance between the silicate layers increased from 12.1 Å to 14.2 Å and 18.9 Å with the presence of surfactant and initiator. The organophilic clay was then swollen in styrene monomer and PS-clay masterbatch with 27% filler were prepared by free radical bulk polymerization of styrene. The interlayer separation was 25 Å after polymerization reaction confirming that the polymerization had occurred

between the clay layers. SEM image also confirmed the homogeneous dispersion of nanofiller even at this high level of loading (Figure 2.17a). PS-organoclay masterbatch was then melt blended with with styrene-b-(ethylene- co-butene)-b-styrene (SEBS) copolymer-PP(40/60 wt/wt) blend in a Brabender mixer. SEBS acted as a compatibilizer between PS domains and PP matrix as it was clearly observed from the homogeneous dispersion of small PS droplets and the absence of distinct interphases in SEM images (Figure 2.17b) and also it provided rubbery properties to the final product. SEM images (Figure 2.17c) also showed that the morphology of the product was changed from PS droplets in PP continuous matrix to two co-continuous phase by increasing PS amount from 20% by wt. to 27% by wt. It was also reported that the tensile strength, modulus and tear strength properties of SEBS-PP blend were improved with the addition of PS-organoclay nanocomposite.

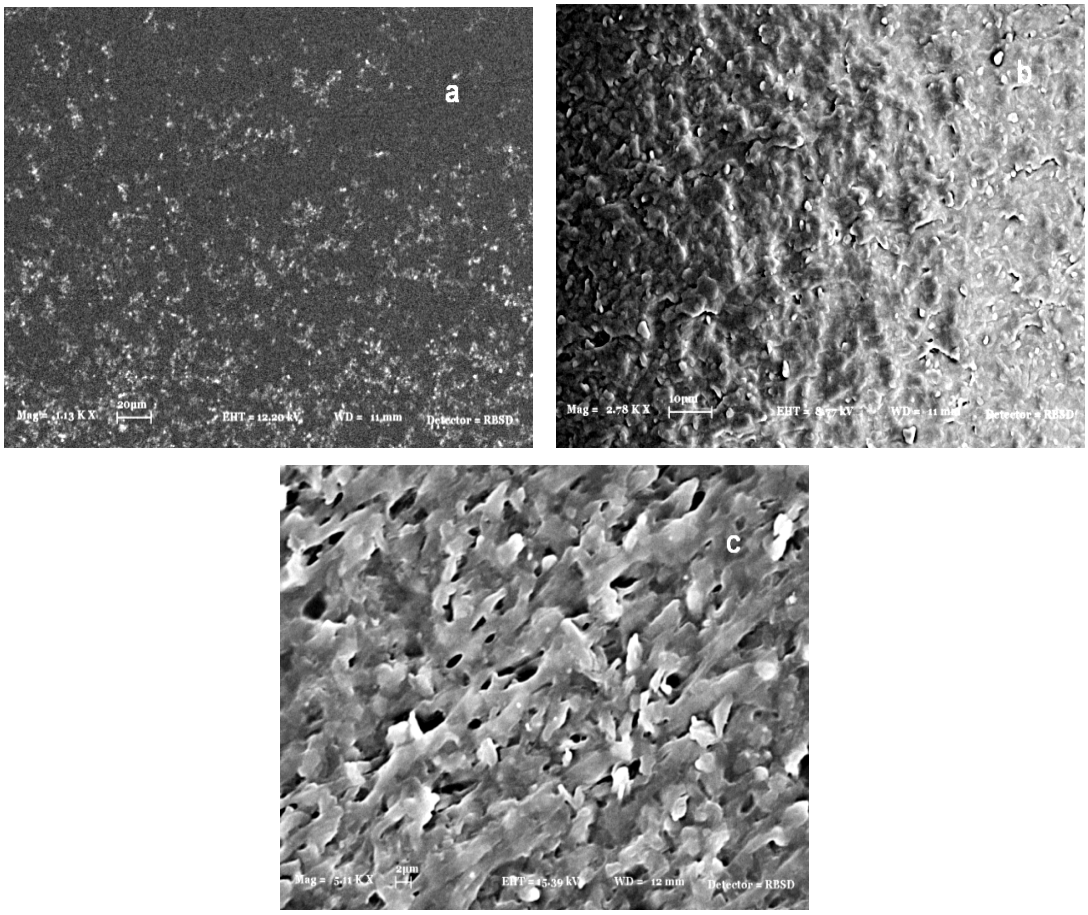

Figure 2.17 SEM images of (a) PS-organoclay masterbatch, (b) SEBS-PP/PS20%-organoclay3% (c) SEBS-PP/PS27%-organoclay3% films.

In order to obtain nanocomposite of polyethylene, Rong et al. studied in-situ coordination polymerization techniqe. They first support the Ziegler-Natta catalyst on

the surface of nanowhiskers by the possible coordination reation of $TiCl_4$ with the magnesium vacancies present in the surface of palygorskite (a kind of natural fibrous silicate) and then initiate the polymerization of ethylene using this nanowhisker system. As the polymerization proceeed, the surface of the nanowhiskers was covered with polyethylene and became a reinforcement material after polymerization. The uniformity of the dispersion was releaved by SEM and TEM microphotographs. The tensile test results showed that the tensile modulus incresed, and the elongation at break decreaed with the clay content. However, there was no well-defined behavior tensile strength and this observation was assigned to the formation of network like "chain brush" or "macromolecular comb" structures in which great number of polymer chains rooted on one whisker. The idea was confirmed by the measurement of gel content that is greatly affected by the clay content. Consequently, the orientation of polymer segments before breaking is inhibiting by inorganic filler and break can occur at any extent of orientation. It was suggested that in this situation the yield strength is better defined, since yield occurs when the lamellae strat to slide, which is not impeded by the silicate. [73].

Heinemann et al. investigated the intercalative polymerization to produce (co)polyolefin nanocomposites [74]. They carried out the polymerizations in the presence of modified layered silicates having dimethyldistearylammonium or dimethylbenzylstearylammonium cations in between the layers. For the purpose of comparison, unmodified clays such as synthetic hectorite and fluoromica were also studied. Different catalysts were used, affording HDPE and ethylene-octene copolymers (zirconium-based catalyst), and branched polyethylene (nickel and palladium-based catalysts). It was found that the modified bentonites had a negative effect on the polymerization activity of the zirconium-based catalyst, while Ni- and Pd-based catalysts were much less affected by the nature of the clay. This effect was attributed to the high sensitivity of the Zr-based active species towards any kind of polar functionality, including the anionic silicate layers covered by the alkylammonium cations. Nanocomposites were observed to be formed when polymerization was carried out by using organomodified clays. At the opposite, composites prepared either by in situ polymerization with nonmodified silicates or by melt-blending a preformed HDPE with a modified bentonite, only gave microcomposite structure as demonstrated by TEM and XRD. The presence of n-alkyl branches along the polyethylene chains (as a

result of 1-octene copolymerization or migratory insertion ethylene polymerization promoted by Ni and Pd-based catalysts) was reported to enhance compatibility between the (co)polyolefin matrix and the dispersed layered silicates, improving the mechanical properties of the resulting nanocomposite materials.

The synthesis of poly(ethylene terephtalate) (PET) nanocomposites by using the in situ intercalative polymerization was discussed by Ke et al. [75]. The organophilic montmorillonite was reacted with PET comonomers (ethylene glycol and terephtalic acid derivatives) to form an intercalated nanocomposite with an interlayer distance increased from 14 to 35 Å depending on the clay content.

Epoxy, acrylate and unsaturated polyester based thermoset nanocomposite structures via in-situ polymerization technique were also extensively studied after realising the outstanding effects of silicates as a reinforcing nano-filler in thermoplastic systems. Nigam et al., for example, synthesized the nanocomposites of epoxy resin with montmorillonite and montmorillonite modified with octadecylamine by swelling of clay in a diglycidyl ether of bisphenol-A followed by in situ polymerization with aromatic diamine as a curing agent. The organoclay was found to be intercalated easily by incorporation of the epoxy precursor and the clay galleries were simultaneously expanded. However, Na-montmorillonite clay could not be intercalated during the mixing or through the curing process. In the kinetic studies, it was found that the cure rate of the epoxy resin was increased by the addition of organoclay. A rise in the clay concentration from 0 to 6% leads to 100% increase in the tensile modulus, 20% increase in ultimate tensile strength, and 80% decrease in elongation at break values. It was also reported that beyond a 6 wt % loading of the organoclay, the elongation at break value is lowered substantially due to the improper filler dispersion by the formation of clay agglomerates so that a further increase of filler concentration was considered unnecessary [76].

Inceoglu et al. combined the advantegeous of UV-curing and nanocomposite technologies in their study to prepare acrylate-based nanocomposite film [77,78]. The clay was modified with dimethyl dihydrogenated-tallow quaternary ammonium salt and made organophilic. The extent of opening of clay galleries after modification was upto 3.3 nm. The organoclay with different amount (2-10 phr) was then allowed to swell and

homogenously dispersed in the presence of arylate monomer and urethane-acrylate oligomer with the aid of ultrasonic bath. After adding the photoinitiator, the liquid reactants are polymerized under UV-light. XRD measurement illustrated that in most of the samples the clay galleries were opened up to 4.0 nm after the polymerization reaction, indicating the highly intercalated morphology. At 3 phr organoclay addition, the presence of both intercalated and exfoliated morphologies was reported. The effect of nanoclay on the progress of polymerization was investigated through gel-content measurement. The rate of polymer conversion was found to be increased rapidly with the time of UV exposition for clay-free resin and reached a plateau at 94% conversion at 60. A much faster polymerization rate was observed in nanocomposite films, reaching the same level of conversion at much shorter time of UV-irradiation as shown in Figure 2.18. This behavior was assigned to two different mechanisms. First of all, strong interaction between polymer matrix and silicate layers might have occurred through the formation of hydrogen bonds which could act as a physical crosslink. Secondly, clay layers might have reduced the rate of termination by inhibiting the mobility of polymer chains, resulting in increased rate of polymerization [79].

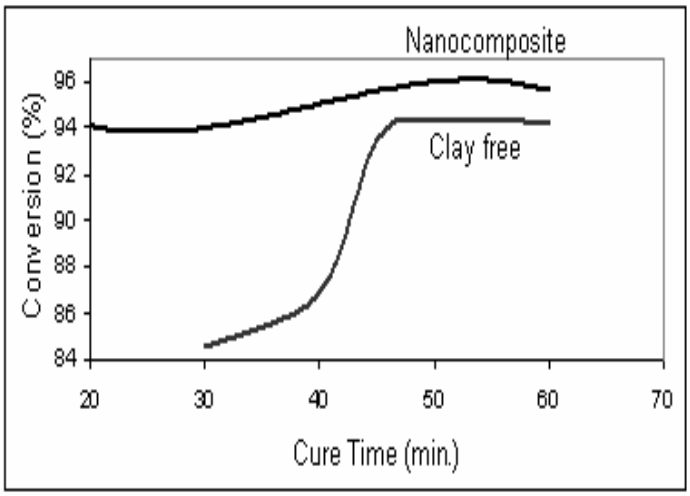

Figure 2.18 Change of % polymer conversion with UV-radiation exposure time for clay-free and nanocomposite resin with 3 phr organoclay.

All the nanocomposite samples exhibited enhanced tensile strength, young's modulus and strain properties compared to neat resin and the peak in all the properties was attained at 3 phr organoclay loading. This observation was related to the layered dispersion and the optimum amount of reinforcing filler in that sample. The increase in % elongation properties with organoclay was explained by the plasticizing effect of

long alkyl chains in quaternary ammonium salt and this suggestion was found to be in consistent with the glass transition temperatures (T_g) of the film, determined from DSC analysis. The lowest T_g value was belong to the nanocomposite film with 3 phr organoclay because of the presence of dangling chains with higher degree of freedom that would contribute to better flexibility. The layered dispersion of organoclay in nanocomposite samples was also evident from AFM and SEM images (Figure 2.19).

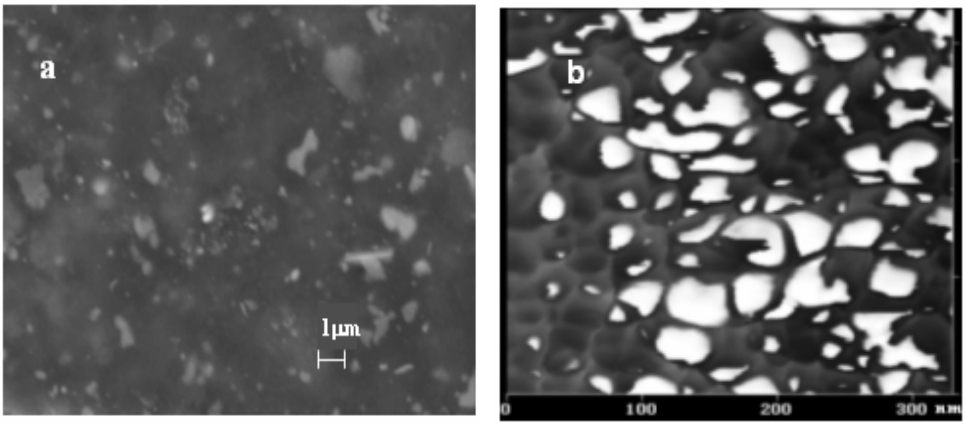

Figure 2.19 SEM images of urethane-acrylate films with 5 phr (a), AFM image of nanocomposite film with 3 phr organoclay (b).

b) Intercalation of polymer from solution

This is based on a solvent system in which the polymer or pre-polymer is soluble and the silicate layers are swellable. The layered silicate is first swollen in a solvent, such as water, chloroform, or toluene. When the polymer and layered silicate solutions are mixed, the polymer chains absorb onto the delaminated sheets and displace the solvent within the interlayer of the silicate. Upon solvent removal, the intercalated structure remains, resulting in PLS nanocomposite.

This technique has been widely used for water-soluble polymers to produce intercalated nanocomposites based on poly(vinyl alcohol) (PVOH), chitosan, poly(ethylene oxide) (PEO), poly(vinylpyrrolidone) (PVPyr) or poly(acrylic acid) (PAA) [80-82]. Layered silicates have also been used with starch in order to increase the mechanical properties of this polymer and find a way to use it more efficiently in plastic industry as it exists abundantly and may form a cost-effective plastic.

Pandey et al. investigated the effect of the mixing methods on the nature of the resulting product, whether it will be a nano-level or micro-level distribution, in starch clay nanocomposites prepared by the solution method [83]. It was shown that the interplanar distance of clay strongly depends on the sequence of mixing. Better dispersion was achieved by first mixing of starch and filler followed by plasticization. Other ways of mixing and the resultant product structures are given in Figure 2.20.

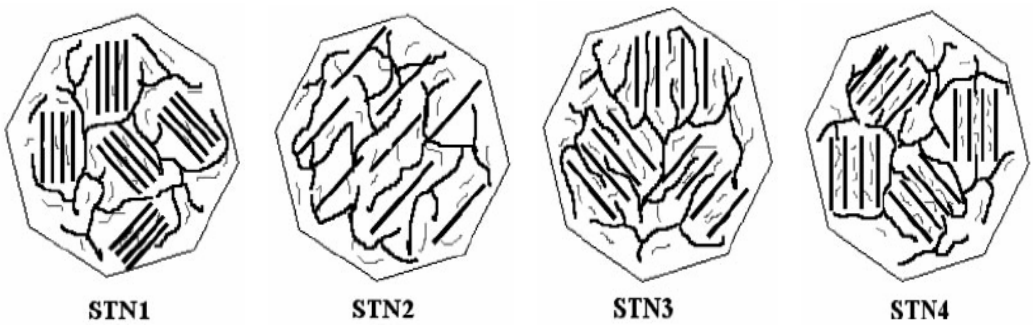

Figure 2.20 Different structure of starch-clay composites: composite formed by the mixing of filler into plasticized starch (STN1), composite structure formed by the mixing of filler into starch followed by plasticization (STN2), composite structure formed by the together mixing of all components (clay / starch / plasticizer) (STN3) and composite structure formed when starch was mixed into slurry of plasticizer and clay (STN4). The thick bold rods indicate the silicate layers, whereas long and short chains denote starch and plasticizer, respectively [83].

Although an enhancement of mechanical properties have been observed in the clay-filled composites, still the water resistance was too poor to use these composites in packaging applications. From a moisture sensitivity point of view, well-ordered intercalated structure reduced the moisture sensitivity. Diffusion of plasticizer inside the clay was found to be easier than diffusion of starch due to the smaller size of the former. It was pointed out that starch chains must penetrate through clay galleries first, followed by plasticization in order to maintain the plasticization efficiency. The composites obtained were very far from becoming substitutes for traditional commodity plastics like polyethylene and polypropylene, mainly because of their extreme moisture sensitivity. The nanocomposites with higher moisture resistance was reported to be prepared by the same group by modification of starch and plasticizers, i.e. starch esters and ethers.

Wilhelm et al. modified glycerol-plasticized starch films by the addition of various layered compounds as filler, two being of natural origin (kaolinite, a natural mineral

clay and hectorite, a cationic exchange mineral clay) and two synthetic (layered double hydroxide, LDH, an anionic exchanger, and brucite having a neutral structure) [84]. Glycerol-plasticized starch/layered compounds composite films were prepared from the aqueous suspensions by casting. XRD patterns demonstrated that the inter-planar basal distance of kaolinite, LDH-CO_3 and brucite was not affected by the presence of a starch matrix while the hectorite showed an increase in interlayer spacing. In this composite, the hectorite dispersion was governed by the glycerol plasticizer. In unplasticized composite films, hectorite was exfoliated. Substitution of plasticized starch matrix by a plasticized oxidized starch or native/oxidized starch blend gave rise to composite with higher interlayer basal distances, indicating that both short oxidized starch chains and glycerol molecules were intercalated between clay layers. In the absence of glycerol, oxidized starch was preferentially intercalated in relation to native starch chains that was explained by its lower chain size and probable higher diffusion rate.

Polymer nanocomposites using this technique can also be performed in organic solvents. Manias, et al. prepared PP-nanocomposite by applying ultrasonic wave to trichlorobenzene solution of PP and organomontmorillonite (o-mmt) [85]. The solvent was then evaporated untill a very viscous gel was obtained. The gel was then placed in a vacuum oven to remove the solvent completely. The resultant nanocomposite material exhibited enhanced mechanical, thermal and solvent resistant properties. High density polyethylene (HDPE)-based nanocomposite has been produced by using a similar technique by Jeon and coworkers [86]. The polyolefinic chains were dissolved in a mix of xylene and benzonitrile with 20 wt.% modified clay dispersed within. The composite material was then recovered by precipitation from tetrahydrofuran (THF). The interlayer spacing of clay increased to 17.7 Å by intercalation of polymer chains. TEM observation showed small stacks of flake-like particles.

c) Melt intercalation method

This method involves annealing, statically or under shear, a mixture of the polymer and layered silicate above the softening point of the polymer. This method has great advantages over either in situ intercalative polymerization or polymer solution intercalation. First, this method is environmentally benign due to the absence of organic solvents. Second, it is compatible with current industrial process, such as extrusion and

injection molding. The melt intercalation method also allows the use of polymers which were previously not suitable for in situ polymerization or solution intercalation.

The thermodynamics that drives the intercalation of a polymer inside a modified layered silicate while the polymer is in the molten state has been approached through a lattice-based mean field theory by Vaia et al. [87,88]. They found that, in general, the outcome of polymer intercalation is determined by an interplay of entropic and enthalpic factors. In fact, although the confinement of the polymer chains inside the silicate galleries results in a decrease in the overall entropy of the macromolecular chains, this entropic penalty may be compensated by the increase in conformational freedom of the alkyl surfactant chains as the inorganic layers separate, due to the less confined environment. Since small increases in the gallery spacing do not influence strongly the total entropy change, intercalation will rather be driven by the changes in total enthalpy. In this study, the enthalpy of mixing has been classified in two components: apolar interactions generally unfavorable and arising from interaction between polymer and surfactant aliphatic (apolar) chains, and polar interactions which originate from the Lewis acid/Lewis base character of the layered polar silicates interacting with the polymer chains. Indeed, since in most conventional organo-modified silicates, the surfactant chains are apolar, dispersion forces dominate polymer-surfactant interactions. On the other hand, a favorable energy decrease is associated with the establishment of many favorable polymer surface polar interactions. The enthalpy of mixing can thus be rendered favorable by maximizing the magnitude and number of favorable polymer-surface interactions while minimizing the magnitude and number of unfavorable apolar interactions between the polymer and the aliphatic chains introduced along the modified layer surfaces. Polymers containing polar groups, for example, intercalate between the silicate layers more easily because they are capable of interact with the layered silicate through Lewis-acid/base interactions or hydrogen bonding. The greater the polarizability or hydrophilicity of the polymer, the shorter the functional groups in the layered silicate should be in order to minimize unfavorable interactions between the aliphatic chains and the polymer.

PS was the first polymer used for the preparation of nanocomposites using the melt intercalation technique with alkylammonium cation modified MMT [89]. PS was first mixed with organically modified layered silicate and the mixture was pressed into a

pellet, and then heated under vacuum at 165 ^{o}C. This temperature is well above the bulk glass transition temperature of PS, ensuring the presence of a polymer melt. It was shown by wide angle x-ray diffraction pattern (WAXD) that during heating the OMLS peaks (at around 1.3 and 2.6 nm) were progressively disappeared while a new set of peaks (at around 1.6 nm and 3.2 nm) corresponding to the PS/OMLS appeared. The same authors also carried out the same experiment under the same experimental conditions using unmodified Na-MMT, but WAXD patterns did not show any intercalation of PS into the silicate galleries, emphasizing the importance of polymer/ OMLS interactions. They also attempted to intercalate a solution of PS in toluene with the same OMLS used for melt intercalation, but this resulted in intercalation of the solvent instead of PS. Therefore, direct melt intercalation enhances the specificity for the intercalation of polymer by eliminating the competing host–solvent and polymer–solvent interactions.

Even though, nylon-6 based nanocomposites preparation using the in situ intercalative polymerization technique has been widely studied, less attempt has been observed in the literature to the preparation of nylon-6-based nanocomposites by melt blending. Liu et al. have prepared nanocomposites by melt blending nylon-6 with an octadecylammonium-exchanged montmorillonite in a twin screw extruder [90]. They prepared composites with a filler content ranging from 1 to 18 wt.%. An intercalated structure was observed to be formed by XRD for composites having more than 10 wt.% of the organoclay, with an interlayer spacing increasing from 15.5 Å for the pristine organoclay to 36.8 Å for the intercalated species. At filler content lower than 10 wt.%, no interlayer spacing could be detected through XRD. TEM micrographs showed the formation of an exfoliated structure at filler content lower than 10 wt.%, indicating that exfoliation is highly dependent upon the filler content. XRD and DSC data also showed that exfoliated structures strongly influenced the nature of the nylon-6 crystallization, favoring the formation of γ-crystals in addition to the crystals of the α-form observed in the native nylon-6 matrix. Moreover, DSC cooling scans showed that exfoliated layered silicates highly increased the crystallization rate, having a strong heterophase nucleation effect.

In order to produce nanocomposite structures with nonpolar polyolefin like polypropylene or polyethylene by melt intercalation method, initial attempts were based

on the introduction of a modified oligomer to overcome the polarity difference between the silicate and polymer. One of the typical example to this approach is the study of Toyota research group on the production of PP/silicate nanocomposite. They used polypropylene oligomer modified with about 10 wt % of maleic anhydride (MA) as a compatibilizer and silicate modified with stearylammonium cation. They obtained exfoliated or semiexfoliated silicate morpholgy. In the nanocomposite system with three components, the miscibility between maleated oligomer and matrix polymer played a key role in the composite properties [91].

Cho, et al. investigated the effect of melt-mixing type on organoclay dispersion and nanocomposite properties [92]. They used both single screw with four different mixing sections including standard flight section, dispersive mixing section (union carbide mixind section), a distributive mixing section and a newly developed dispersionary mixing section and twin screw extruder including three kneading disc blocks. The clay filled PP products were prepared with two different processes; one include the preparation of masterbatch with 50 wt.% organoclay (octadecylamine modified montmorillonite) and 25 wt% compatibilizer (polypropylene-graft-maleic anhydride) and then dilution of masterbatch with PP/compatibilizer mixture and the second one includes the compounding of all the components with the final formula of PP/5% PP-g-MA/6% organoclay. The results showed that very intensive dispersionary mixing is required to make sure that organoclay particles are uniformly and thoroughly dispersed and distributed throughout the molten polymer. In general, nanocomposite prepared by two-step process exhibited enhanced properties than the nanocomposite obtained by direct compounding method. Even though masterbatch prepared by two step process in twin screw extruder provided nearly complete dispersion and superior mechanical properties, a masterbatch prepared with a specially designed single screw extruder showed a reasonably good dispersion and comparable mechanical properties as a master batch prepared with a twin screw extruder. Optical photomicrographs of PP nanocomposites obtained with different mixing types are given in Figure 2.21.

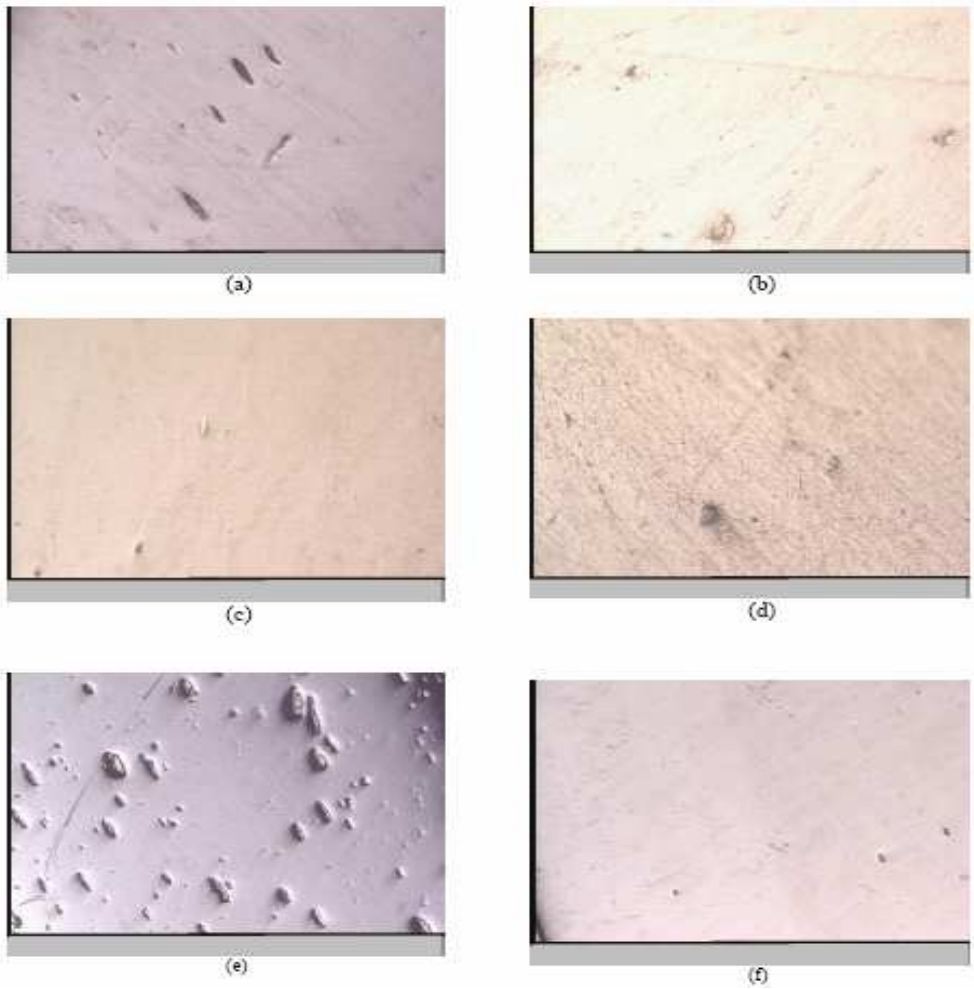

Figure 2.21 Optical photomicrographs (Magnification=200X) of PP nanocomposites obtained by using single screw extruder with (a) Flighted End (b) Distributive Mixer (c) Dispersionary Mixer (d) Union Carbide Mixer sections and PP nanocomposites prepared using (e) Direct Compounding (f) Masterbatch processes with a twin screw [92].

2.7.1.4 Degradability of PLS Nanocomposites

The effect of layered silicates on mechanical, thermal, gas barrier and flame retardant properties of polymeric matrix have been extensively studied by many researchers and it became certain that there are significant improvements on these properties after the formation of nanocomposites. On the other hand, the effect of layered silicates on the degradation mechanisms of polymers was not extensively studied and it is still not clear.

There are some works in the literature concerning the photo-oxidative degradation of PLS nanocomposites. The photo-aging behaviors of polyethylene/ montmorillonite (PE/MMT) and polyamide 6/montmorillonite (PA6/MMT) nanocomposites, for example, have been investigated by Qin et al. [93,94]. The rate of photo-oxidative degradation of PE/MMT nanocomposite was found to be much faster than that of pure PE. The acceleration of photo-oxidation of PE/MMT nanocomposite was explained by the nature of MMT and interlayer ammonium ions. It is known that the thermal decomposition of alkyl ammonium salts in the clay interlayer is known to take place following the Hoffman mechanism. The resultant is ammonia, corresponding olefin and an acidic site on layered silicate as shown equation below.

$$LS^{-+}[NH_3\text{-}CH_2\text{-}(CH_2)_n\text{-}CH_3] \xrightarrow{\Delta} LS^{-}H^{+} + NH_3 + CH_2{=}CH\text{-}(CH_2)_{n-1}\text{-}CH_3$$

It was assumed that during the melt processing and UV exposure period, the decomposition of the ammonium ions in the galleries might have been happened partially. The decay products, such as the acidic sites and corresponding olefin, could lead to the formation of free radical and accelerate the photo-oxidative degradation of polymer matrix upon UV irradiation.

Tidjani et al. reported that the photo-oxidative degradation of polypropylene/montmorillonite (PP/MMT) nanocomposites was faster than that of pure polypropylene. They suspected that the acceleration was caused by clay or the structure form of the nanocomposites [95].

In the recent study of Qin et al., PP/MMT nanocomposite was prepared using the compatibilizer PP-g-MA through melt processing and the influence of pristine MMT, alkylammonium and compatibilizer on photo-oxidative degradation mechanism of PP were investigated, respectively [96]. The rate of photo-oxidative degradation of PP/MMT nanocomposite was found to be much faster than that of pure PP. It was shown that acceleration of photo-oxidative degradation of PP clay nanocomposite is due to the influence of compatibilizer, pristine MMT and interlayer ammonium ions, in which the influence of compatibilizer and pristine MMT is primary. The compatibilizer, PP-g-MA, can introduce some photoresponsive groups (such as carboxylic acid and anhydride carbonyl groups) to PP matrix. The complex crystallographic structure and

habit of clay minerals could also result in some catalytic active sites, such as Bronsted acidic sites like the weakly acidic SiOH and strongly acidic bridging hydroxyl groups at the layer edge of the silicate, un-exchangeable transition metal ions in the galleries, and crystallographic defect sites within the layers. Moreover, the decomposition of ammonium ions could lead to catalytic acidic sites created on the layers and correspondingly olefin generated. Consequently, these photoresponsive groups and catalytic active sites might accept single electrons from donor molecules of PP matrix with low ionization potential. Under UV exposure, free radicals formed in the polymer matrix and the materials suffered photo-oxidative degradation. All these proposed mechanisms of the photo-oxidative degradation of PP-clay nanocomposite was schematically shown by the authers as given in Figure 2.22.

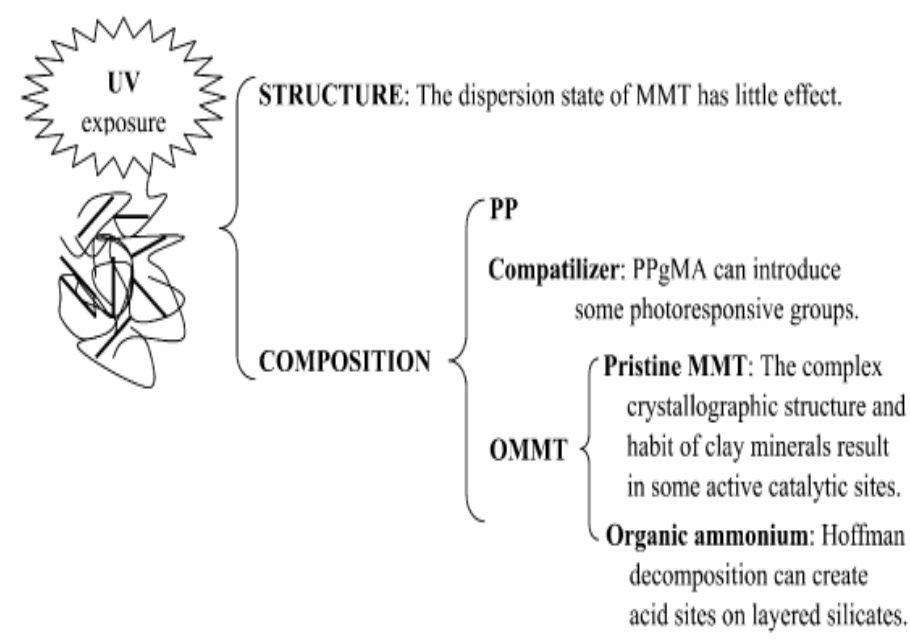

Figure 2.22 Schematic representation of catalysis mechanism of photo-oxidative degradation of PP clay nanocomposite [96].

The effect of layered silicate on biodegradation of biodegradable polymers was also investigated by some researchers. Tetto et al. first reported results on the biodegradability of nanocomposites based on PCL, reporting that the PCL/OMLS nanocomposites showed improved biodegradability compared to pure PCL [97]. The improved biodegradability of PCL was attributed to a catalytic role of the OMLS in the biodegradation mechanism, but this was not clear. Lee et al. reported the biodegradation of aliphatic polyester-based nanocomposites under compost [98]. In

biodegradation test, they observed that biodegradation was retarded by the addition of OMLS and the effect of this behavior increased with increasing clay content. This observation was attributed to the improvement of the barrier properties of the aliphatic polyester after nanocomposite preparation with clay. However, they did not provide any permeability data.

The biodegradability of neat PLA and the corresponding nanocomposites prepared with octadecyltrimethylammonium-modified MMT was investigated in a compost medium at 58^{o}C by Sinha Ray et al. [99]. The decrease in M_w and residual weight percentage of the initial test samples were reported as the indication of extent of biodegradation. It was found that the biodegradability of neat PLA was significantly enhanced after the additon of OMLS. Within one month, both the extent of M_w and the extent of weight loss were similar for both neat PLA and PLA with OMLS. However, after one month, a drastic increase in the weight loss of PLA/OMLS was observed. It was assumed that the presence of terminal hydroxylated edge groups in the silicate layers could be one of the factors responsible for this behavior by initiating the heterogeneous hydrolysis of the PLA matrix after absorbing water from the compost. This type of hydrolysis caused the matrix to decompose into very small fragments and eventually it disappeared with the compost. Because this process would take some time to start, the weight loss and degree of hydrolysis for PLA and PLA/OMLS were similar at the beginning of the test. This assumption was confirmed by conducting the same experimental procedure with PLA and OMLS prepared with dimethyl dioctdecyl ammonium salt modified synthetic mica, which has no terminal hydroxylated edge group. The same degradation tendency was reported with PLA.

CHAPTER 3

3. EXPERIMENTAL

3.1 Choice of the Raw Materials and Processing Method

■ **Choice of the starch type:** The particle size of the disperse phase determines many of the properties of the final product, such as mechanical, optical and barrier properties.Generally, the smaller the disperse phase the better the final properties due to obtaining more homogeneous dispersion in the main matrix. Among different sources of starch like corn, rice, wheat and potato, corn starch has the smallest particle size and therefore it was prefered to be used as a biopolymer component in the present study [100].

■ **Choice of the filler:** Due to being environmentally friendly, cost-effective and providing good interaction with hydrophilic starch by its polar structure, natural montromorilonite was considered to be a suitable filler. It is also known to provide good performance with thermoplastic starch [17].

For the sake of comparison, two types of organoclay, namely Nanofil and Viscobent that are compatible with the main matrix were chosen. Both filler includes dimethyditallow quaternary ammonium salt between their layers but one of them has additional surface coating in order to provide better compatibility with the nonpolar matrix.

■ **Choice of the thermoplastic polymer matrix:** Low density polyethylene (LDPE) with low melt flow index (MFI) value was prefered to be used as a main matrix

as it has good film forming properties, high melt and solid strength. It is also the most commonly used commodity polymer in the industry and research field. Another important property of LDPE is its low crystallinity as compared to that of HDPE and this property provides it high transparency as well as ease of bio- and photo-oxidative degradation.

■ **Choice of the compatibilizer:** Maleic anhydride grafted polyethylene and ethylene-glycidyl methacrylate copolymer with epoxy functionality were preffered with the idea of providing good interfacial adhesion by reacting with the hydroxyl groups of starch and clay.

■ **Choice of the processing method:** The processing of composite in a twin screw extruder is the most efficient way to obtain a good dispersion. Starch granules and clay agglomerates can be disrupted by the help of high shear that is generated in a twin screw extruder. It is also known that using twin screw extruder for polymer composite system provides better mechanical properties compared to those of solution cast method.

3.2 Materials

Exxon Mobil D156 BW grade LDPE with MFI value of 0.75 g/10 min was kindly supplied by Alcan Packaging, Istanbul. Corn starch was provided by Cargill, Turkey. G-105 PGN and PGW polymer grade sodium montmorillonite type of clays (Na^+mmt) with cation exchange capasity (cec) of 120 and 145 meq/100g were obtained from Nanocor, USA. Organoclay (Viscobent) having dimethyldistearyl ammonium component, was provided by Bensan, Turkey. The same type of organoclay (Nanofil SE 3000) but additionlly modified with organic components to improve the dispersibility in polyolefin matrix, was supplied by Sud-Chemie, Germany. Clay samples were dried at 120^{o}C under vacum for at least 2 hours prior to using.

Aldrich grade maleic anhydride and analytical grade dimethyl sulfoxide (dmso) and glycerol were used as received. Styrene monomer was purified by passing through the alumina in column and kept at -4^{o}C in refrigerator. Benzoyl peroxide was obtained from Aldrich Chemical Company, Inc. with 75% purity and used as received.

Maleic anhydride grafted polyethylene (MAgPE) under the trade name of Polyglue LE102T was supplied from SK Corporation, Korea. Ethylene-butyl acrylate-glycidylmethacrylate terpolymer (E-BA-GMA terpolymer) containing epoxy functionality with the trade name of Elvaloy PTW was donated by Dupont Company. Their molecular structures are given in Figure 3.1.

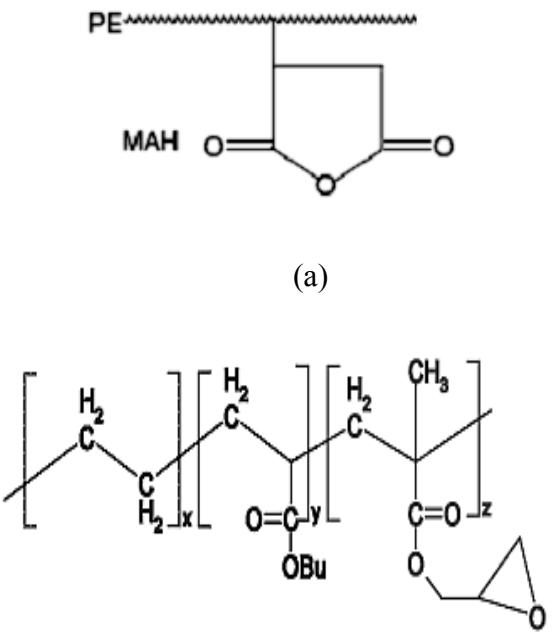

Figure 3.1 Molecular structures of (a) MAgPE, (b) E-BA-GMA terpolymer.

3.3 Instrumental

Leistritz Micro 27-GL 44D twin screw extruder with 27 mm screw diameter and L/D ratio of 44 was used to prepare polyethylene-starch blends. Schematic representation of typical twin-screw extruder is presented in Figure 3.2.

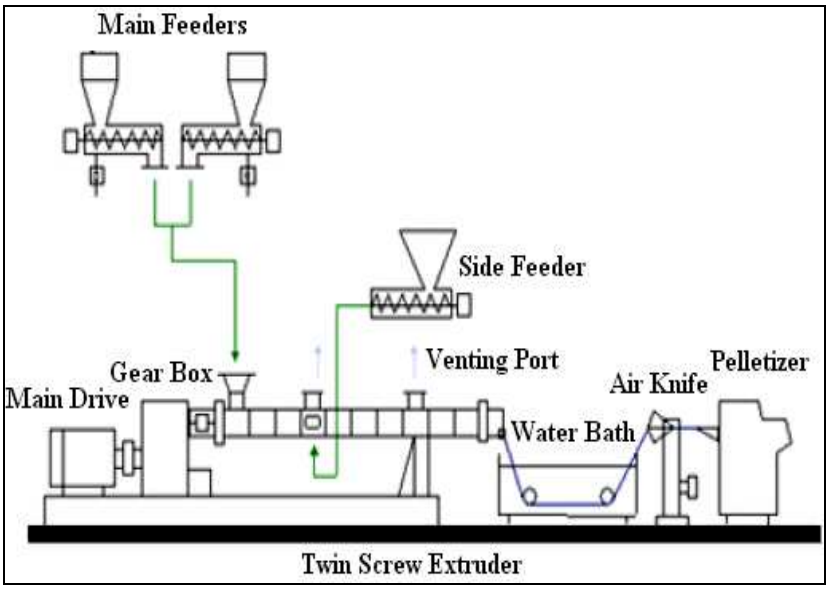

Figure 3.2 Schematic representation of twin-screw extruder and its components.

Polymer granules obtained from twin-screw extruder were first melted and mixed in Scientific LRM-S-110 two-roll mills and than hot pressed into the films using Scientific LP-S-50 at a pressure of 100 bars. The thickness of the films was 400 µm.

Scientific Single Screw Extruder Type LE25-30/CV with Scientific Laboratory Cast Film and Sheet Attachment Type LCR-300 was used to produce cast film with the thickness of 60-70µm. The barrel temperature of the chill-roll line was adjusted between 160-180^{o}C, cast roll to 40^{o}C and cast die to 180^{o}C. The screw speed and rolling speed were 40 and 26 rpm, respectively.

Blown film samples with the thickness of 40-60µm were prepared in Petkim, Turkey. Plasticisers extruder with L/D=24 and die diameter of 63 mm was used. The temperature profile were adjusted betweeen 120-160^{o}C.

ENGEL Victory 200/50 Tech Injection Moulding Machine with L/D of 20.5 and 30 mm screw diameter was used to produce tensile and impact test sample according to ASTM D-638. The barrel temperature was set between 150-170^{o}C and the mould was kept at room temperature.

The compatibility between polyethylene and starch were evaluated by Fourier Transform Infrared (FT-IR) measurements that were carried out by using Bruker Equinox 55 instrument with attenuated total reflectance (ATR) attachment.

The level of separation of clay layers and the crystallograpic structure of starch, clay and polyethylene were determined by X-ray diffraction (XRD) analysis conducted using a Bruker AXS-D8 diffractometer with CuKα radiation, operating at 40kV and 40 mA.

A Leo G34-Supra 35VP scanning electron microscope (SEM) operating with an accelerating voltage of 10kV was used for the morphology observation of the samples after they were coated with thin carbon film in an Emitech K950X sputter coater to avoid charge built up.

A Netzsch DSC 204 was used to determine the percent crystallinity of LDPE matrix and its nanocomposites. The samples were heated to 150 ^{o}C at a rate of 10 K/min. The enthalpy of melting was calculated from the area of the melting peak.

The transmission of UV-Vis light through the films was detected using Shimadzu UV-3150 spectrophotometer in a wavelenght range of 200-800 nm.

Contact angle analysis of the samples was performed by using sessile drop method with a Krüss GmbH DSA 10 Mk 2 goniometer with DSA 1.8 software. Advancing angles (θ_A)were determined by measuring the contact angles at the onset of advancing of the three phase contact lines while slowly injecting water to pre-deposited drops, with the help of a 1 mL syringe equipped with a micrometer. Measurements from at least 5 different regions were averaged. During the analysis, the tip of the syringe was kept in the drops within the measurements and a tangent method, in which the part of the profile of a sessile drop lying near the baseline is adapted to fit a polynomial

function, is employed to calculate the contact angles from the slope at the three phase contact line.

Surface energies of the films were calculated from advancing contact angle measurements of water, ethylene glycol and n-hexadecane by using Owen, Wendt, Fowkes concept [101-103]. This approach states that surface energy of a solid γ_{SV} can be broken into a dispersive γ_{SV}^{d} and a polar γ_{SV}^{p} component as:

$$\gamma_{SV} = \gamma_{SV}^{d} + \gamma_{SV}^{p} \tag{3.1}$$

and the advancing contact angle of a liquid can be related to the interfacial surface energies as:

$$\tfrac{1}{2}(1+\cos\theta_A)\,\gamma_{LV}/(\gamma_{LV}^{d})^{0.5} = (\gamma_{SV}^{p})^{0.5}\,(\gamma_{LV}^{p}/\gamma_{LV}^{d})^{0.5} + (\gamma_{SV}^{d})^{0.5} \tag{3.2}$$

Through this equation, by using at least two liquids, whose surface tension (γ_{LV}) and the dispersive and polar components are known, if the $\tfrac{1}{2}(1+\cos\theta_A)\,\gamma_{LV}/(\gamma_{LV}^{d})^{0.5}$ is plotted against $(\gamma_{LV}^{p}/\gamma_{LV}^{d})^{0.5}$ and fit to a linear equation, then the polar component of the solid-vapor interfacial energy (γ_{SV}^{p}) can be calculated from the slope of the line, and dispersive component (γ_{SV}^{d}) can be evaluated from the y-intercept.

Biodegradation degree was evaluated by calculating the amount of glucose that was evolved due to the degradation of starch molecules by AG-Amiloglucosidase. The film samples were incubated in a enzyme solution at 50^{o}C and pH of 4.8 for 3 days. The samples were taken at each 24 hours interval and the glucose amount in the samples was calculated from the absorbance measurement conducted on Shimadzu UV-3150 spectrophotometer [104].

The tensile tests were performed on Zwick/Roell Z100 BT1-FB100TN tensile tester at a cross speed of 50mm/min according to ASTM D 638 and ASTM D 882-02. Tensile tests for films were conducted by using 200N load cell, while 10kN load cell was used for injection molded samples.

The charpy impact tests were performed using Ceast Resil 25 Instrument according to ISO 179-1. Ceast Notchvis-Manual Version was used to prepare 1.0 mm single notched specimen.

The barrier properties of the films were evaluated using Labthink TSY-T3 Water Vapor Permeability Tester and Labthink TOY-C2 Film-Package Oxygen Permeability Tester. The water vapor permeability test was performed at 90%RH (relative humidity), 38^{o}C and the results were expressed as grams of moisture vapour permeated through the film for 1 m^2/d. The oxygen permeability test was done at 23^{o}C and 0 RH conditions and the results were expressed as cc/m^2/d.

The tear strenght of the film samples with 7.5x 2.5 cm dimensions were measured via Instron Model No. 5565. Each sample was cut 5 cm. from the middle and the two arms of the samples were attached to the grips of tensile machine. The strength was measured while the sample is tearing down.

Heat seal strength of film samples were determined by applying tensile load via Instron Model No. 5565 after standardizing the sealing temperature, dwell time, and pressure conditions.

Flow properties of the samples was evaluated using Malvern Advanced Capillary Rheometer RH10 Instrument at different temperatures. The shear viscosity values of the samples were recorded under the shear rates of between 10-100 that correspond to the shear rate range developed in a typical extrusion process.

3.4 Sample Preparation

3.4.1 Preparation of Starch-Na^+mmt Nanocomposite by Solution Method

Starch was dissolved in 90 % (by volume) dimethyl sulfoxide solution at room temperature and kept in ultrasonic bath for two hours. To obtain clay slurry, Na^+mmt with an amount of 8 phr based on starch content was dispersed in a distilled water untill

the formation of homogeneous dispersion and the resultant dispersion was added to the starch solution. The mixture was than stirred mechanically at 600 rpm for 24 hours at room temperature. The small portion of the solution was poured onto the teflon plate and the solvent was allowed to evaporate slowly at 40^{o}C in order to obtain thin films for tensile tests. The remaining portion of the solution was than poured into acetone to precipitate the resultant product**.** The product was filtered and the solvent was evaporated at 65 ^{o}C in an oven. The solid particles formed was than grounded into the powder.

Thermoplastic starch(TPS)-Na^{+}mmt nanocomposite film was prepared by heating the starch-clay solution to 80^{o}C for 30 min with continuous stirring and incorporating glycerol (in an amount of 30 wt% of starch) to this solution. After stirring the solution mechanically at 600 rpm for 24 hours at room temperature, the product was poured onto teflon plate and the solvent was evaporated slowly at 40^{o}C.

3.4.2 Preparation of TPS-Na^{+}mmt Nanocomposite by Melt Intercalation Method

Water and glycerol, in an amount of 30 wt % of starch content from each one, were heated to 60^{o}C, separately. Starch-Na^{+}mmt nanocomposite prepared as described in section 3.4.1 was blended with these plasticizers and the blend was kept overnight in sealed PE bags in order to allow starch particles to swell with plasticizer. The mixture was than melt blended via twin-screw extruder at the processing temperature of between 90 and 150^{o}C and screws speed of 100 rpm. The resultant TPS-Na^{+}mmt nanocomposite strands were than granulated in a pelletizer and the granules were kept in sealed polyethylene bags.

For the comparison purpose, TPS-Na^{+}mmt nanocomposite was also prepared in a single step process using twin-screw extruder. For this aim, 1 kg of starch and 600 g of plasticizer (300 g water and 300 g glycerol) preheated to 60^{o}C were mixed together and the mixture was kept overnight in sealed PE bags. Na^{+}mmt was than added to this mixture at an amount of 8 phr based on starch content and the resultant powdered mixture was fed through the extruder. The same processing conditions were used as described above.

3.4.3 Preparation of TPS by Melt Blending

The same procedure was followed with that given in section 3.4.2 except that instead of using starch-Na^+mmt, starch powder was used to blend with preheated plasticizers.

3.4.4 Preparation of Maleic Anhydride Grafted Polyethylene (MAgPE) by Reactive Extrusion

The grafting reaction of maleic anhydride on LDPE was carried out in a co-rotating twin screw extruder. Maleic anhydride (1.5 wt% based on polymer matrix), benzoyl peroxide (0.15 wt% based on polymer matrix) and purified styrene (1.5 wt% based on polymer matrix) were premixed with LDPE before feeding into the extruder. The blend was extruded at a screw speed of 100 rpm with barrel temperature profile between 140-200 ^oC. This conditions was found to be the optimum conditions in obtaining high yield of grafting reaction. The grafting reaction was summarized in Figure 3.3.

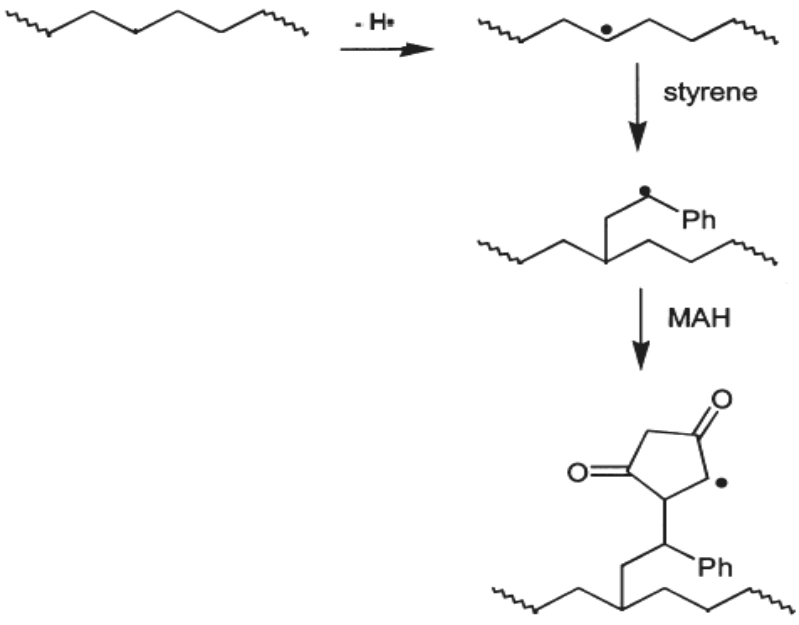

Figure 3.3 Reaction scheme for maleic anhydride grafting onto polyethylene.

In order to determine the efficiency of grafting reaction, 5 g of the product was refluxed in hot xylene to remove any unreacted monomers. The solution was than

poured into acetone in order to precipitate the pure product. The precipitate was washed several times with acetone, dried in an oven at 80^{o}C. The presence of maleic anhydride that is reacted with polyethylene was checked with FT-IR analysis.

The degree of grafting was determined by titration method. The product (0.4 g) was first dissolved in hot toluene and than several drops of water was added to this solution in order to hydrolyze all anhydride groups into the carboxylic acid groups. After adding thymol blue as an indicator, the solution was titrated with 0.05 N KOH solution until the formation of stable blue color. The amount of carboxylic acid was than calculated with the following formula;

Carboxylic acid content (% wt) : (45 * N * V) *100 / M
N: KOH concentration (mol/L)
V : The amount of KOH solution that is consumed (mL)
M: The amount of grafted PE (g)

3.4.5 Organoclay Masterbatch Preparation

LDPE, compatibilizer and organoclay at 70:10:20 by weight compositions were fed through the main feeding port of twin screw extruder. The temperature of the barrel was adjusted between 160-170^{o}C and the screw speed to 300 rpm in order to introduce high shear to break-up the clay agglomerates. The process was performed using two different compatibilizers namely Polyglue and Elvaloy and two different organoclays which are called as Viscobent and Nanofil SE3000, for the sake of comparision.

3.4.6 Preparation of LDPE/Starch (or TPS) Composites and Nanocomposites

The samples with compositions given in Table 3.1 were prepared using twin screw extruder operating at screw speed of 200 rpm and the barrel temperature of betwen 155-175 ^{o}C . All the components were introduced from the main feeding port of the extruder.

The name of the samples were given to show which compatibilizer, clay, form of starch and how much starch content are used to prepare it. For example, sample with the name of PE/MA/20St-Na^+mmt includes MAgPE as a compatibilizer and 20 wt% of starch and 2 phr Na^+mmt, whereas PE/Elv/20TPS contains elvaloy as a compatibilizer and 20 wt% TPS. Similarly, PE/PG/40TPS/Nanofil contains polyglue as a compatibilizer, 40 wt% TPS and 2 phr organoclay (Nanofil SE3000). Otherwise mentioned, all the blend samples with TPS contain 20 wt% compatibilizer and all the nanocomposite samples include 2 phr clay.

The effect of compatibilizer, compatibilizer type, clay type, starch form and its content as well as preparation methods on the mechanical and physical properties of the final product were investigated. After deciding in suitable composition, blown and sheet films were produced to evaluate the possibility of our products to be used in packaging industry.

Table 3.1 Formulations used throughout the study.

Sample Name	Wt (%)							Clay (phr)		
				Compatibilizer						
	LDPE	Starch	TPS	MA	PG	Elv	EVOH	Na^+ mmt	Vis	Nano fil
St-Na^+mmt		100						8		
TPS- Na^+mmt			100					8		
PE/20St	80	20								
PE/MA/20St	60	20		20						
PE/MA/20TPS	60		20	20						
PE/MA/20TPS-Na^+mmt	60		20	20					2	
PE/Elv/20TPS	60		20			20				
PE/PG/20TPS	60		20		20					
PE/PG/30TPS	50		30		20					
PE/PG/40TPS	40		40		20					
PE/PG/50TPS	30		50		20					
PE/EVOH/20Vis	87.5						12.5		25	
PE/Elv/20Vis	87.5					12.5			25	
PE/PG/20Vis	87.5				12.5				25	
PE/EVOH/Vis	99						1		2	
PE/Elv/Vis	99					1			2	
PE/PG/Vis	99				1				2	
PE/PG/20 Nanofil	87.5				12.5					25
PE/PG/Nanofil	99				1					2
PE/PG/40TPS-Na^+mmt	40		40		20			2		
PE/PG/40TPS-Nanofil	40		40		20					2

CHAPTER 4

4. RESULTS AND DISCUSSION

4.1 Properties of Starch-Na^+mmt and TPS- Na^+mmt Nanocomposite Films

Starch-Na^+ mmt nanocomposite was prepared using solution intercalation method. Dimethyl sulfoxide/water (90/10 v/v) mixture was used as a solvent since it is known to dissolve starch granules at room temperature [105-107]. The separation extent of clay layers in St-Na^+mmt nanocomposite film was investigated using XRD. Figure 4.1 reveals that the interplanar basal spacing (d_{001}) of pure Na+mmt is 1.14 nm and it is increased to 1.79 nm after dispersing in starch solution, indicating the intercalation of clay layers by starch molecules.

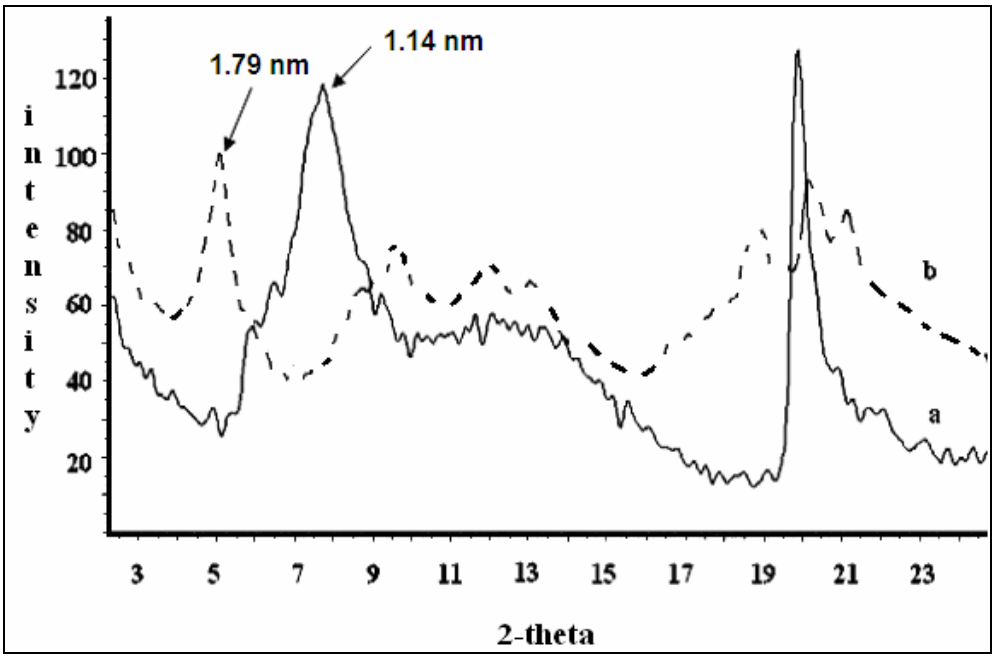

Figure 4.1 XRD pattern of a) Na^+mmt, b) St-Na^+mmt nanocomposite.

SEM image of St-Na^+mmt films, given in Figure 4.2, shows that the clay layers are homogeneously dispersed in starch matrix.

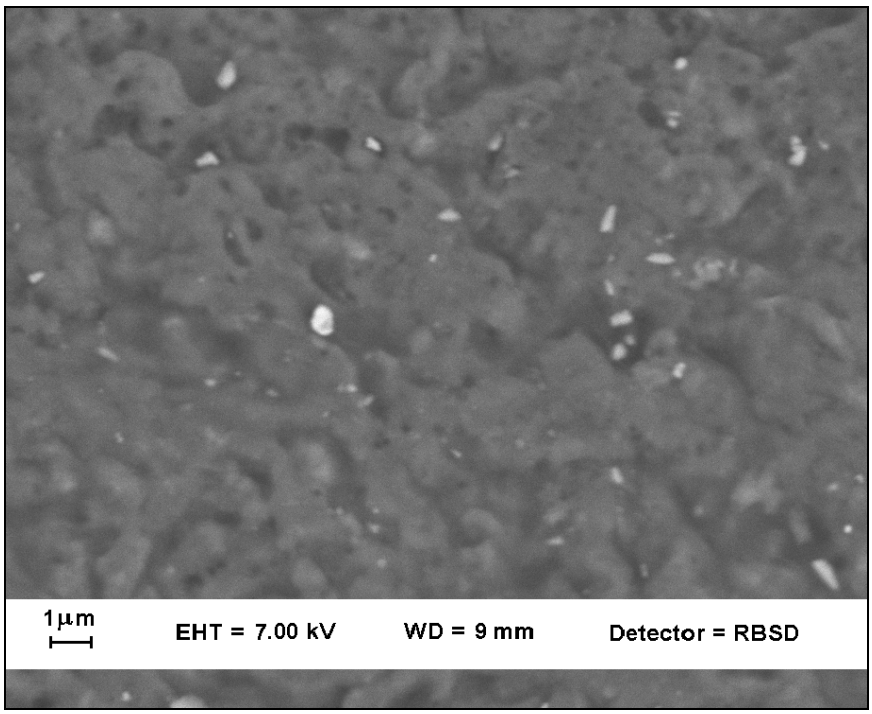

Figure 4.2 SEM image of St- Na^+mmt nanocomposite film.

In TPS-Na^+mmt sample, intercalation occurred with the d spacing of 1.65 nm (Figure 4.3b). Since both starch and glycerol are hydrophilic in nature, they tend to migrate between the clay galleries by polar-polar attraction forces. It is more probable for glycerol to diffuse into the clay layers due to its smaller molecular size compared to that of starch [83]. In order to determine which molecule resides between the clay layers in TPS-Na^+mmt nanocomposite sample, the same procedure described in section 3.4.1 was repeated with the use of glycerol as an intercalant. The xrd pattern (Figure 4.3c) demonstrated that the clay gallery height were very similar with that observed in TPS-Na^+mmt film, indicating the presence of mainly glycerol molecules between the clay layers.

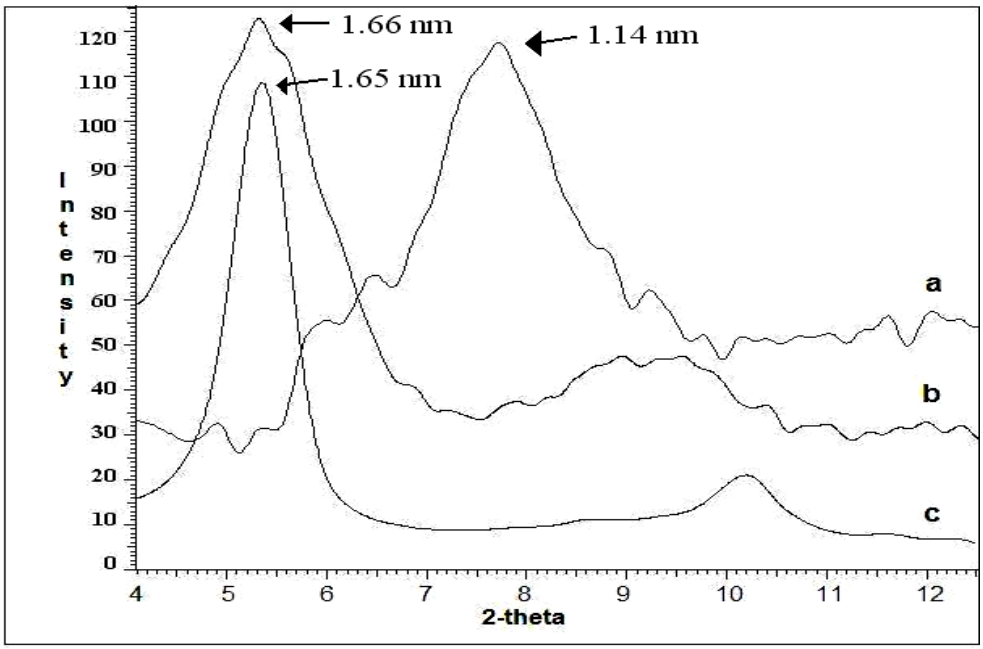

Figure 4.3 XRD pattern of a) Na^+mmt, b) TPS-Na^+mmt, c) Glycerol- Na^+mmt sample.

The tensile properties of TPS, TPS/Na^+mmt and unplasticized St/Na^+mmt films are given in Table 4.1. Even though the elongation property of TPS films is high enough, its tensile strenth is very low making it unsuitable material for many industrial application. The significant increase in tensile strength and modulus of TPS was observed after the addition of clay, indicating the reinforcing effect of the layered filler. However, elongation properties of TPS drasticaly decreased by the presence of clay. This reduction can be attributed to the stiffness of inorganic filler and also reduced plasticization effect of glycerol molecules because some of them reside between the clay layers and therefore they are not available to disrupt the hydrogen bonding between the starch molecules. The unplasticized St-Na^+mmt film exhibited the highest modulus and lowest elongation at break value compared to glycerol added films indicating the plasticization efficiency of glycerol molecules.

Table 4.1 Mechanical properties of TPS and Starch nanocomposite films.

Sample	Tensile Stress at Break (MPa)	Tensile Strain at Break (%)	Young's Modulus (MPa)
TPS film	1.75	189	193
TPS/ Na^+mmt film	3.98	56	362
St/ Na^+mmt film	6.35	11	571

All the film samples exhibited drastic change in their flexibility depending on the environmental conditions, such as temperature and moisture. The film samples were very flexible at high humidity but becomes fragile when dried. This behavior was attributed to the high water absorption property of TPS which was determined by drying the samples until constant weight in an vacum oven and than keeping the films at high humidity in desicator for 4 days. The film samples were than weighted again and the percentage of water absorption was calculated by the formula,

$$\% \text{ Water Absorption} = (W_f - W_i) / (W_i) \times 100 \quad (4.1)$$

where W_i is the initial weight of dried samples and W_f is the final weight of the samples measured after keeping them at high humidity.

The water absorption level of TPS nanocomposite films was found to be 46.7% and that of starch film was 26.5%. The much higher water absorption capasity of the TPS nanocomposite film is due to its less crystalline structure and swelling property of Na^+mmt.

The properties of TPS as well as its nanocomposites revealed that these materials are not suitable to be used in any plastic applications therefore they need to be further improved with much stronger and stable thermoplastics such as polyolefins.

4.2 Properties of LDPE/Starch Composite and Nanocomposite Samples

4.2.1 Effect of Using Compatibilizer on Starch Dispersion

In order to provide the compatibility between starch and LDPE, maleic anhydride was grafted into polyethylene chains. Figure 4.4 shows FTIR spectrum of MAgPE that was taken after purification in xylene. The peak at 1781 cm^{-1} is assigned to stretching vibrations of carbonyl groups in maleic anhydride, showing the success of the grafting reaction. The amount of maleic anhydide that is grafted onto LDPE chains was found to be 1.0 wt% of LDPE content from the titration method.

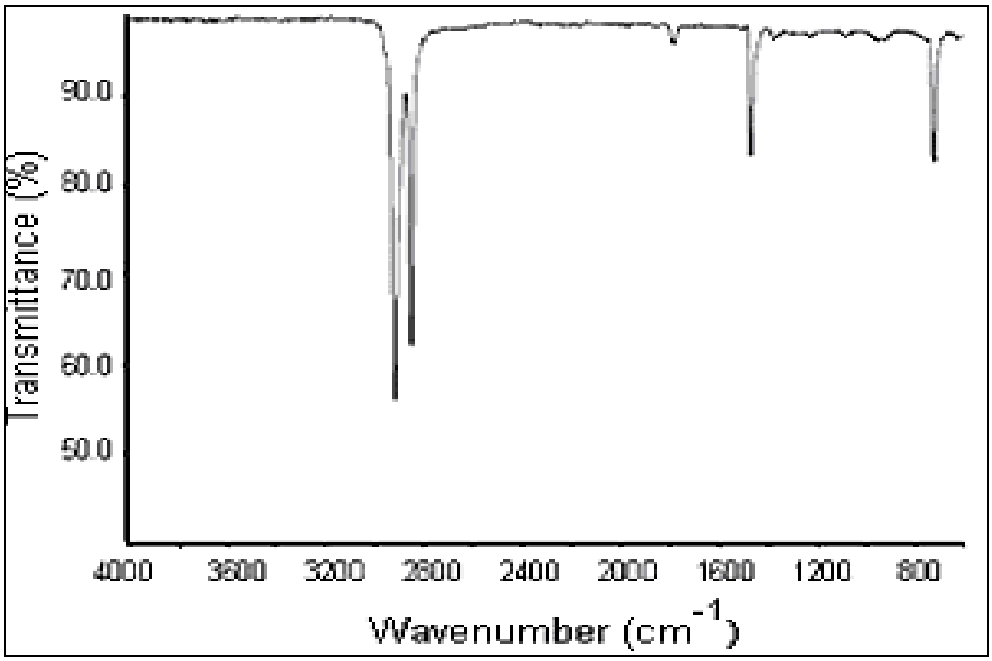

Figure 4.4 FTIR spectrum of MAgPE.

The effect of compatibilizer on the morphology of the samples is clear from SEM images (see Figure 4.5). The presence of large starch granules on the order of 500-600μm and the poor interfacial adhesion between starch and LDPE matrix showed that starch acted as physical filler in PE/20St blends (Figure 4.5a) due to their different polarities. Figure 4.5b shows that by the addition of MAgPE, the size of the starch granules was reduced to a maximum size of 20μm and the voids between the two phases disappeared.

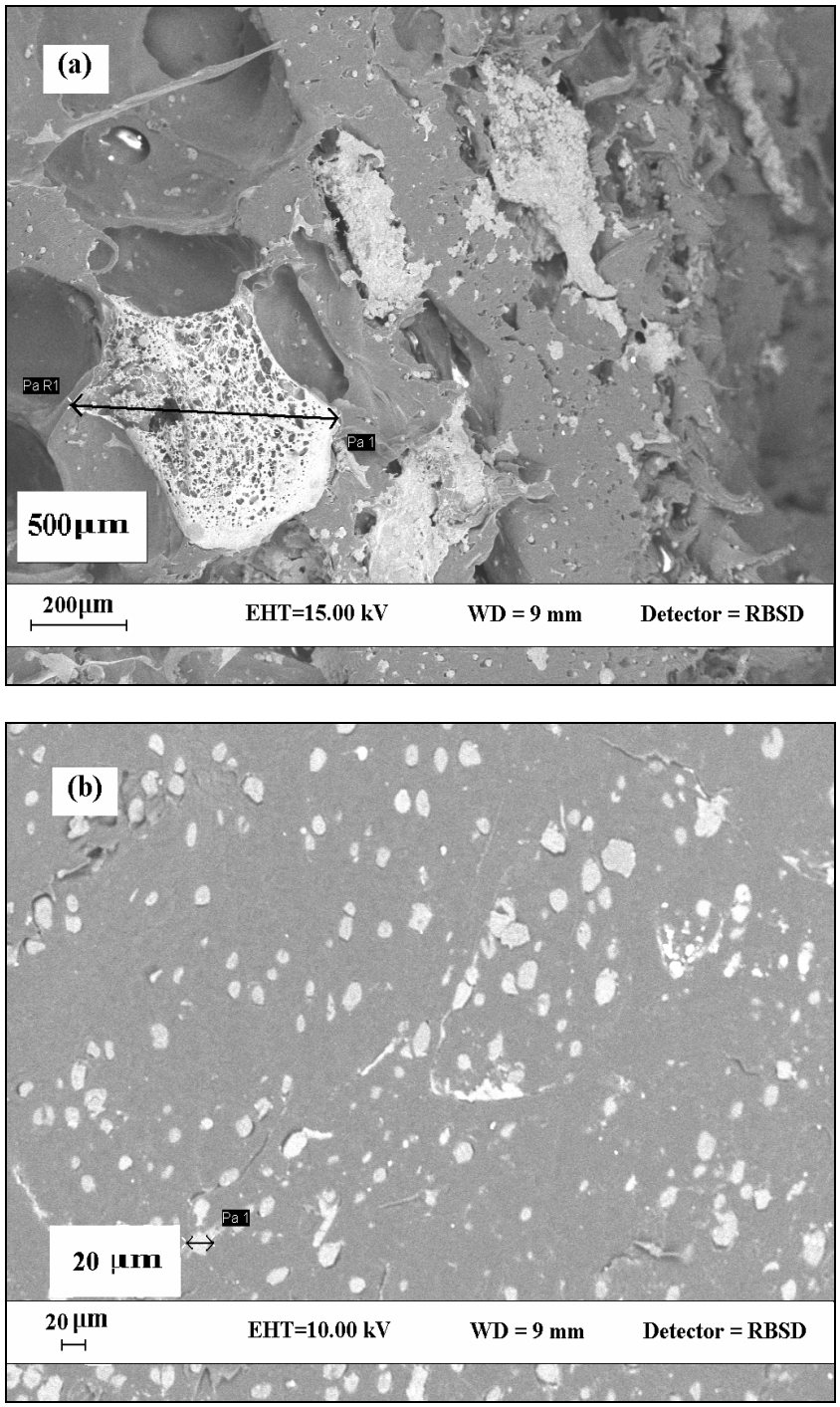

Figure 4.5 SEM images of (a) Uncompatibilized, (b) Compatibilized PE/20St Composites.

The FTIR (Figure 4.6) spectrum of PE/MA/20St composite film shows chemical bond formation between hydroxyl groups in starch and carboxylic groups in maleic anhydride, with the peak appearing at around 1740 cm^{-1}, corresponding to the C=O group of ester linkage. The absence of peak at 1781 cm^{-1} shows that all the cyclic maleic anhydride groups in compatibilizer were opened up and reacted with the hydroxyl groups in starch molecules, as schematically illustrated in Figure 4.7.

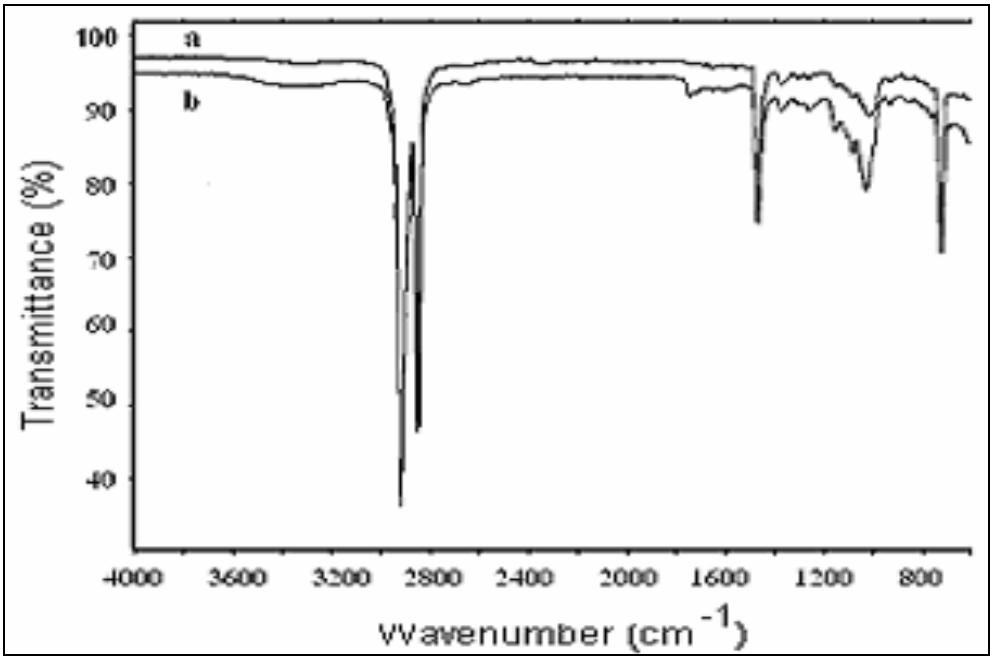

Figure 4.6 FTIR spectra of (a) PE/St, (b) PE/MA/St.

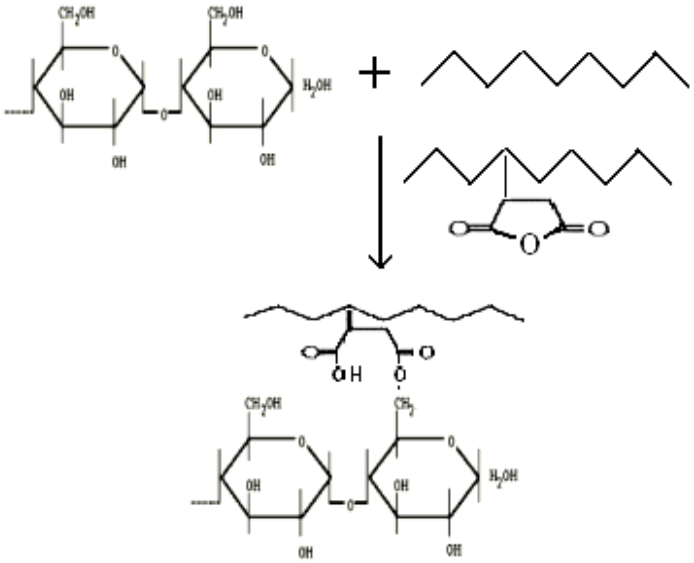

Figure 4.7 Reaction scheme for MAgPE and starch molecules.

The mechanical strength of the composite materials depends strongly on the homogenoneous dispersion of the disperse phase and its adhesion to the polymeric matrix. Table 4.2 compares the tensile properties of PE/20St blends with and without compatibilizer. Mechanical properties confirms the necessity of using compatibilizer between starch and LDPE in order to prepare composite material with improved mechanical strength.

Table 4.2 Effect of using compatibilizer on mechanical properties of LDPE/starch composite.

Sample	Tensile Strength (MPa)	Tensile Strain at Break (%)	Young's Modulus (MPa)
PE	9.7±0.3	~500	107.9±3.3
PE /20St	6.6±0.1	22±2	123.8±13.4
PE/MA/20St	8.9±0.2	25±3	151.5±5.9

4.2.2 TPS Formation by Extrusion and Its Effect on Mechanical Properties

Addition of starch to LDPE matrix resulted in deterioration of the mechanical properties as well as the physical appearence of polyethylene film, which could be partially overcome by the addition of MAgPE as a compatibilizer. The tensile strength of the LDPE film recovered back from 6.6 MPa to 8.9 MPa with the aid of compatibilizer. However, the most serious reduction occurred in the percent elongation properties of LDPE, even in the presence of compatibilizer. In order to improve the flexibility of the films, strong intermolecular interactions between starch molecules were broken up with plasticizer during the extrusion process. In an extrusion process, the granular starch is exposed to shear stress by compression and friction processes and converted to a highly amorphous structure. The X-ray diffraction pattern of starch sample before and after extrusion process is showing this transformation in Figure 4.8.

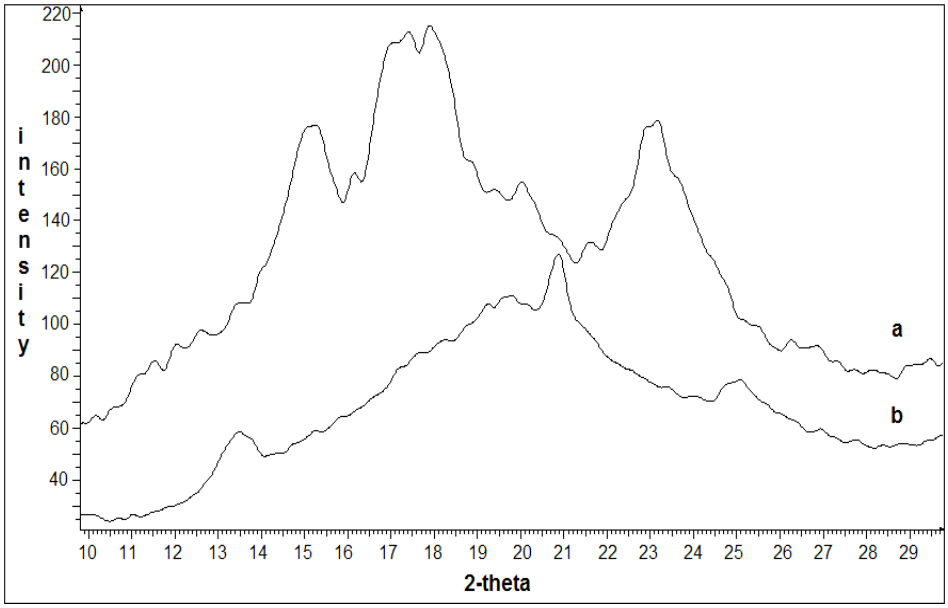

Figure 4.8 Xrd patterns of (a) native starch, (b) Plasticized starch (TPS)

The native corn-starch gives an X-ray scattering pattern that is typical A-type pattern with strong reflections at 2θ about 15° and 23° and an unresolved doublet at a 2θ of 17° and 18°. The corn starch contains 30 wt % amylose and 70 wt % amylopectin that leads to about 25% crystallinity. It is known that the degree of crystallinity is inversely proportional to the amylose content in the starch and it is commonly accepted that amylopectin, the high molecular weight (10^8 g/mol), highly branched constituent of the starch granule, is predominantly responsible for the crystalline structure of native starch [108,109].

During the extrusion process of starch with glycerol, a drastic reduction in crystallinity was detected by xrd analysis. The formation of a new structure was observed with the peaks appearing at 2θ =13.5° and 21°. This structure has been attributed to a complex formation between the amylose and the lipid fraction of starch, probably as a helical form of six and/or seven glucose residues per turn by [109]. These two small peaks indicate that a very small amount of crystallinity still exists in the material that can be further destroyed during the compounding, injection molding or film processing.

The SEM images of granular corn starch and plasticized corn starch are presented in Figure 4.9. After extrusion process, transparent and highly amorphous starch structure was obtained.

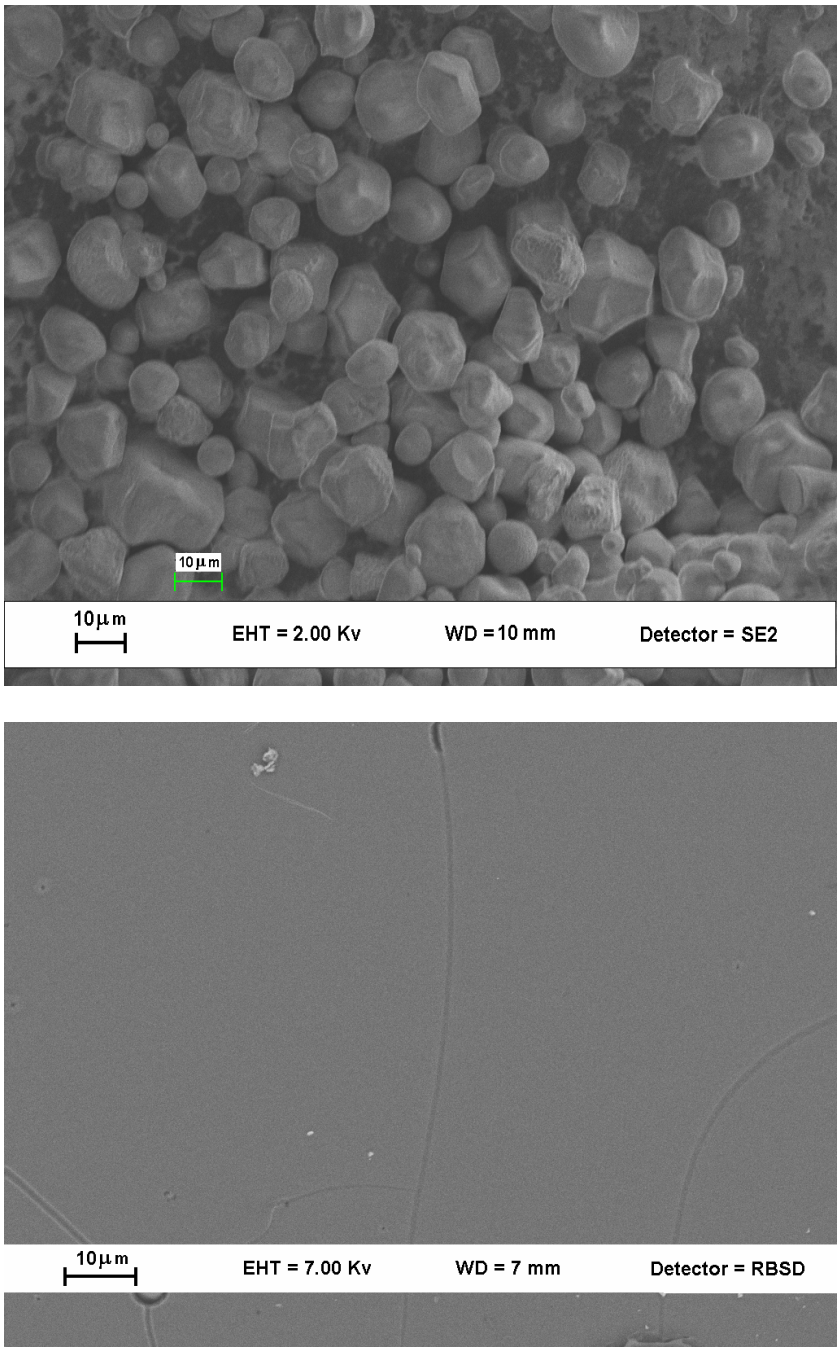

Figure 4.9 SEM images of (a) native granular starch (b) Plasticized starch (TPS).

The plasticized starch (TPS) was melt blended with LDPE matrix in the presence of compatibilizer and resulted in a product with more homogeneous structure compared to the sample with unplasticized starch. The formation of better morphology was attributed to the reduced size of the starch granules through the formation of amorphous starch morphology. The big granules are still present in the blend but they are very few compared to the number of finely dispersed particles. The SEM image of the blend is presented in Figure 4.10.

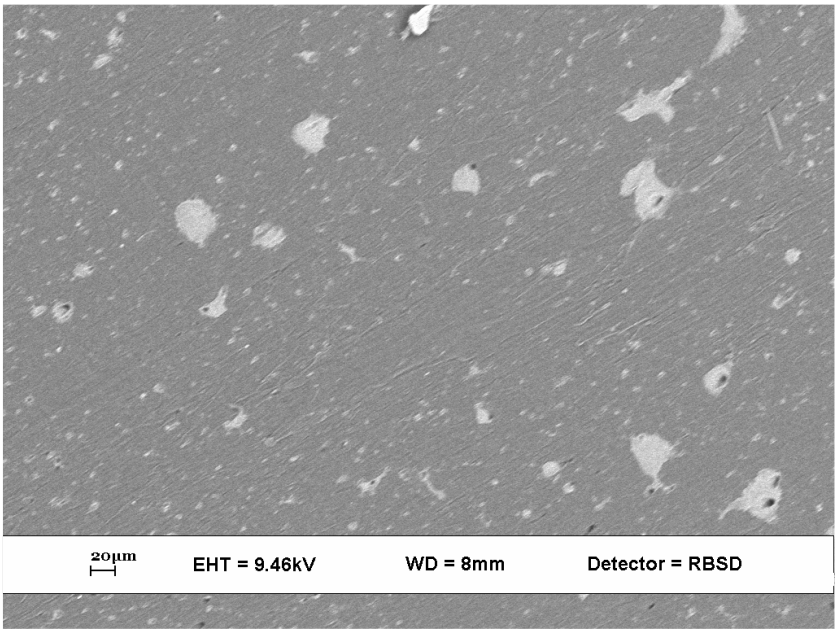

Figure 4.10 SEM image of blend containing 20 wt% TPS.

Table 4.3 presents the tensile properties of LDPE containing 20 wt% of unplasticized and plasticized starch, respectively. The percent elongation was found to be increased from 24.8 to 55.2 without losing much from the tensile strength by using TPS instead of granular starch in the blend. As expected, the stiffness of the blend decreased by the presence of plasticizer.

Table 4.3 Effect of starch form on mechanical properties of LDPE/starch composite.

Sample	Tensile Strength (MPa)	Strain at Break (%)	Young's Modulus (MPa)
PE/MA/20St	8.9±0.2	25±3	151.5±5.9
PE/MA/20TPS	8.3±0.1	55±5	125.5±5.8

4.2.3 Effect of Layered Clay on Physico-Mechanical Properties

Na^+mmt is not a suitable filler for LDPE due to its high polarity but it is highly compatible with starch. Therefore, Na^+mmt was pre-dispersed in starch matrix by preparing starch-clay masterbatch in powdered form. The clay layers were intercalated with starch molecules after this process, as shown previously in Figure 4.1. The masterbatch was than blended with plasticizer and converted into the tps-clay masterbatch by extrusion process, since plasticized starch was previously found to be

the best form of starch in LDPE matrix in partially regaining the reduced elongational properties.

Figure 4.11 illustrates the morphlogy obtained when starch was incorporated into the LDPE matrix in the form of TPS-Na^{+}mmt nanocomposite. The better dispersion with the reduced size of starch granules is evident from the SEM image compared to that observed in compatibilized PE/TPS sample (Figure 4.10). The same micrograph, when viewed at a higher magnification (Figure 4.11b), showed the nano-sized clay layers. It was further realised from SEM images that most of the clay layers reside inside the starch particles. This morphology is expected to be highly beneficial in providing moisture barrier in this region since one of the most biggest obstacle in using biodegradable polymers for packaging applications is their high moisture permeability.

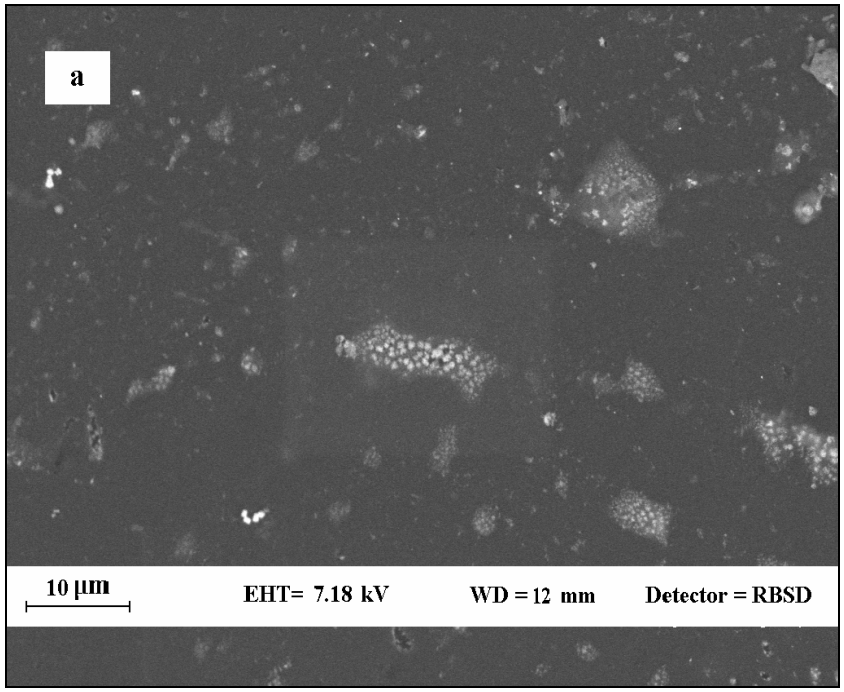

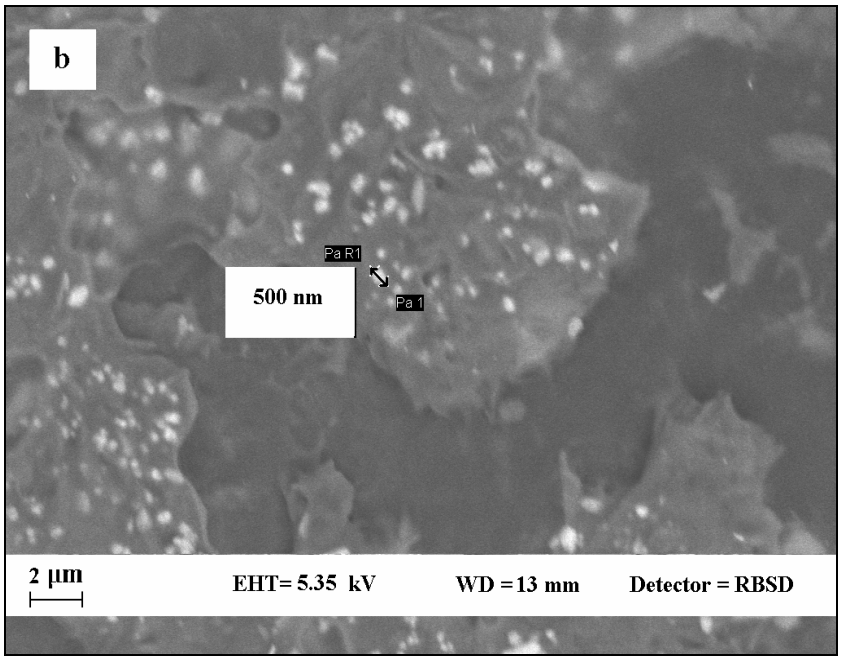

Figure 4.11 SEM images of PE/MA/20TPS-Na^{+}mmt.

The presence of finely dispersed starch particles with good interfacial adhesion, as it is evident from the SEM images, as well as the dispersion of clay layers in nano-size strongly affected the mechanical performance of the blend. The tensile strength and elongation at break value increased much more significantly than all the other trials (Table 4.4). The tensile strength increased to 10.6 MPa (better than that of LDPE itself) and percent elongation increased to %125.2.

Table 4.4 Mechanical properties of 20 wt% starch filled LDPE samples.

Sample	Tensile Strength (MPa)	Strain at Break (%)	Young's Modulus (Mpa)
PE	9.7±0.3	~500	107.9±3.3
PE / 20St	6.6±0.1	22±2	123.8±13.4
PE/MA/20St	8.9±0.2	25±3	151.5±5.9
PE/MA/20TPS	8.3±0.1	55±5	125.5±5.8
PE/MA/20TPS-Na^{+}mmt	10.6±0.2	125±6	137.6±5.8

The significant improvement in elongation properties of PE/MA/20TPS-Na^+mmt film was attributed to different mechanisms. First of all, it was previously shown that the plasticizers disrupts both the intermolecular and intramolecular H-bonds and provides homogeneous dispersion of starch molecules in LDPE matrix. Therefore, clay layers that had been intercalated with starch molecules were also uniformly dispersed in LDPE matrix. This improved dispersion increases the nano-scale reinforcing effect of clay layers and results in better tensile properties in nanocomposite film compared to other blend samples. Moreover, clay helps to keep plasticizers inside the matrix due to its barrier properties and its polar structure which enable it to interact strongly with water and glycerol. This moisture retention ability of clay in TPS-clay nanocomposite sheets was stated as being one of the possible reason for observing less reduction in elongation at break value of TPS-clay as compared to more conventional polymer nanocomposites by Dean et al. [110]. Clay is also known to inhibit the evaporation of plasticizer during extrusion process [111], so it may effectively increase the effect of plasticizer on the elongation properties. Finally, clay may inhibit the recrystallization process of starch molecules in TPS which normally occurs due to the evaporation of plasticizer and causes the embrittlement of the TPS materials in time.

Although clay particles have diameters in the micron range, when their layers are well dispersed in the polymer matrix, the resulting nanocomposite can be transparent in the visible light. Figure 4.12 represents the UV-Vis transmission spectra of the samples. The transparency of polyethylene film was not affected significantly by the presence of TPS-Na^+mmt disperse phase, indicating the homogeneous dispersion of clay layers and starch molecules inside the matrix. The LDPE film including starch and compatibilizer, on the other hand, exhibited much poorer optical transparency (Figure 4.12c) due to the presence of large starch granules.

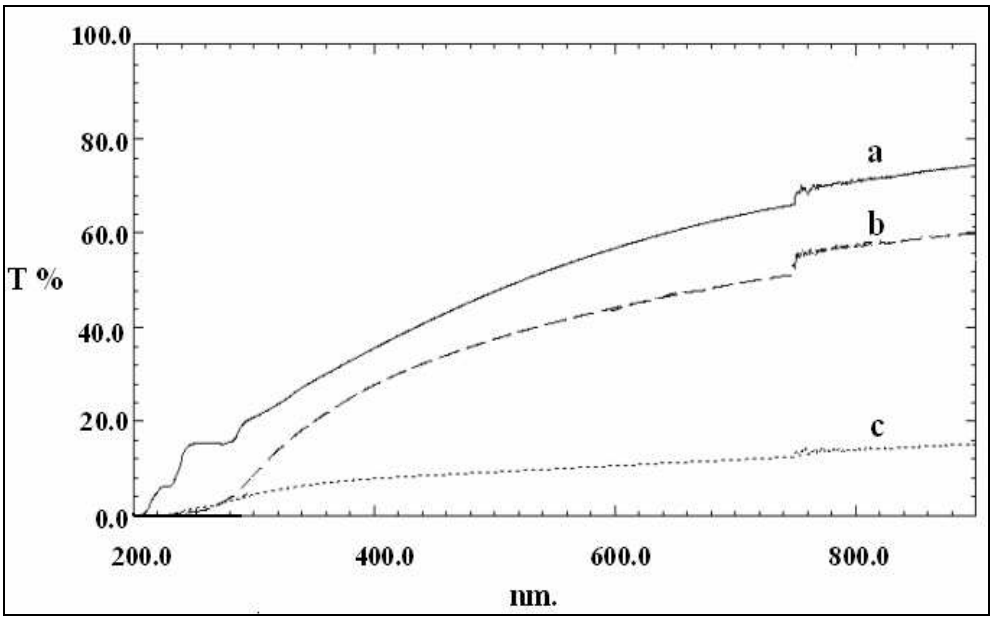

Figure 4.12 UV-Vis transmission spectra of (a) PE , (b) PE/MA/20TPS-Na^+mmt, (c) PE/MA/20St films.

4.2.4 Effect of Using Different Compatibilizer on TPS Dispersion

The size of biopolymer phase determines many of the important properties of the final blends, as it was discussed in the sections above. The size of the disperse phase mainly depends on the presence of strong interfacial adhesion between the filler and the matrix. This interaction can only be achieved with the use of correct compatibilizer type. In the present study, the effect of two different functional groups, which are epoxy functionality of E/BA/GMA terpolymer (Elv) and maleic anhydride functionality of MAgPE, was investigated. For the sake of comparison, besides using MAgPE (MA) that was produced as described in Section 3.4.5, commercially available MAgPE with the trade name of Polyglue (PG) was used.

The morphology analysis of the blend samples prepared using different compatibilizers demonstrated that epoxy functional group did not work in this blend and resulted in the product with uncompatibilized structure (Figure 4.13a). Whereas, the use of PG as compatibilizer provided very fine dispersion of TPS phase and free of voids morphology, indicating strong interfacial adhesion between the filler and the matrix (Figure 4.13b). When compared with the morphology obtained by using MA (see

Figure 4.10), the use of PG seems to exhibit slightly better dispersing efficiency. Therefore, PG was used for the preparation of other blends.

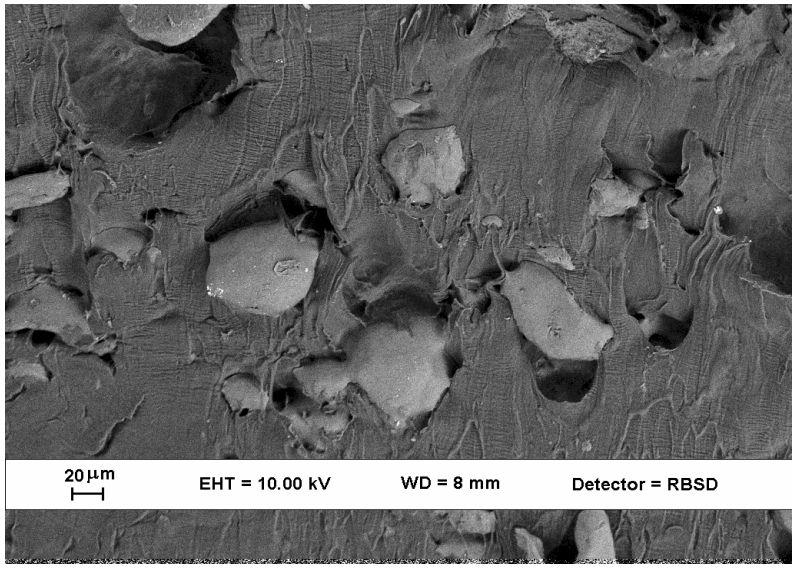

(a)

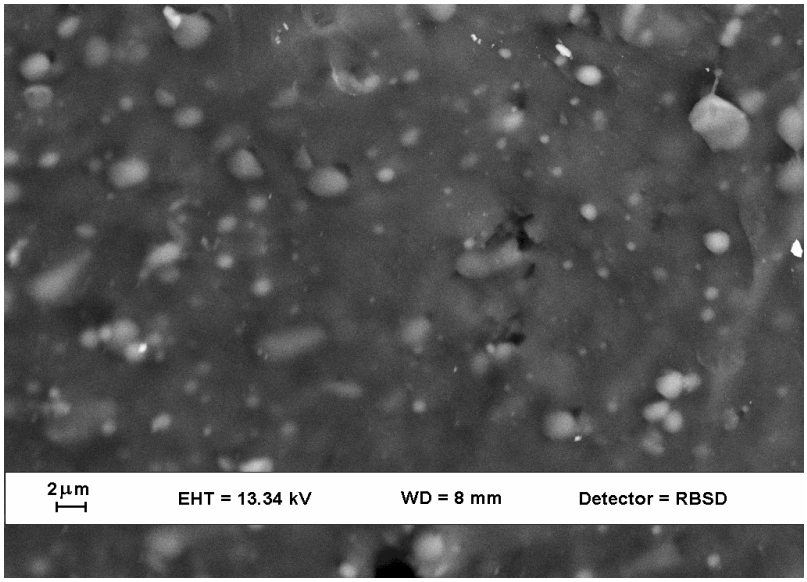

(b)

Figure 4.13 Morphology of (a) PE/Elv/20TPS, (b) PE/PG/20TPS blend samples.

4.2.5 Effect of TPS Content on Fracture Behavior

Our preliminary experiments showed that LDPE/Starch blends with good dispersion of biodegradable component can be prepared by using plasticized starch in

the presence of reactive compatibilizer, such as MAgPE. The results also revealed that using intercalated TPS-Na^+mmt nanocomposite as a disperse phase increases the mechanical properties of the blend much more significantly than using clay-free TPS. Because the ultimate goal of the present study is to increase the degradation rate of LDPE through increasing the number of chain ends on the surface that is in contact with the oxygen, the preparation of blends with higher TPS content was studied. The critical properties for such blends to be used in industrial applications, especially in sheet or blown film applications are their tensile strength and percent elongation properties. It is generally known from literature that as the biodegradable content increases, the tensile strength and the flexibility of the synthetic polymer reduce and normally ductile polymers become fragile at high biopolymer concentration. Therefore, the highest limit of TPS content below which the blend still shows acceptable mechanical properties was investigated.

Figure 4.14 shows the variation of the tensile properties of injection-molded samples with TPS content. The tensile strength of the blends increased slightly with TPS content, reaching the maximum value at 40 wt% (Figure 4.14a). This was attributed to the very fine dispersion of TPS content as well as the strong interfacial adhesion between the components so that efficient stress transfer has occurred during the tensile test. The fine dispersion of TPS is evident from the SEM images given in Figure 4.15-18 with the average particle size of about 1 μm in all the blend formulations.

The elongation at break values for the blends is given in Figure 4.14b. The results revealed that the flexibility of LDPE decreases with TPS loading and the most drastic reduction occurred at 50 wt%. It was also realized that the elongation properties of the blend with 20 wt% TPS is very close to that of 30 wt% TPS, whereas significant change has occurred above 30 wt% TPS addition and the most drastic change was observed at 50 wt% TPS. The reason for this behavior was investigated by examining the tensile fracture surface of the samples. The morphology of the fracture surface for 20 wt % and 30 wt% TPS containing blends are given in Figure 4.15 and Figure 4.16, respectively. The photographs illustrate the formation of fibrous fractured surface, indicating the difficulty of breaking through highly stretched polymer chains. Above 30 wt% TPS loading, the fracture mode starts to change from ductile failure to brittle failure. This

conversion is clear from the SEM images of the blends with 40 wt% and 50 wt% TPS, as shown in Figures 4.17 and 4.18, respectively. Both ductile and brittle fracture mechanisms have been observed for 40 wt% TPS loaded sample. The fracture mechanism involves crack development due to stress concentration at the interface, debonding of the filler-matrix interface and yielding of LDPE chains by forming microfilaments. It is apparent from Figure 4.18b that the brittle fracture has taken place at the interface between the matrix and TPS particles with the formation of cavities, indicating the removal of TPS phase from the interface. This behavior can be due to the discontinuity of LDPE matrix at very high TPS contents (50 wt %), as the disperse phase starts to occupy very large volume. The formation of starch clusters is also evident from SEM image.

The impact test results provided in Figure 4.14c are also consistent with the above discussion that blends with 20 wt% and 30 wt% TPS exhibited similar resistance against breaking while fracture occurred with very low impact energy for the samples with 50 wt% TPS.

The modulus of the samples increased with TPS content due to the presence of rigid starch particles (Figure 4.14d). Matzinos et al. prepared injection molded TPS samples in their study and reported that the modulus of the samples is 2 GPa, tensile strength is 18.5 MPa and elongation at break is 0.8% [109]. These values explains the reinforcing and stiffing effects of plasticized starch in a more flexible and less strong LDPE matrix when sufficient interfacial adhesion has been provided.

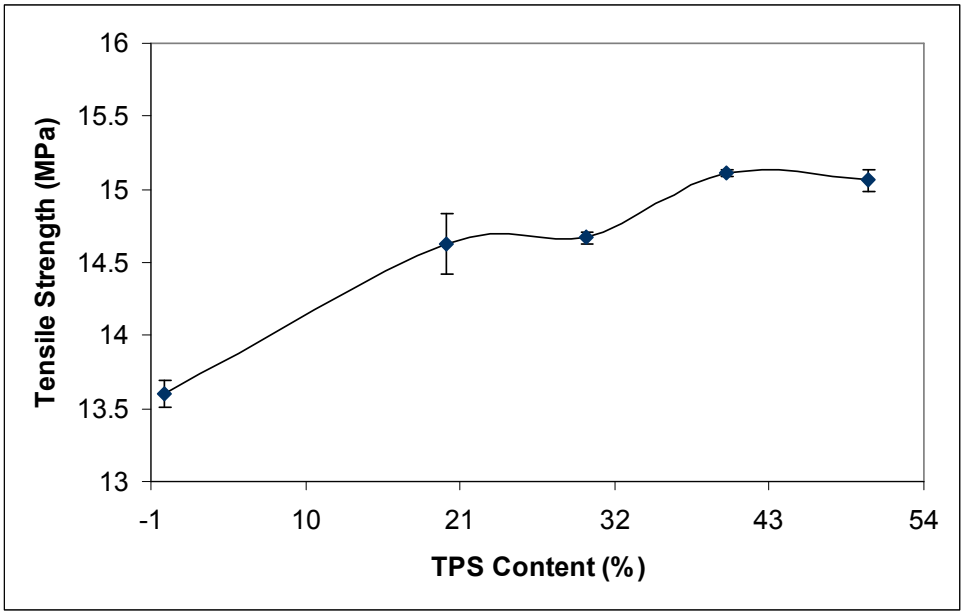
Tensile Strength (MPa)
16
15.5
15
14.5
14
13.5
13
-1
10
21
32
43
54
TPS Content (%)

(a)

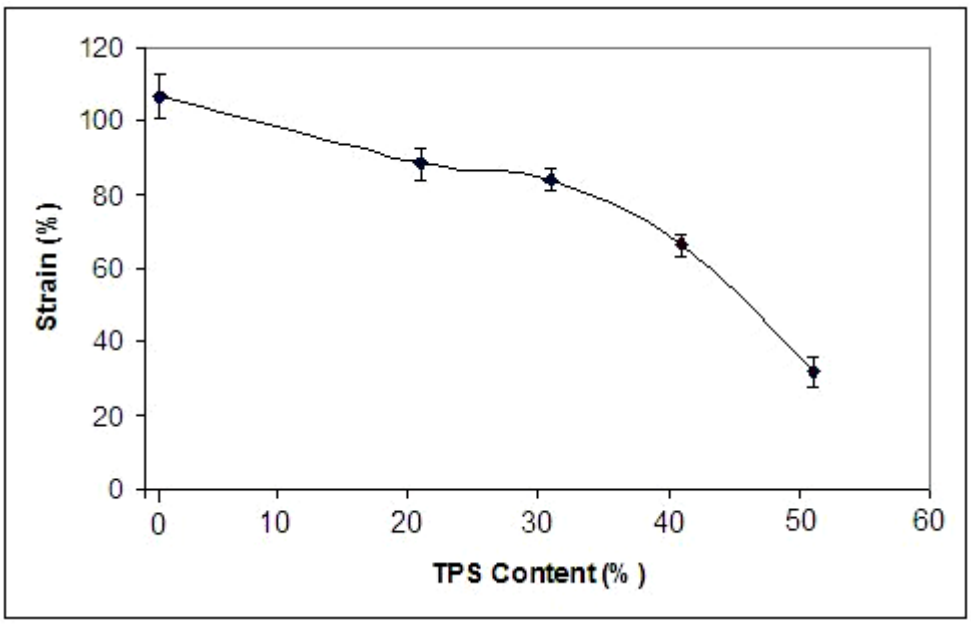
Strain (%)
120
100
80
60
40
20
0
0
10
20
30
40
50
60
TPS Content (%)

(b)

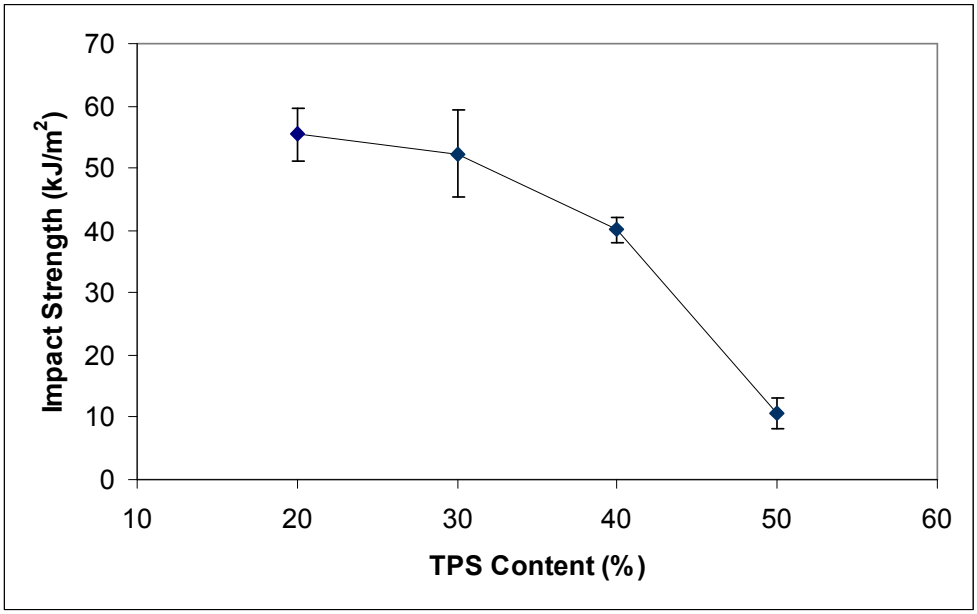

(c)

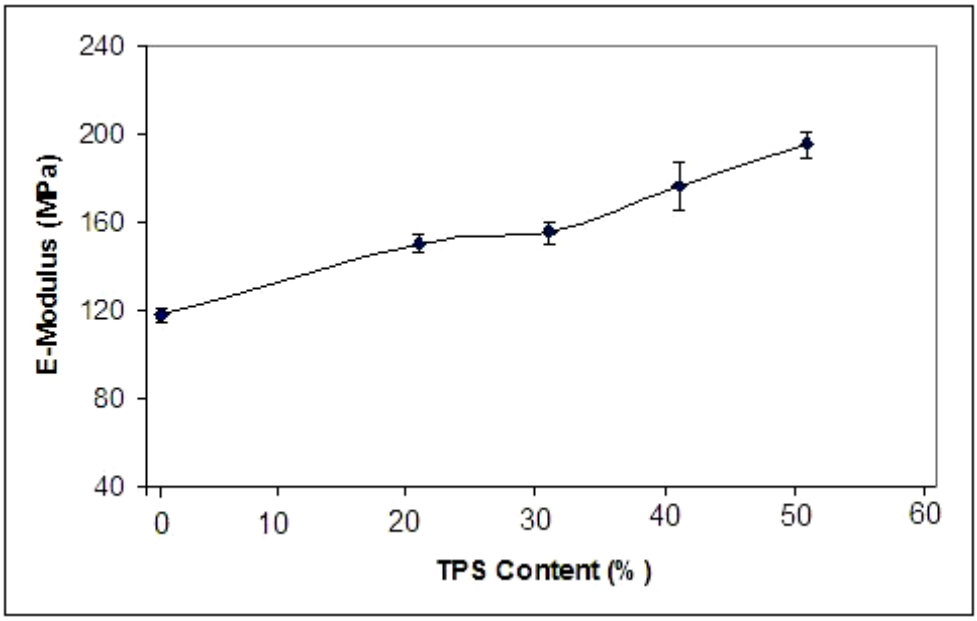

(d)

Figure 4.14 The change in (a) tensile strength, (b) elongation at break, (c) impact strength and (d) Young's modulus, of the blends with TPS content.

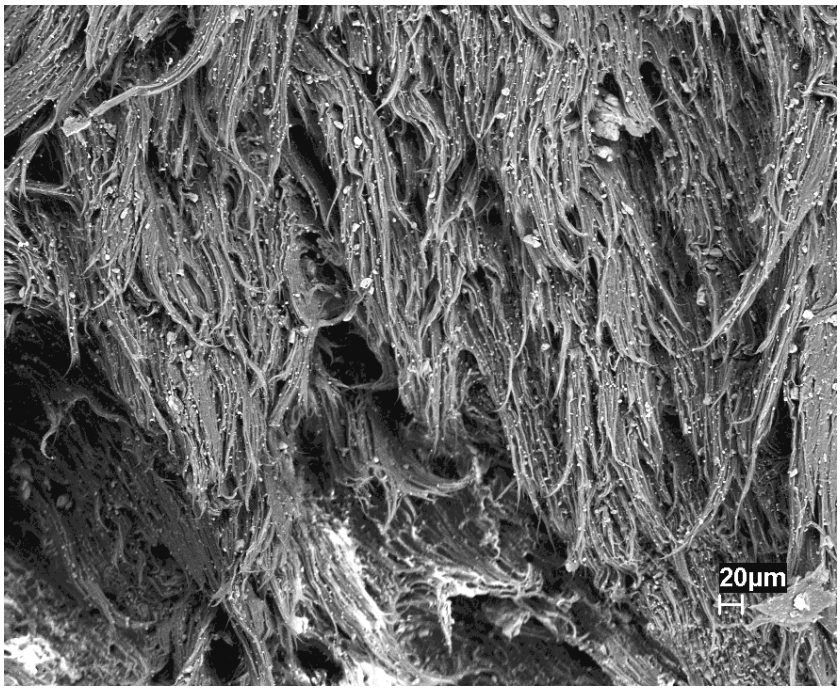

(a)

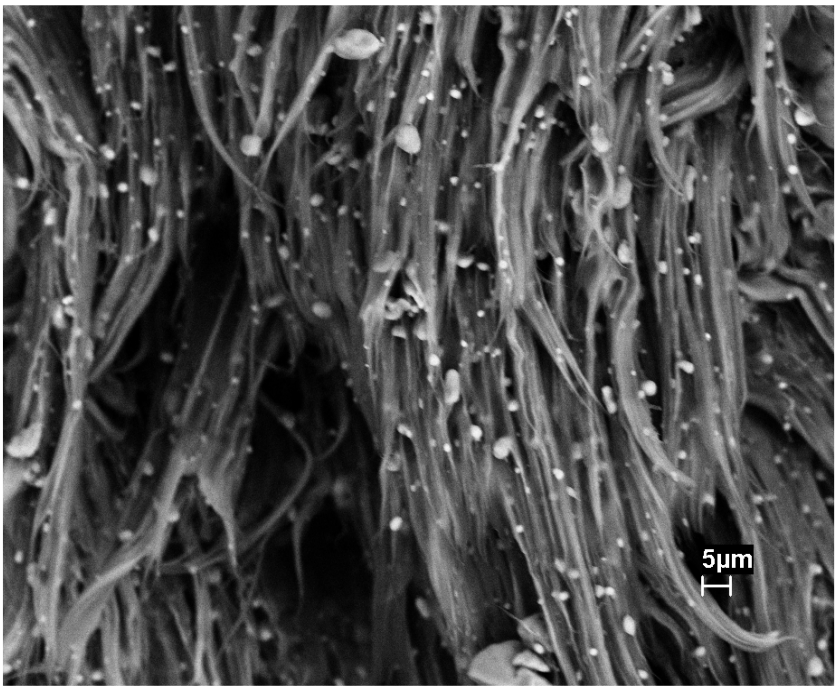

(b)

Figure 4.15 SEM images for fractured surface of blends with 20 wt% TPS.

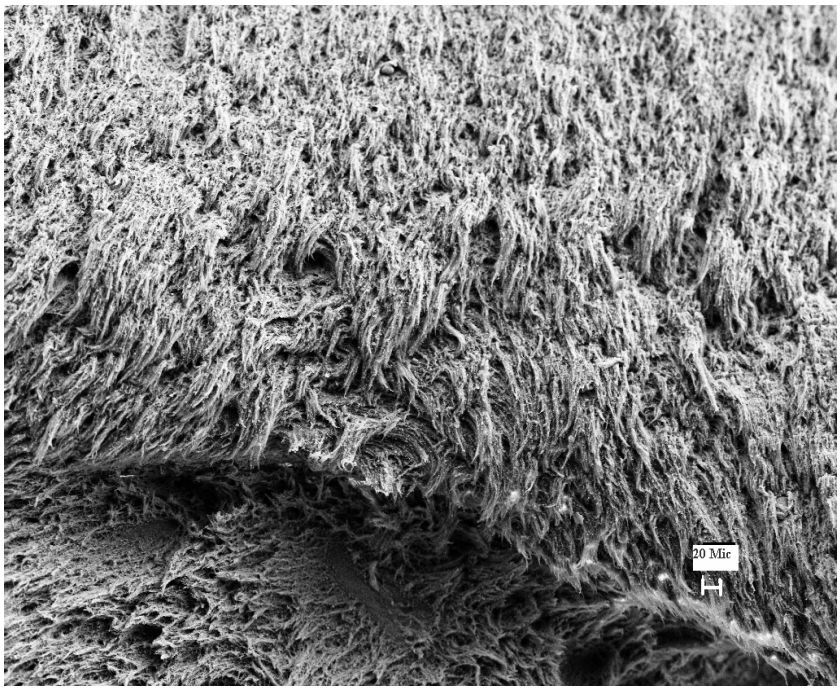

(a)

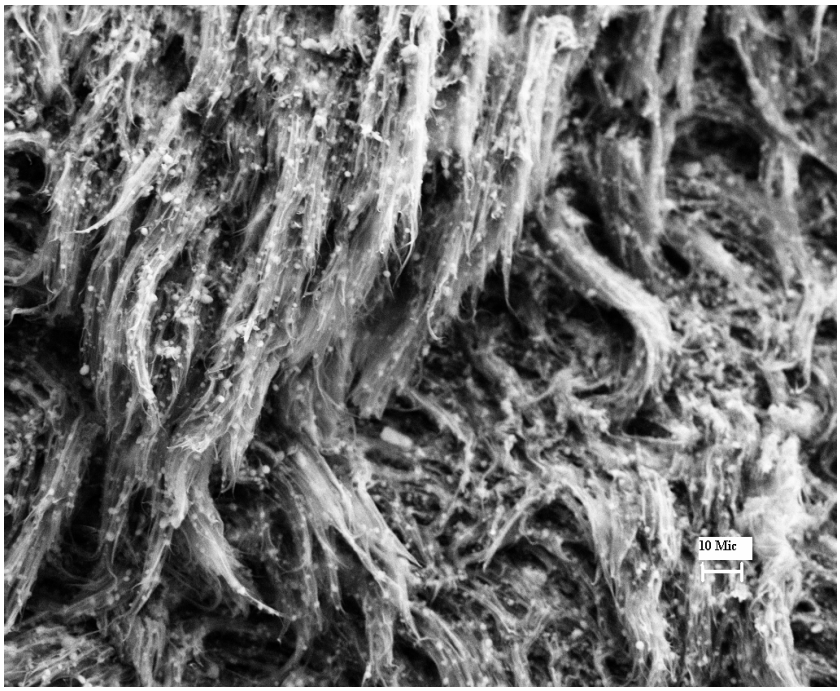

(b)

Figure 4.16 SEM images for fractured surface of blends with 30 wt% TPS.

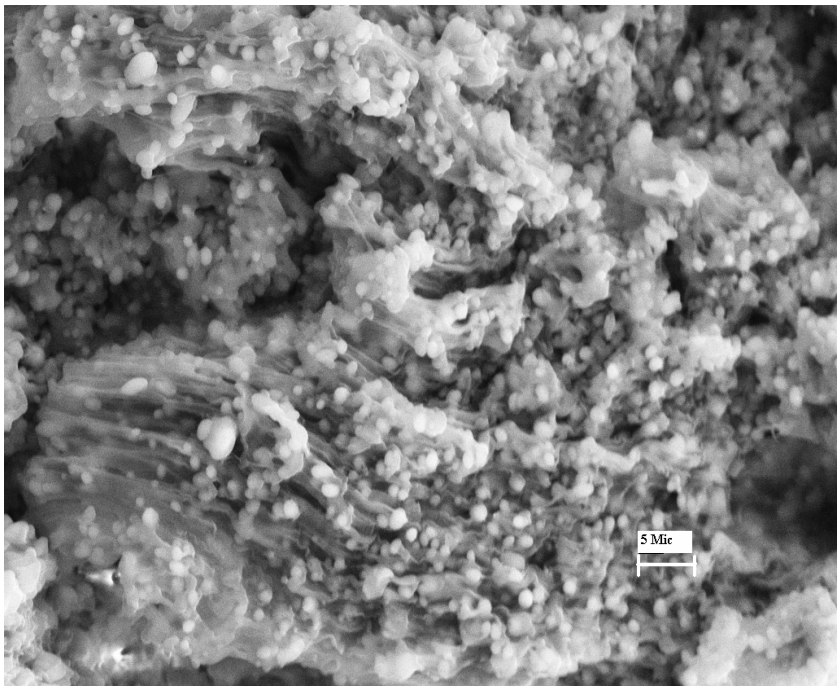

(a)

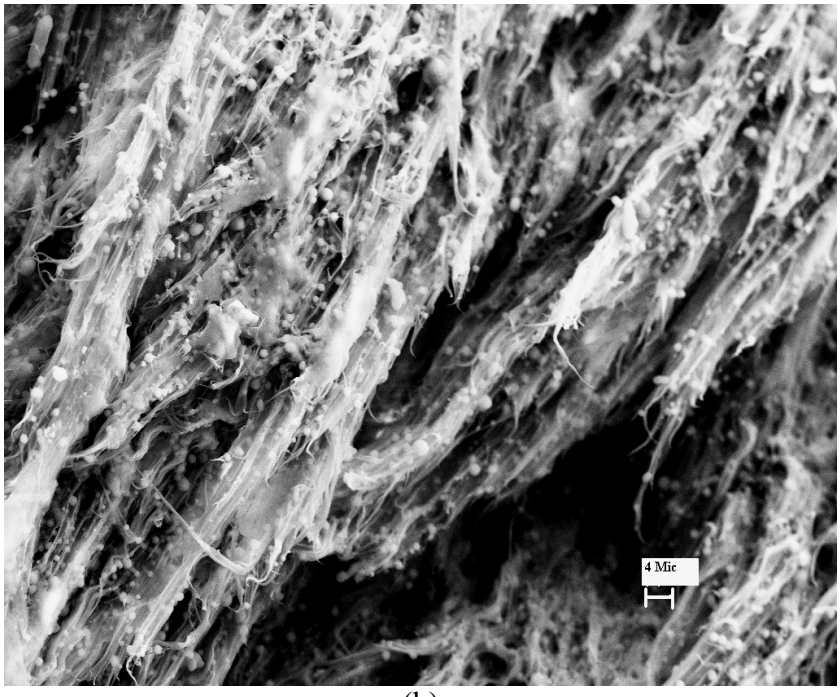

(b)

Figure 4.17 SEM images for fractured surface of blends with 40 wt% TPS.

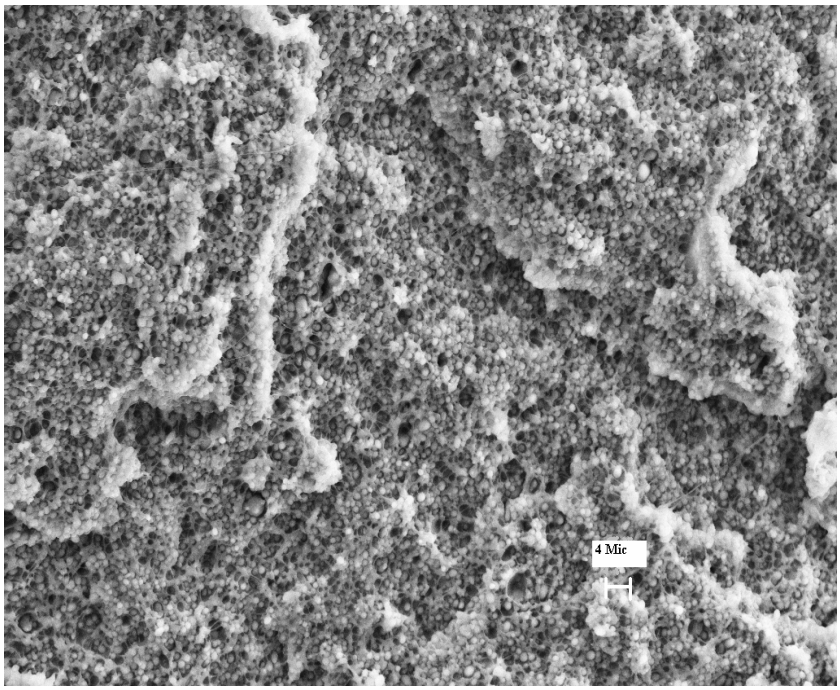

(a)

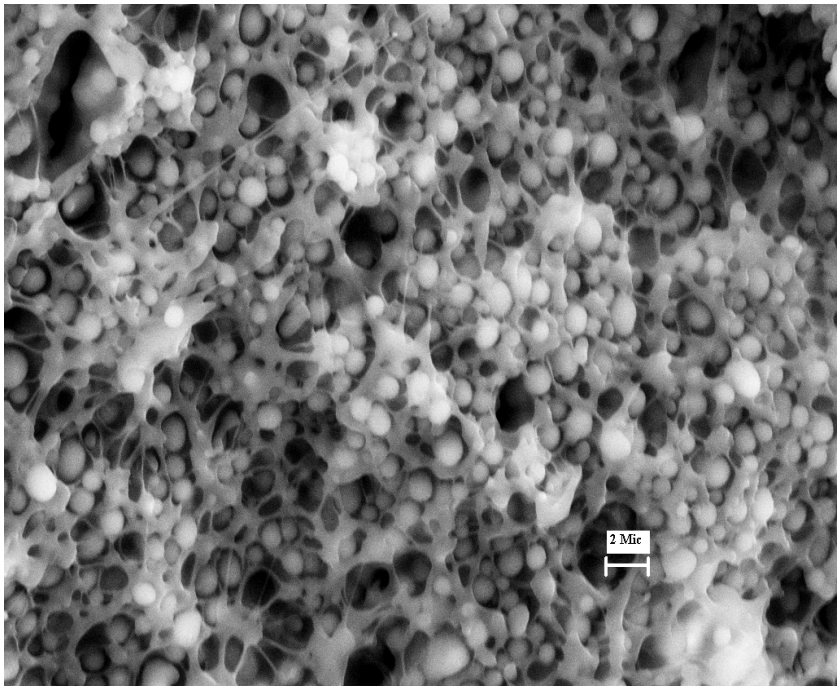

(b)

Figure 4.18 SEM images for fractured surface of blends with 50 wt% TPS.

4.3 Rheological Properties of Blend Components at Processing Temperature

Polymeric materials exhibits an unusual deformation and flow behavior due to their viscoelastic behaviour. The deformation of a polymer is due to stresses imposed on it. During extrusion processes, polymer melts are exposed to shear stress that is increasing with increasing shear rates. In a typical extrusion process, shear rate varies between 10-100 s^{-1} and it is directly proportional to the screw speed.

The production of polymeric blends with good morphology does not only depend on the nature and amount of the components or type of the compatibilizers, but it is also significantly affected by the processing conditions. In order to achieve good mixing by melt compounding process, it is important to provide good interaction between the components during flow inside the extruder. This can be achieved by performing the extrusion process at the optimum processing conditions, like temperature and screw speed, so that the flow characteristic of each components are similar. By this way, the efficient contant area can be provided between the polymeric materials.

The apparent viscosity data as a function of shear rate for LDPE, TPS and compatibilizer (MAgPE), for the temperature range at which the extrusion process was performed, are shown in Figure 4.19. As observed from these figures, with increasing shear rate, the apparent viscosity of the three samples exhibited a declining trend, and such flow behavior is mainly due to the shear thinning (or pseudoplastic) behavior of the polymers. The results also showed that at the temperature of 155, 165 and 175^{o}C and the shear rate of around 70 s^{-1}, corresponding to the shear rate generated during processing of the components, the viscosity of the components are very similar, especially for LDPE and MAgPE (see Figure 4.20). These flow behaviors confirm the formation of good morphology with fine dispersion of TPS phase by providing interaction at the molecular level during melt blending process.

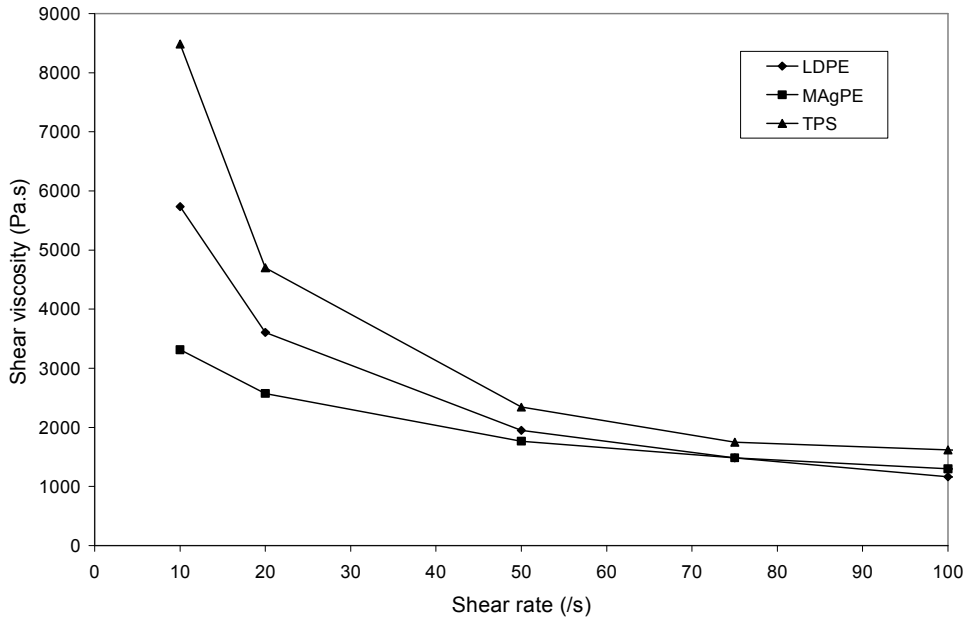
9000
8000
7000
6000
5000
4000
3000
2000
1000
0
Shear viscosity (Pa.s)
0
10
20
30
40
50
60
70
80
90
100
Shear rate (/s)
LDPE
MAgPE
TPS

(a)

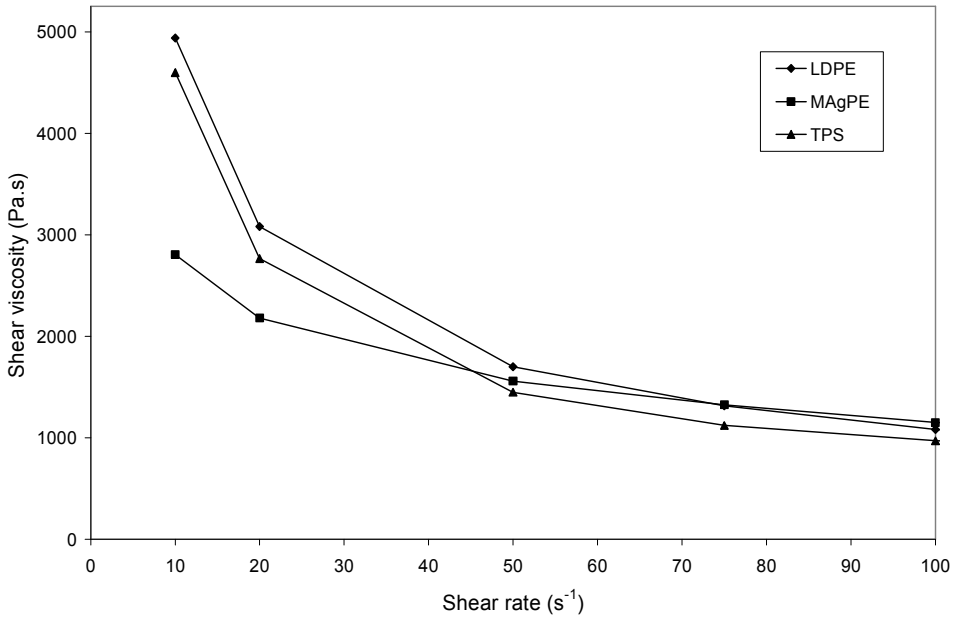
5000
4000
3000
2000
1000
0
Shear viscosity (Pa.s)
0
10
20
30
40
50
60
70
80
90
100
Shear rate (s-1)
LDPE
MAgPE
TPS

(b)

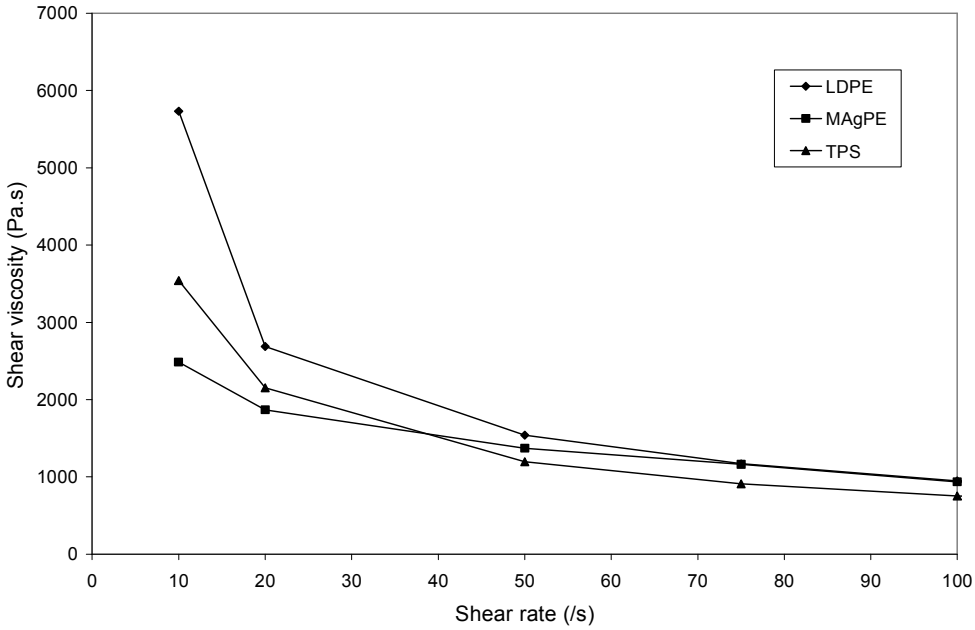

(c)

Figure 4.19 Flow properties of the blend components at (a) 155°C, (b) 165°C and (c) 175°C.

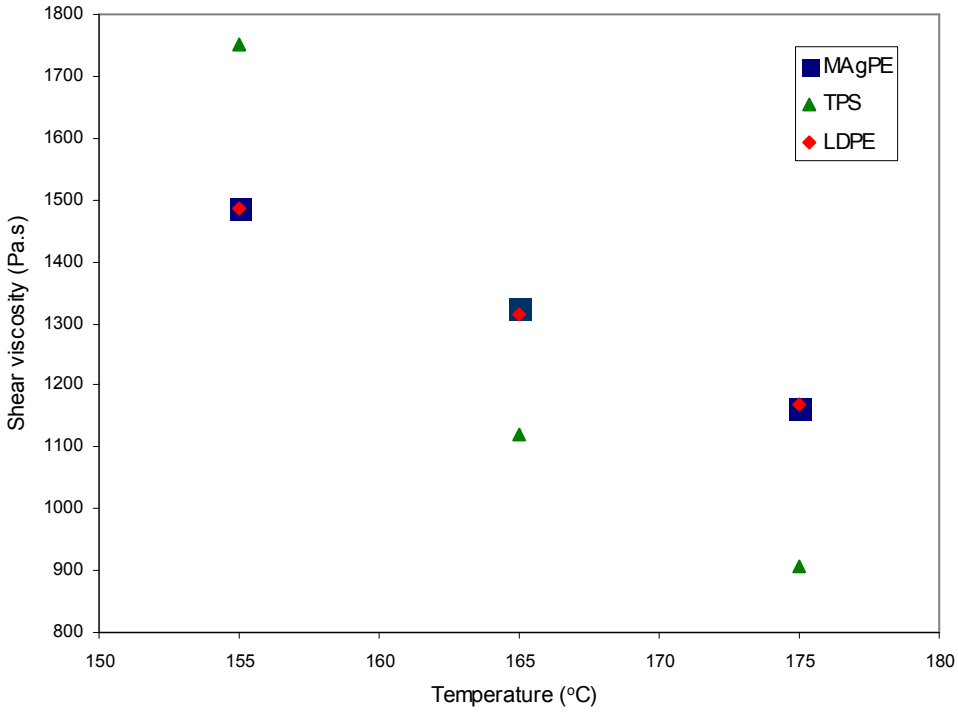

Figure 4.20 Change in shear viscosities of LDPE, TPS and MAgPE with temperature at shear rate of ~70 s^{-1}.

4.4 Properties of Polyethylene-Organoclay Masterbatch Samples

Previously, it was found that the preparation of TPS-Na^+mmt nanocomposite and its melt blending with LDPE resulted in product with improved mechanical properties as compared to the blends containing clay-free biopolymers. The clay used was natural clay due to its similar polarity with starch molecules and therefore it mainly resides inside the starch phase after blending with synthetic polymer. In order to understand the effect of clay type and its incorporation method on the mechanical as well as physical properties of the blends, besides natural clay, two types of organoclay namely Viscobent and Nanofil SE3000 that are compatible with polyethylene matrix were used to prepare biodegradable nanocomposite products. Both are alkyl ammonium modified organoclays but the later was additionally coated with organic compound (silane coupling agent) in order to make its surface more compatible with polyolefins.

4.4.1 Effect of Compatibilizer and Organoclay Type

Polyethylene and clays have very different polarities therefore most of the time their combination results in microcomposites having phase separated morphology. Even though clays are made organophilic by the treatment with alkyl ammonium salt, their surface are still polar and therefore they need compatibilizer to be dispersed at nano-scale in polyethylene.

In the present study, LDPE-organoclay masterbatches with 20 wt% Viscobent were prepared by using three different compatibilizers which are E-BA-GMA terpolymer, MAgPE and EVOH. The effect of compaibilizers on the dispersion of organoclay in LDPE matrix was investigated by determining the height of the organoclay layers using x-ray diffractometer, the size of the clay particles in polymer matrix using SEM images and the change in mechanical properties of the main matrix using tensile test of the injection molded samples. The compatibilizers were used in the preparation of masterbatch and than masterbatch was diluted with LDPE in a twin screw extruder. The amount of clay in the final formulation was fixed at 2 phr.

Xrd results given in Figure 4.21 revealed that the clay layers heights initially being 3.3 nm increased to 3.5 nm in masterbatch with EVOH (PE/EVOH/20Vis), and to 3.6 nm in masterbatch containing Elvaloy (PE/Elv/20Vis). The peak remained at 3.3 nm in masterbatch with PG (PE/PG/20Vis) but the peak with d-spacing of 1.2 nm corresponding to unmodified clay layers seems to be shifted to the lower angle with $2\theta=5^{o}$, indicating the efficiency of the compatibilizer in driving the polymer chains between the clay layers. Comparing the intensity ratios of peaks at around $2\theta=3^{o}$ and $2\theta=5^{o}$ for different masterbatches, the highest ratio belongs to the sample having PG as compatibilizer. This indicates that the number of clay layers that have been intercalated upto 3.3 nm is higher in masterbatch containing PG.

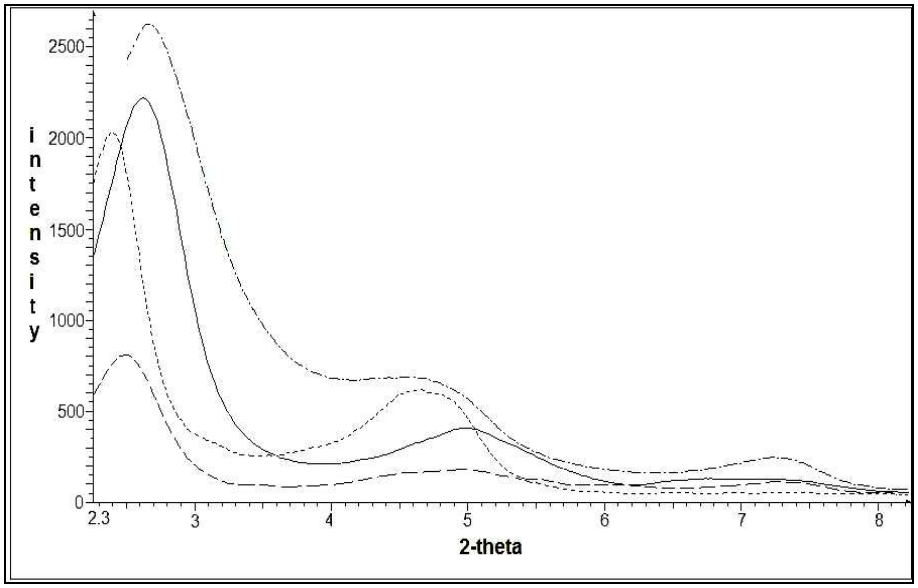

Figure 4.21 X-ray diffraction patterns of a) virgin organoclay (viscobent), indicated by, discontinuous line and points (_._._) b) PE/PG/20Vis, indicated by continous line (___), c) PE/Elv/20Vis, indicated by points (.....) and d) PE/EVOH/20Vis, indicated by discontinuous line (- - -).

Figure 4.22 shows the effect of using different compatibilizer on the dispersion of organoclay. The presence of clay agglomerates were observed in the sample with EVOH compatibilizer (Figure 4.22a). The voids between the matrix and the fillller indicates the formation of uncompatible microcomposite structure in this composition. Whereas, the finer dispersion of the filer with better interfacial adhesion is evident from the SEM images of the samples with PE/Elv/20Vis and PE/PG/20Vis formulations given in Figure 4.22b and Figure 4.22c.

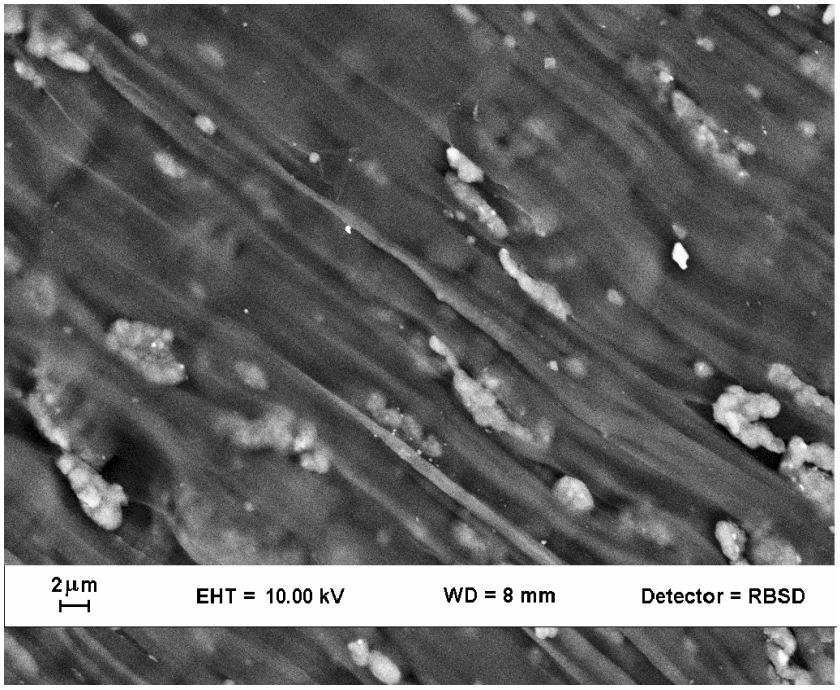
2µm
EHT = 10.00 kV
WD = 8 mm
Detector = RBSD

(a)

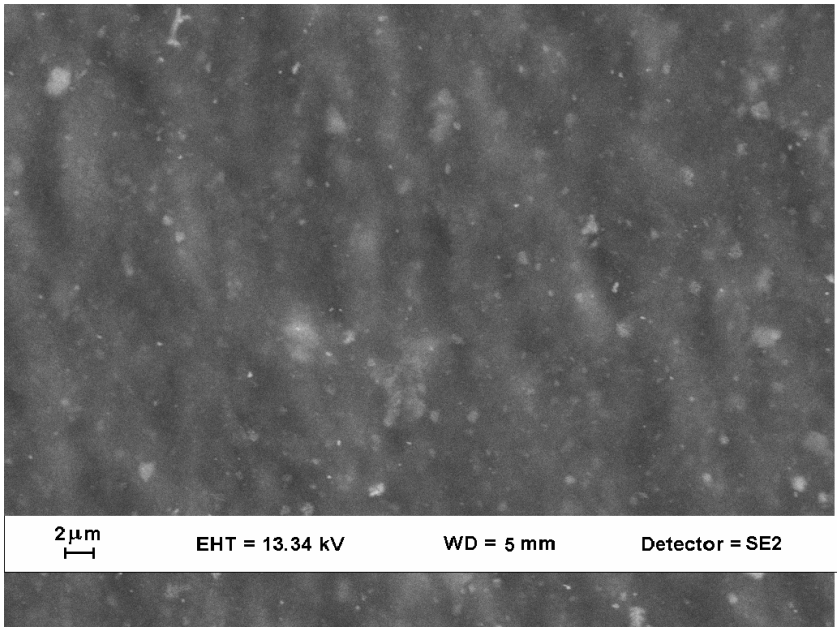
2µm
EHT = 13.34 kV
WD = 5 mm
Detector = SE2

(b)

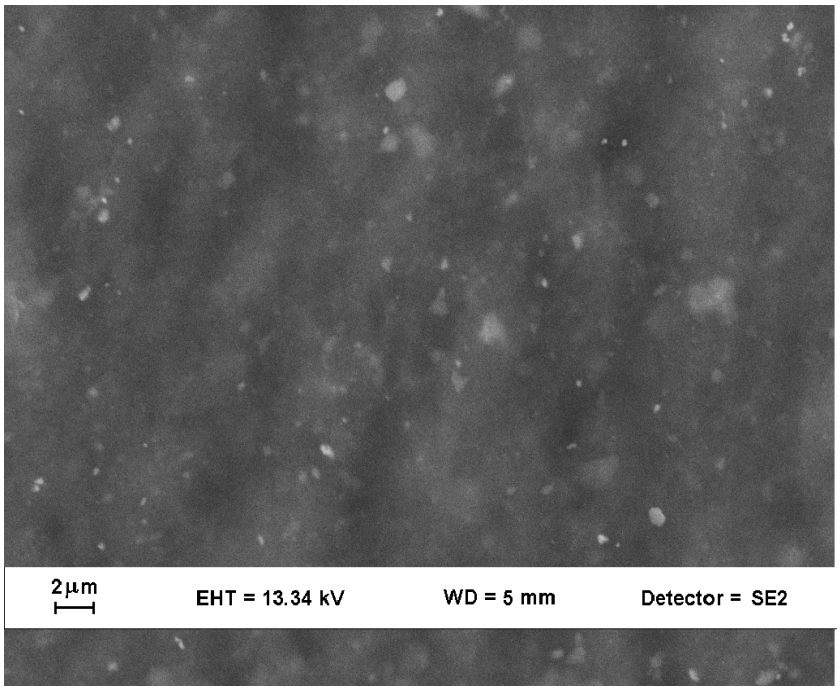

(c)

Figure 4.22 SEM images a) PE/EVOH/20Vis, b) PE/Elv/20Vis and c) PE/PG/20Vis samples.

The change in mechanical properties of injection molded samples having 2 phr organoclay and different compatibilizers (2 wt% based on polymer amount) are provided in Table 4.5. The masterbatch sample with E/BA/GMA terpolymer exhibited slightly reduced tensile strength and modulus even though it contains inorganic filler with good dispersion as observed from xrd pattern as well as SEM images. This behavior is probably due to the low T_g and T_m values of terpolymer compared to LDPE matrix. Even though the tensile properties of the samples are close to each other, PE/PG/20Vis seems to be slightly better in mechanical strength.

Table 4.5 Effect of using different compatibilizers on tensile properties of LDPE-Organoclay samples.

Sample	E (MPa)	F max (MPa)	Strain (%)
PE	133.57 ±10.08	12.04 ±0.08	164 ±13
PE/Elv/Vis	131.04 ±3.22	11.86 ±0.12	156 ±9
PE/PG/Vis	143.91 ±5.10	12.24 ±0.14	156 ± 6
PE/EVOH/Vis	141.02 ±6.63	12.01 ±0.06	149 ±5

After deciding the suitable compatibilizer as being PG for masterbatch production, another type of organoclay (Nanofil SE3000), the surface of which is coated additionally with organic compound, was studied for masterbatch preparation. The same procedure was followed as described above in order to produce masterbatch with 20 wt% organoclay and than nanocomposite with 2 phr organoclay. Xrd pattern of the resultant samples was given in Figure 4.23. It is appearent from the pattern that the polymer chains entered between the clay layers and increased the d-spacing of original organoclay from 3.0 nm to 3.6 nm. The intercalation of polymer chains is indicating the compatibility of the filler with polymer matrix.

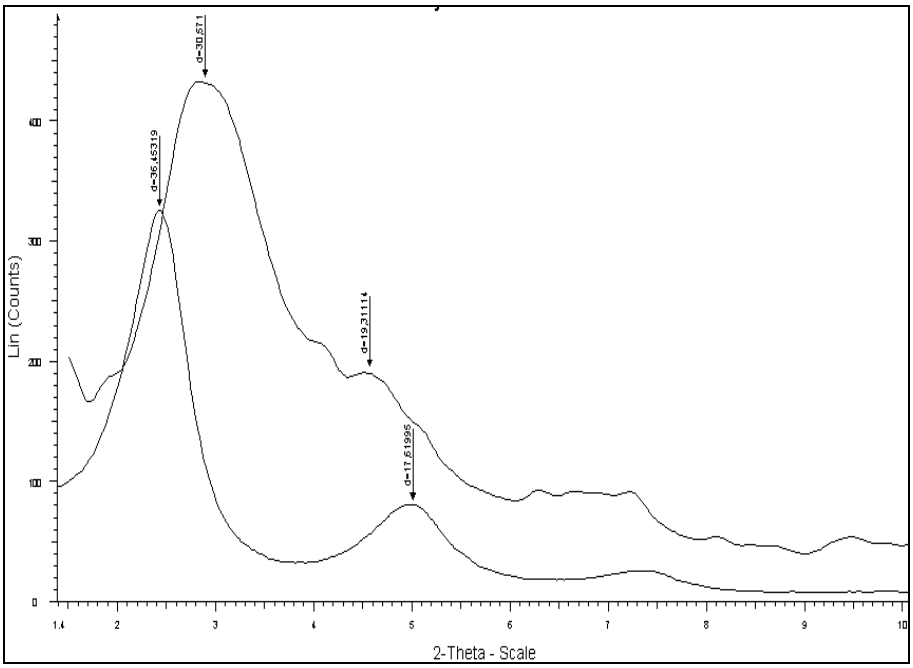

Figure 4.23 X-ray diffraction patterns of a) virgin organoclay (Nanofil SE3000), b) PE/PG/20Nanofil

The fine dispersion of Nanofil SE3000 organoclay particles can be seen in SEM images of Figure 4.24.

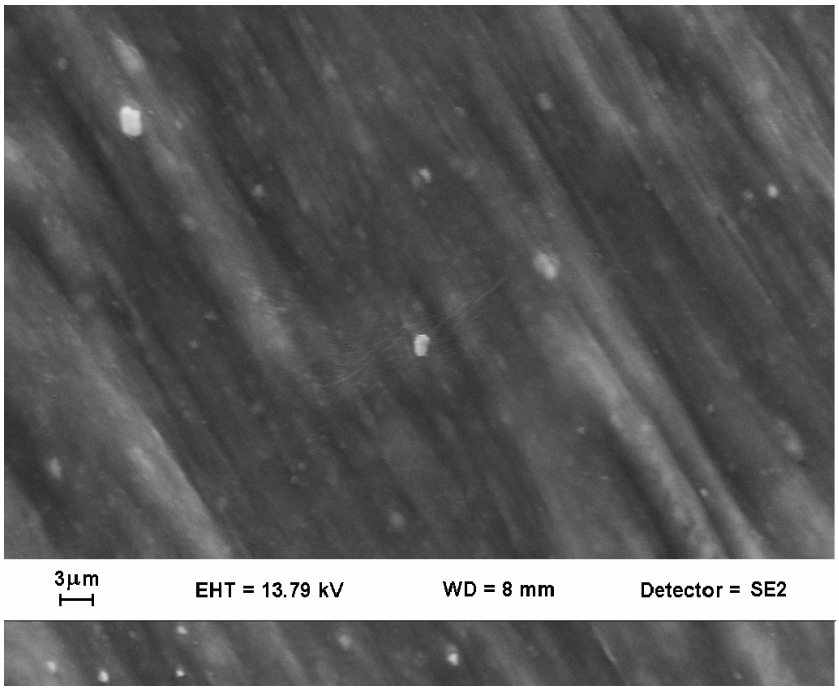

Figure 4.24 SEM image of PE/PG/20Nanofil.

The effect of organoclay type on the mechanical performance of LDPE matrix was shown in Table 4.6. The tensile strength, especially the elongation at break of polyethylene matrix were found to be improved with Nanofil SE3000 more pronouncedly than with Viscobent, indicating the strong interfacial adhesion and efficient stress transfer mechanisim between the filler and polymer matrix. The reason for significant improvement in elongation at break of LDPE with 2 phr Nanofil might be related with the change in crystallinity of polymer chains. The clay layers can inhibit the growing of polymer crystallites by decreasing the chain mobility and result in reduced degree of crytallinity [89]. The occurance of this mechanism was investigated by DSC analysis and the related thermogram was illustrated in Figure 4.25. The percent crystallinity (X_c) of the LDPE phase was determined with the following equation:

$$X_c = \Delta H_f / \Delta H^o_f \times 100 \qquad (4.1)$$

The heat of fusion (ΔH_f) of the samples was determined by the calculation of the area under the peaks. ΔH^o_f is the heat of fusion for the 100% crystalline LDPE and was taken to be 287.6 J/g. [112]. The results exhibited that the crystallinity decreased by the presence of organoclay particles but the highest reduction occurred with Nanofil

organoclay, exhibiting the formation of more amorphous morphology with higher flexibility.

Table 4.6 Tensile properties and degree of crystallinity (X_c) of LDPE nanocomposite samples with different clay types.

Sample	E (MPa)	F max (MPa)	Strain (%)	X_c (%)
PE	133.57 ±10.08	12.04 ±0.08	164 ±13	36.3
PE/PG/Nanofil	137.62 ±7.86	12.42 ±0.16	190 ±10	32.9
PE/PG/Vis	143.91 ±5.10	12.24 ±0.14	156 ±6	35.9

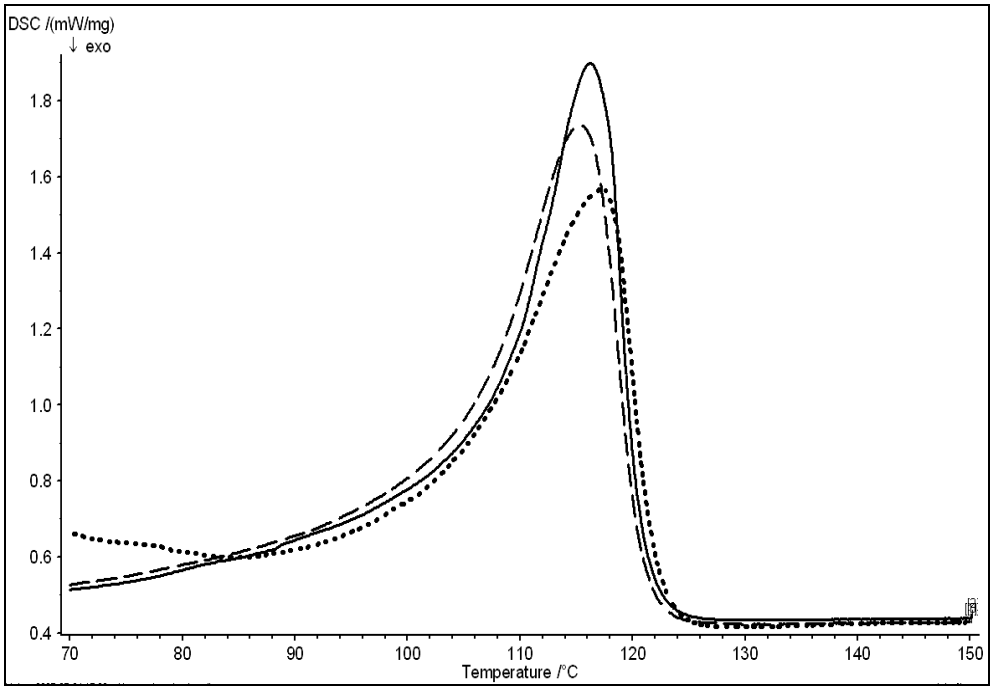

Figure 4.25 DSC thermograms of LDPE shown by straight line(——), PE/PG/Vis shown by discontinous line (- - -) and PE/PG/Nanofil shown by points (**.....**).

4.5 Preparation and Properties of LDPE/TPS Nanocomposite Cast Films

In order to evaluate film-forming abilities of the samples, the granules obtained in twin-screw extruder were extruded onto a cast roll to produce continuous films with about 70 μm. The performance of the films was evaluated by determining mechanical

properties, heat seal properties, tear strength properties, transparency and barrier properties.

Nanocomposite films were prepared in two different ways: first one includes Nanofil as organoclay that had been incorporated into LDPE matrix as it was previously mentioned in Section 4.4.1 to produce masterbatch (MB), which has a composition of LDPE/PG/20Nanofil. The product was than prepared by melt blending of LDPE, TPS, PG and MB. Second one includes Na^+mmt in TPS matrix that was prepared by single step melt intercalation technique as described in Section 3.4.3. TPS-Na^+mmt granules were than melt blended with LDPE in the presence of PG as compatibilizer.

Obtained TPS-Na^+mmt granules were characterized by X-ray diffractometer and the resultant pattern was given in Figure 4.26. The characteristic pattern of TPS as described in Section 4.2.2 is apparent from the figure showing the conversion of starch crystalline domains into TPS with more amorphous morphology. The peak which corresponds to d_{001} spacing of Na^+mmt was observed at around 5^o indicating the intergallery expansion up to 1.76 nm. The absence of any peak at 1.14 nm shows the efficiency of intercalation mechanism in an extrusion process.

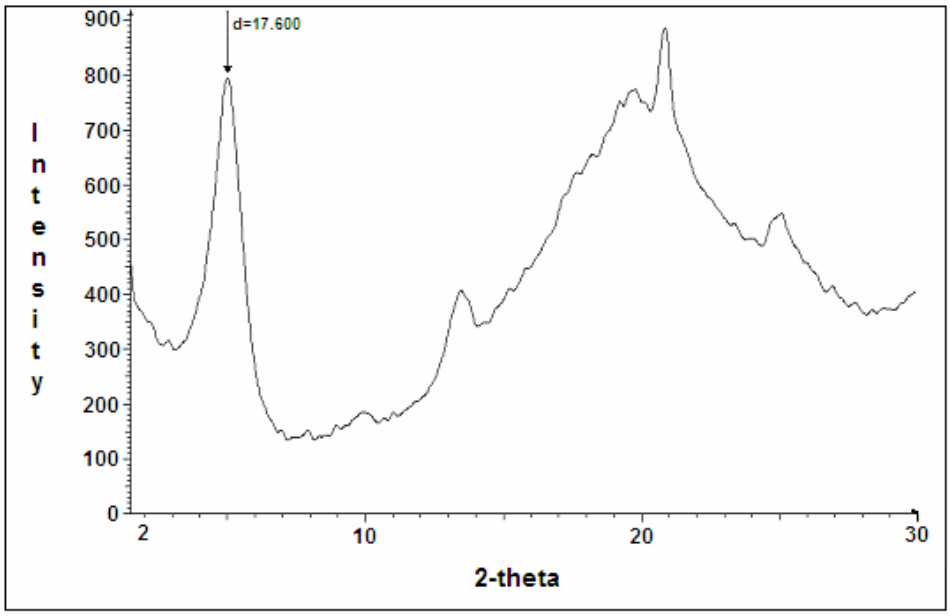

Figure 4.26 X-ray pattern of TPS-Na^+mmt granules prepared by melt intercalation technique.

The homogeneous dispersion of clay layers in TPS matrix is also apparent from SEM image given in Figure 4.27.

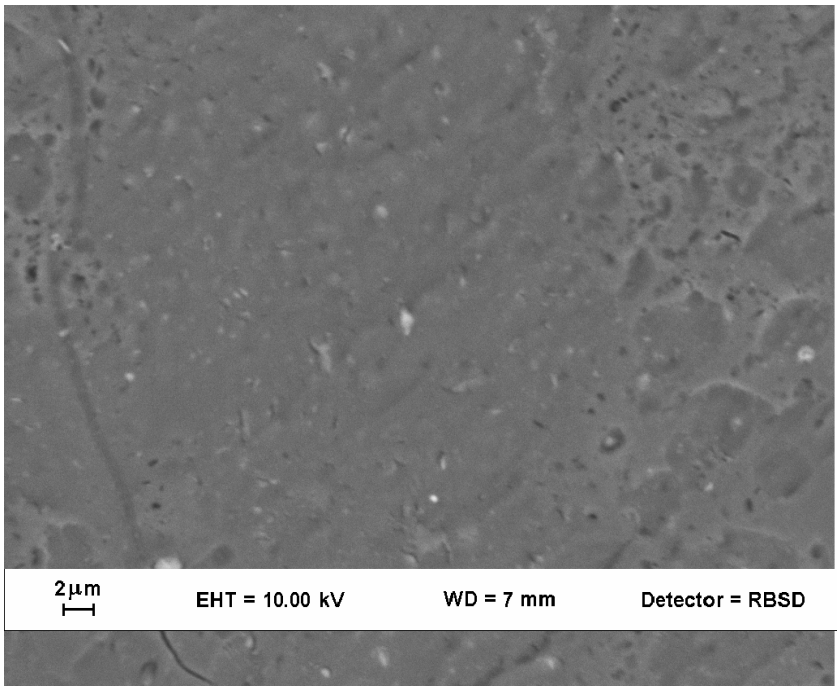

Figure 4.27 SEM image of TPS-Na^{+}mmt film prepared by melt intercalation technique.

4.5.1 Tensile Properties

Table 4.7 illustrates the mechanical properties of the cast films. Tensile strength of LDPE film was found to decrease with TPS incorporation as opposite to the reinforcing effect observed in injection molded samples. This difference is mainly due to the different orientation of polymer chains in two different processes. In injection process, the orientation takes place at the wall of the mold while the interior remains more amorphous. [113]. Therefore, entanglement occurs between PE and MAgPE chains at the interior of material. These entanglements act as physical crosslinking points and make the stress transfer from matrix to starch particles more efficient through the formation of interpenetrating polymer chains system. In cast films, on the other hand, stress transfer between the components are inhibited by higher degree of polymer chain orientation.

Considering the effect of dispersed particle size on the mechanical properties of the blends, it is appearent that larger TPS size, in the range of 1-3 μm in cast films, (see Figure 4.28) as compared to the average size of 1 μm particles in injection molded samples should also be effective in observing the decrease in tensile strength. The

processing conditions are considered as the reason for different TPS size in different shaping processes since all the other factors affecting the size of the disperse phase were the same. In injection molding process, the polymer injection and the cooling process are performed under high pressure in a very short time so that the moisture or any unreacted plasticizer can not leave the system. However, in film process, the polymer melt that was under pressure untill the die are cooled in normal atmospheric conditions and at low pressure so that any remainig plasticizer (water or glycerol) in TPS can evaporate and cause TPS particles to swell. The similar results were also reported in other studies related with LDPE/Starch blown film [109] and cast films [5].

The tensile strength of PE/PG/40TPS film was improved by the addition of organoclay, while it remained almost at the same level with the addition of Na^+mmt. In LDPE/MA/20TPS-Na^+mmt film samples, the effect was the opposite (see Section 4.2.3). This is due to the different fracture mechanisms observed in these samples. The load applied during the tensile test is carried by both starch and LDPE matrix at low TPS content such as 20 wt%. Therefore, any filler having reinforcing feature in any phase would be effective in stress transfer mechanism and makes the film more resistant to the applied load. However, as TPS content increased to 40 wt%, the fracture occurs first at the weak interface between TPS and LDPE with the formation of voids that has been observed during tensile tests, so that only LDPE matrix with smaller cross section continues to carry the load until the chains are broken. Thus, reinforcing LDPE matrix with nanoclay resulted in improved tensile strength while reinforcing mainly TPS phase with Na^+mmt does not have any influence on the stress transfer mechanism.

The modulus increased and elongation at break decreased with TPS addition in a similar manner as it was observed in injection molded samples and this was attributed to the stiffenning effect of rigid TPS particles. The presence of organoclay or Na^+mmt had little effect on elongational properties but increased the modulus about 40%.

Figure 4.29 shows the dispersion of clay particles in cast films. In both nanocomposite formulations prepared with different type of clays, the homogeneous dispersion of clay layers with the absence of any tactoids or agglomerates is evident from SEM images.

Table 4.7 Tensile properties of LDPE with 40 wt%TPS cast films.

Sample	Tensile Strength (MPa)	Strain at Break (%)	Young's-Modulus (Mpa)
PE	26.9±1.4	166±13	250.2±11.5
PE/PG/ 40TPS	20.7±0.4	117±26	404.0±17.2
PE/PG/40TPS-Na^+mmt	19.4±0.7	97±18	570.1±25.7
PE/PG/40TPS/ Nanofil	23.4±0.9	105±9	576.3±34.6

* All the properties were measured in machine direction.

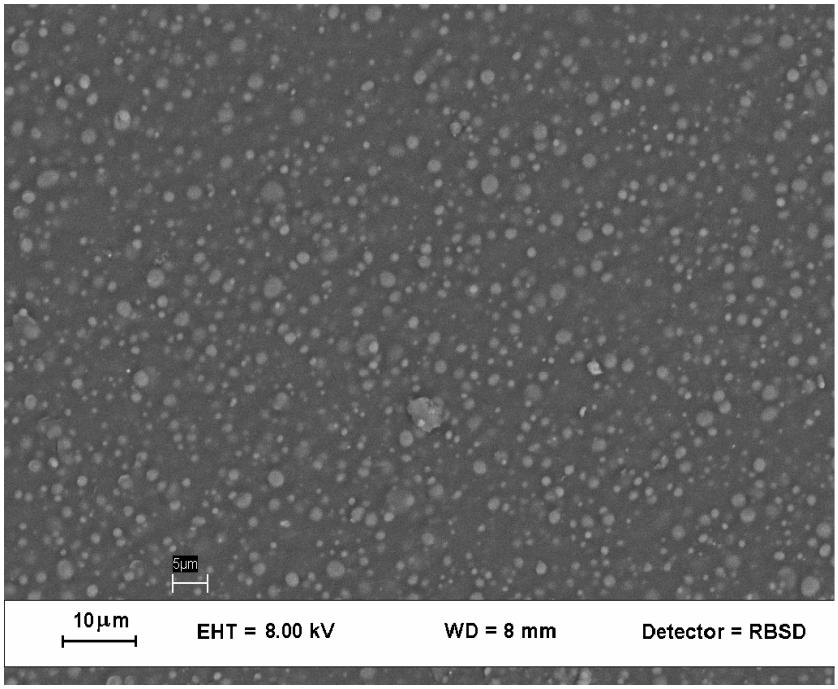

(a)

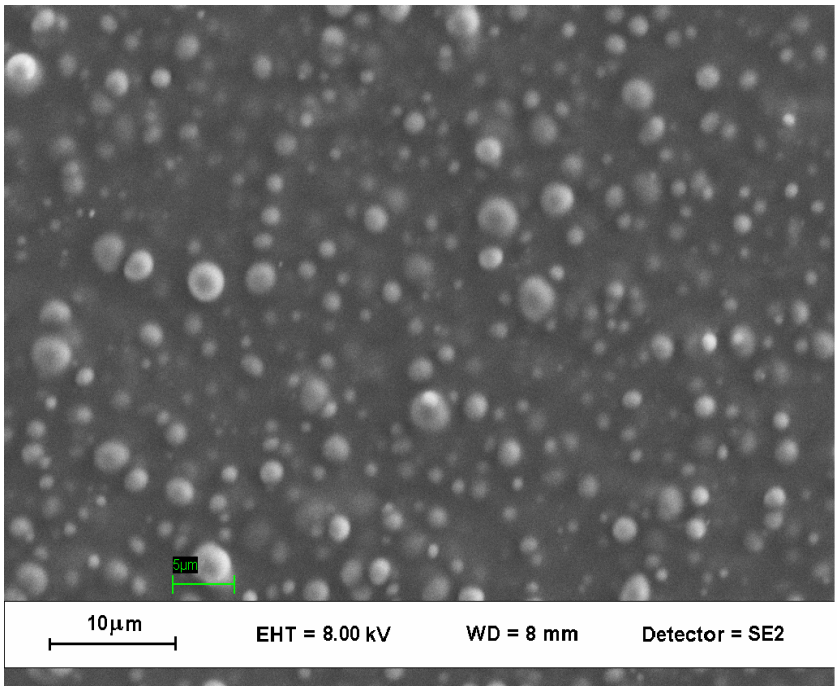

(b)

Figure 4.28 SEM images of PE/PG/ 40TPS cast films.

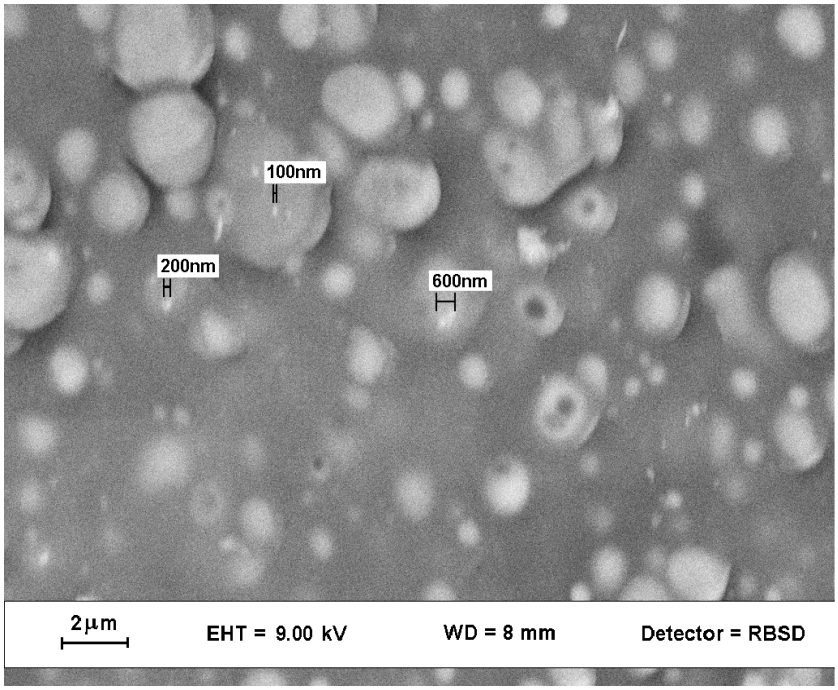

(a)

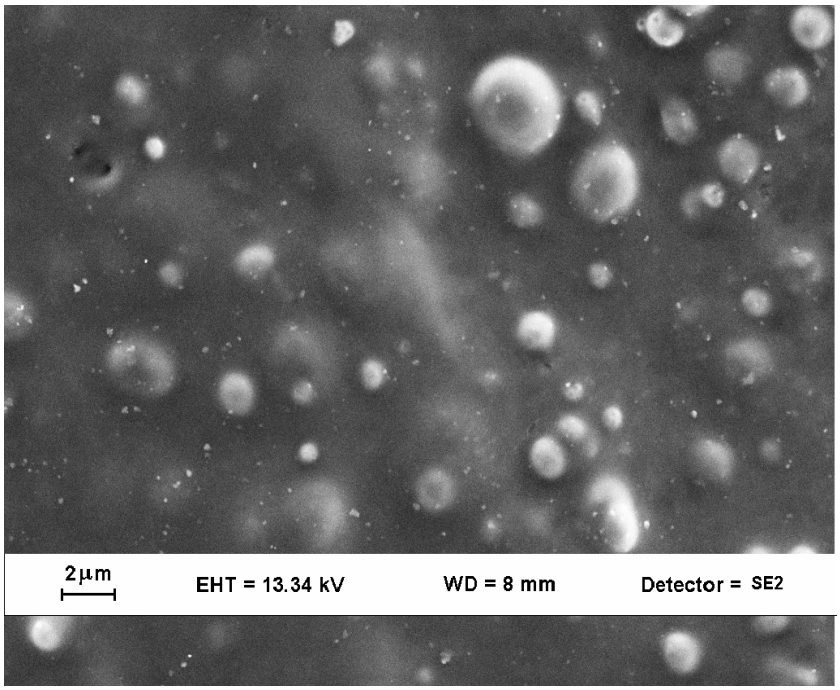

(b)

Figure 4.29 SEM images of (a) PE/PG/40TPS-Na^{+}mmt, (b) PE/PG/40TPS/Nanofil cast films.

4.5.2 Tear and Heat Seal Strengths

Tear strength is an important property for packaging applications. In easy opening solid food packaging applications such as coffee, ketchup, soup, snack food stick packs, etc., the low tear strength property in both MD and CD directions is highly desired. LDPE has high tear strength property in both directions. Therefore, to make easy opening packaging using LDPE, three layer co extruded films are produced where HDPE is blended with LDPE in the core layer in order to have lower tear strength in MD or CD by creating some incompatibility to start and propagate the tearing. Table 4.8 illustrates tear strength properties of biodegradable blend films. The incorporation of TPS into LDPE matrix satisfied the requirement necessary for easy opening packaging applications by reducing the tear strength properties of LDPE in both directions. No significant change in tear strength values was observed after the addition of clay.

Heat seal strength is another important property for packaging applications since it prevents the leakage or lose of the contents from the sealed section of the packaging

material and it is directly proportional to the weight of the contents. It is generally known that heat seal strength of commercial compostable plastics such as PLA is very low (about 200 gf/15 mm for PLA film of NatureWorks Company) [114] and therefore they are mostly used in the outside layer of the packaging materials.

Seal strength of LDPE/ starch blend films were determined by tensile load after finding the seal initiation temperature, under standard dwell time, and pressure condition. The results were presented in Table 4.8. The seal initiation temperature of the films were close to each other i.e., there was no negative effect of TPS on heat sealability of LDPE film. It was observed that heat seal strength of LDPE itself dropped by 65% with the addition of 40 wt% TPS but the value is still higher than 1000 gf/15mm, indicating that it is strong enough to carry the heavy loads without bursting. It was found that the presence of Na^+mmt did not affect the result significantly while the incorporation of organoclay into LDPE matrix improved the heat seal property of the blend by %23. This improvement is in consistent with the enhancement observed in tensile strength of PE/PG/40TPS film with organoclay addition and it is related with the reinforcement of LDPE matrix which is the main load carrying phase in this blend formulation.

Table 4.8 Tear and Heat Seal Strengths of LDPE with 40 wt%TPS cast films.

Sample	Tear Strength (N)		Heat Seal Temperature (^oC)	Heat Seal Strength (gf/15 mm)
	MD	CD		
PE	1.72±1.56	4.17±0.29	117	4261.34±100.71
PE/PG/ 40TPS	0.22±0.04	2.87±0.16	119	1476.98±168.25
PE/PG/40TPS-Na^+mmt	0.28±0.04	2.38±0.50	114	1818.56±151.13
PE/PG/40TPS/ Nanofil	0.23±0.01	2.99±0.14	117	2483.47±266.52

4.5.3 Barrier Properties

Barrier properties such as water vapour transmission rate (WVTR) and oxygen transmission rate (OTR) of plastic packaging materials play an important role in designing food packaging materials. The barrier requirements for food staffs are complex since foods are often dynamic systems with limited shelf life and require very specific packaging requirements. For example, high WVTR and OTR barrier are necessary for snack food packaging materials while high moisture barrier with high oxygen permebility is desired for fresh meat products [106].

In general, starch-based packaging materials exhibit high water vapour permeability, and therefore need to be improved before used for food packaging where the moisture barrier property is crucial. For example, the WVTR value of commercial PLA film with 40 μm thickness is known to be 120 g/m^2d that is measured at 38°C and 90% RH. [105]. Improved moisture barrier may be achieved by coatings or the use of films with multiple layers of complementary properties. At present, biopackaging is known to be most suitable for food with high respiration (fruit and vegetables) or food with short shelf life (bread, convenience food, etc.) because of the poor water barrier properties of this materials [115-118].

Barrier properties of LDPE-TPS blend cast films were presented in Table 4.9. WVTR value of LDPE film increased after TPS addition from 4.1 g/m^2d upto 15.6 g/m^2d (the thickness of the films are 60 μm). The increase in water permeability properties with increasing starch content in LDPE-Starch blends was also reported in other studies [5, 118-120]. Looking at the WVTR values of nanocomposite film, it was found that the moisture barrier properties of LDPE/40TPS blends were improved by 9% and 16% with the use of organoclay and Na^+mmt, respectively. The better barrier properties of the film samples containing Na^+mmt was attributed to the presence of clay layers mainly in TPS phase where the moisture permeability is very high. The swelling properties of natural clay by water absorption could be the another possible reason for this observation.

Oxygen transmission rate of LDPE was decreased by 21% with the incorporation of TPS. This is because oxygen barrier properties of LDPE film is poor due to its

hydrophobic character, while hydrophilic polymers are known to have lower OTR values. Unexpectedly, the addition of clay decreased the oxygen barrier properties of blend and more pronounce decrease was observed with organoclay. It is generally known that besides the components of blends, the presence and size of microcrystallites significanty affect the gas barrier properties of polymeric materials [119]. The crystal growth in LDPE film was found to be inhibited by clay layers determined from DSC analysis and the percent crytallinity reduced from 35% to 30.8% after incorporation of Nanofil clay (See Table 4.10). Since oxygen gas transmission is more favorable in amorphous or less crystalline polymer films, this result may explain the reason in observing higher OTR in nanocomposite films. This suggestion was also evident from OTR values of LDPE films which is 16.5% less as compared to that of LDPE/Nanofil nanocomposite films.

Table 4.9 Gas Barrier Propeties of LDPE with 40 wt%TPS cast films.

Sample	**WVTR (g/m^2d)**	**OTR (mL/m^2d)**
PE	4.1	2285
PE/PG/ 40TPS	15.6	1809
PE/PG/40TPS-Na^+mmt	13.1	1869
PE/PG/40TPS/ Nanofil	14.2	1950

Table 4.10 OTR values and crystallinity degree (X_c) of LDPE and LDPE/Nanofil nanocomposite films.

Sample	**OTR (mL/m^2d)**	**X_c (%)**
PE	2285	35.0
PE/Nanofil	2662	30.8

4.5.4 Contact Angle and Surface Energy Properties

The results of contact angle and the surface energy measurements conducted using solvents with different polarities are given in Table 4.11. Normally, TPS has hydrophilic character and its presence in 40 wt% in LDPE matrix is expected to increase the wettability of LDPE film by increasing the surface energy. It was reported by Carvaho et al. that the water contact angle and surface energy of TPS films with 30 wt% glycerol are 63^o and 43.6 mJ/m^2 with polar contribution of 14.2 mJ/m^2 and dispersive contribution of 29.4 mJ/m^2, respectively [121]. The unexpectedly low contribution of polar component was explained by the orientation of polar hydroxyl groups either towards the bulk of the material or centre of the helix complexes formed by starch and hydroxyl groups during TPS processing. In the present study, for pure LDPE film, the water contact angle and the surface energy values were found to be 99.9^o, 26.29 mN/m, respectively. According to the *Langmuir's law of surface action*, the surface energy is the sum of the local surface free energies such that:

$$\gamma = r_1\gamma_A + r_2\gamma_B \tag{4.2}$$

where r_1 and r_2 are the fractions of surface covered by componenets A and B, respectively [122]. Thus, this equation states that the surface energy of blend films with %60 wt LDPE should be in between the surface energies of TPS and LDPE components but closer to the value of LDPE. On the contrary, it was experimentally observed that the the surface energy of LDPE itself remained almost unchanged and the water contact angle increased with TPS, indicating the more hydrophobic character of the blend films. This situation can only be explained by *Wenzel state* that was proposed for rough surface where there is a continuous solid-liquid interface by the penetration of the liquid into the grooves completely [123]. According to Wenzel, the appearent contact angle (θ^*) is related to the Young's contact angle (θ) (suggested for the smooth surfaces with the equation of : $\cos\theta = (\gamma_{SV} - \gamma_{SL})/\gamma_{LV}$,where γ_{SV}, γ_{SL} and γ_{LV} represent solid-vapor, solid-liquid and liquid-vapor interfacial tensions), with the ratio of the actual surface area over the projected surface area (σ) such that:

$$\cos\theta^* = \sigma\cos\theta \tag{4.3}$$

This equation suggests that the contact angle of the rough surface should be larger than that observed on the smooth surface.

The PE/PG/40TPS sample with smooth surface was prepared by hot press method and the contact angle of this surface was found to be $88.8^o \pm 5.13^o$. This value explains the reason for observing higher contact angle (114.8^o) for the cast film sample of the same formula. The presence of clay in nanocomposite blend formulations increased the surface wettability only slightly by the polar nature of the clay.

The results also indicate that the cast films produced from LDPE and TPS blends are not printable and require corona treatment for the ink adhesion.

Table 4.11 Contact angles and the surface energies of the cast films.

Sample	Contact Angle (^{o})			Surface Energy (mN/m)		
	Water	HD[1]	EG[2]	γ_{SV}^d	γ_{SV}^p	γ_{SV}
PE	99.9±3.51	11.2±2.86	72.4±2.82	26.97±0.55	0.68±0.08	26.29±0.47
PE/PG/ 40TPS	114.8±1.58	13.8±0.45	80.7±2.33	27.42±0.10	0.18±0.02	27.24±0.08
PE/PG/40TPS-Na^+mmt	107.7±2.86	7.8±0.93	72.8±2.46	28.22±0.18	0.02±0.01	28.20±0.17
PE/PG/40TPS/ Nanofil	107.4±3.71	11.4±1.72	77.7±1.72	26.65±0.31	0.03±0.01	26.61±0.29

γ_{SV}, γ_{SV}^p and γ_{SV}^d indicates total surface energy, polar, and dispersive components, respectively.
[1,2] indicates the use of n-hexadecane and ethylene glycol in contact angle measurements.

4.5.5 Light Transmittance

The transparencies of the cast film samples with similar thickness were determined using UV-Vis spectrophotometer (Figure 4.30). The light transmittance of the films containing 40 wt %TPS was much lower that that of LDPE film. This was attributed to the both surface roughness created by TPS phase with particle size of between 1-3 μm (larger than the wavelength range of the visible light, which is between 400-700 nm), as it was confirmed in Section 4.5.4 and to the presence of second phase with different refractive index.

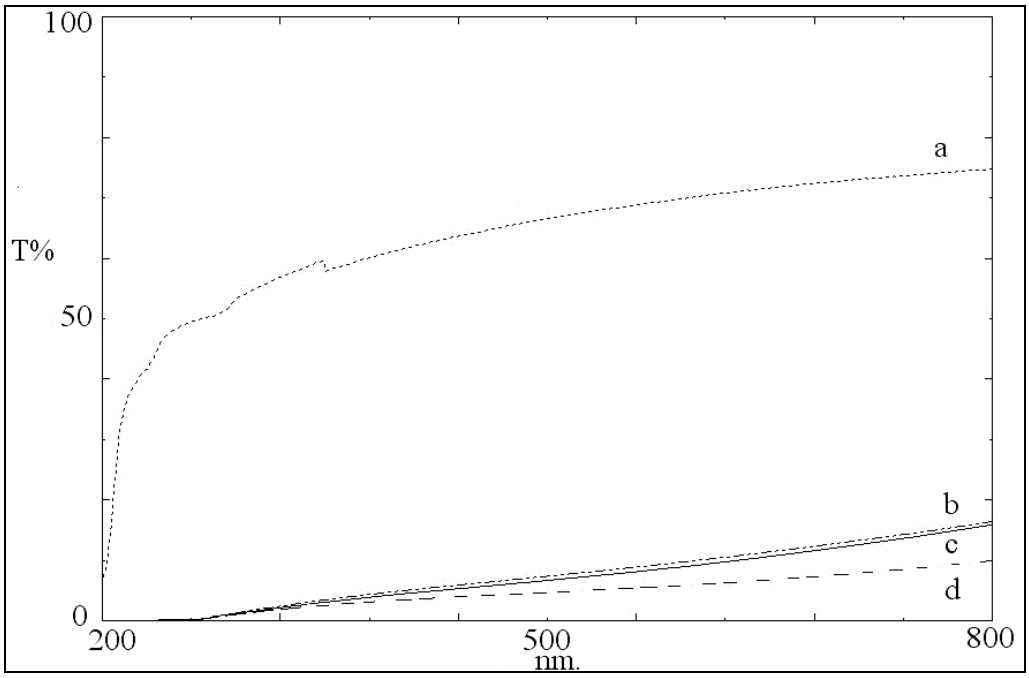

Figure 4.30 UV-Vis transmission spectra of (a) PE , (b) PE/PG/ 40TPS , (c) PE/PG/40TPS/ Nanofil and (d) PE/PG/40TPS-Na^+mmt cast films.

4.6 Properties of LDPE/TPS Nanocomposite Blown Films

The ability of LDPE based biodegradable blends to produce continuous blown film is very important property since most of the LDPE produced commercially are used in blown film application.

The previous results have shown that the enhancement in most of the properties of LDPE/TPS blends were achieved by using organoclay that is mainly present in LDPE phase. Therefore, as nanocomposite formulation, only PE/PG/40TPS/Nanofil was used for the blown film experiments.

Tensile properties of the blown film samples are presented in Table 4.12. Compared with the mechanical properties of the cast films that were given in Table 4.7, the similar tensile strength and % elongation properties were observed in blown film samples. The only significant difference occurred in elastic modulus properties such that blown film samples exhibited higher modulus that was attributed to the higher orientation that was achieved in blown films process. In cast film process, the polymer

melt coming out from the die is cast onto the cold sylinders thus only limited orientation in machine direction during rolling process is allowable before it solidifies. Different from the cast film process, the polymer melt is drawn by passing hot air form the interior surface of the film so that polymer can be oriented while it is still hot. The higher orientation achieved by this cooling and drawn process is the reason for observing higher modulus in blown film samples.

Table 4.12 Tensile properties of the blown films.

Sample	Tensile Strength (MPa)	Strain at Break (%)	Young's-Modulus (Mpa)
PE	24.9±1.4	182±36	333.2±65.1
PE/PG/ 40TPS	20.8±1.4	101±19	559.8±30.6
PE/PG/40TPS/ Nanofil	22.2±1.5	85±21	575.4±27.6

Another important differences between the properties of cast and blown films is the effect of organoclay on the stiffness of the films. In cast film, the organoclay enhanced the modulus of PE/PG/ 40TPS sample by %40, while the improvement is only about %3 in blown film samples. The possible cause for this behaviour in blown film samples is the orientation of the polymer chains that occurs firstly in cross direction due to blowing up process near the die and than in machine direction due to the drawing process. Therefore, besides polymer chains, some of the organoclay layers were also oriented in cross direction so that their effect was decreased in machine direction. On the contrary, as previously mentioned, cast film process induces more orientation towards the machine direction due to the rolling process so that most of the clay layers were oriented in machine direction leading to observe significant stiffness enhancement in this direction. The modulus properties of nanocomposite blown and cast film samples measured from both machine and cross directions corroborate with the discussion above (see Table 4.13).

Table 4.13 Elastic modulus of nanocomposite films measured in machine (MD) and cross (CD) directions.

Sample	Young's-Modulus (MPa)	
	MD	**CD**
PE/PG/40TPS/ Nanofil_ cast film	575.3±34.6	432.5±26.2
PE/PG/40TPS/ Nanofil_blown film	575.4.0±27.6	618.9±35.5

4.7 Normalized Tensile Properties According to Different Shaping Processes

The tensile strength and strain properties of bio-synthetic polymer blends are the most important properties determining the usefulness of the final product. The LDPE/Starch blends obtained in this study were shaped using four different processes, namely hot press, injection molding, film-casting and film-blowing techniques. Each technique provides different tensile properties to the product due to different polymer chain orientations and Figure 4.31 summarizes these properties. Tensile strength values of the samples were normalized according to the maximum tensile strength value of LDPE (26.9 MPa) which was obtained by cast film method and the strain values were similarly normalized by the maximum strain value (about 500%) of LDPE films prepared using hot-press method. In general, it seems that the samples prepared by the same method form their own clusters in the graph. The maximum tensile strain for LDPE was obtained by hot press method and it can never be reached after the addition of starch, irrelavent of the method used. Yet, the 0.2 % normalized strain corresponds to about 100 % and it is high enough for most of the industrial applications. On the contrary, maximum tensile strength value of LDPE belongs to the sample prepared by film-casting method and it can be almost reached by film-casting and film-blowing LDPE/40TPS/Nanofil nanocomposite structures. Compared to different shaping processes, starch containing LDPE samples prepared with film-casting and film-blowing methods seem to be better in tensile strength, while the strain values of the blends are comparable with each other for different methods.

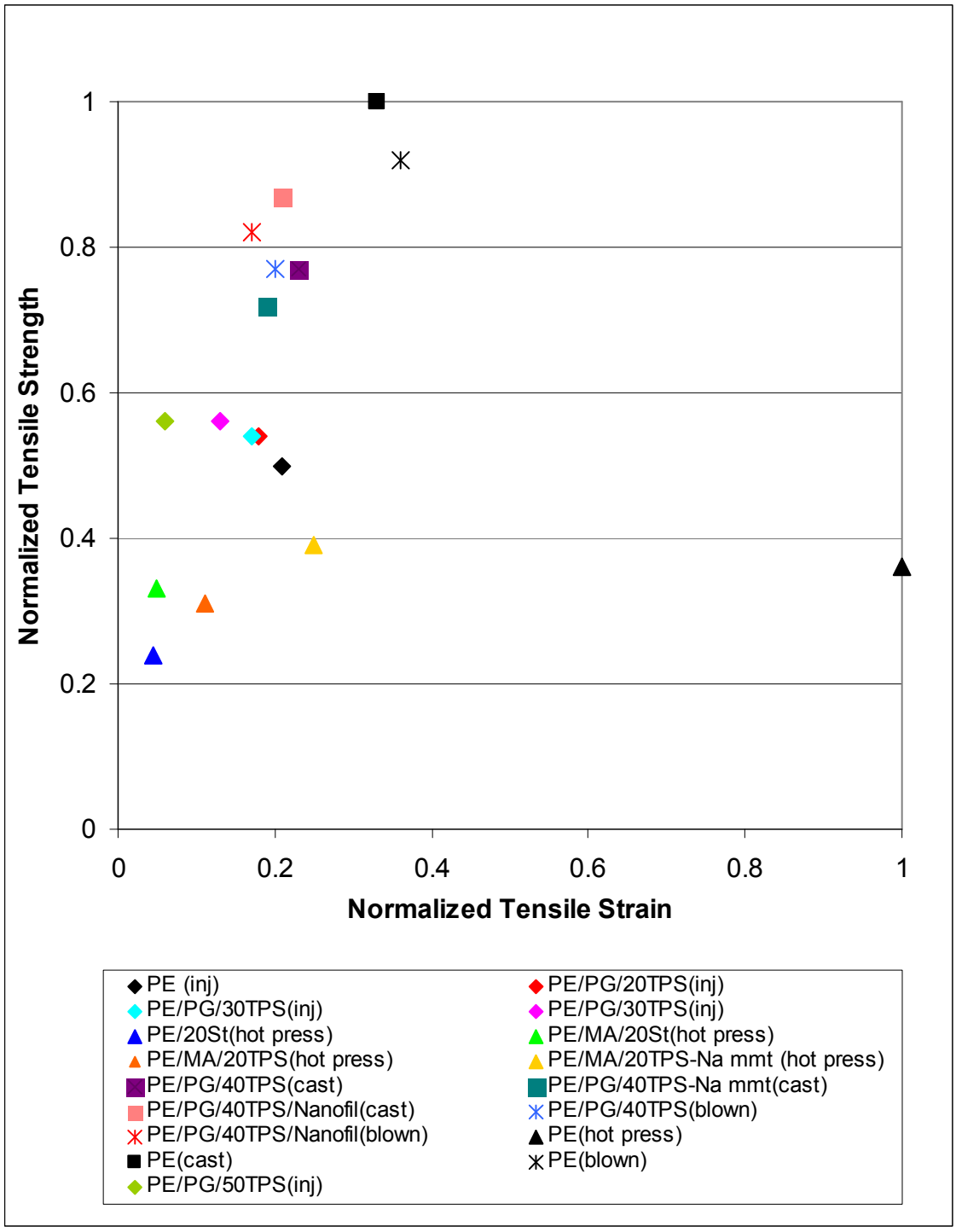

Figure 4.31 Normalized tensile properties of the samples prepared with different shaping processes.

4.8 Biodegradation

The biodegradation test of starch-containing films was performed using AG-Amiloglucosidase that digests both amylose and amylopectin chains and results in the liberation of glucose molecules. The amount of glucose molecules evolved was calculated from the absorbance values of the enzyme solutions at specific wavelength and the morphology of the degraded films were investigated using SEM. In order to investigate the effect of biopolymer particle size in its consumption rate, biodegradation tests were performed for both film samples containing 20 wt.% starch and 40 wt.% TPS. However, it is noteworthy to indicate that the degradation behaviour in soil reflects the most real situation but since it takes place more slowly due to the low percolation rate, the degradation study was performed in enzyme solution in the present study.

Table 4.14 presents the % of starch content that was degraded into glycose molecules after the film samples were incubated in enzyme solution for 3 days. The data were taken in every 24 hours. The noticeable change in starch degradation rate of 20 wt% starch containing samples revealed that as the biopolymer disperse more homogeneously in LDPE matrix, the rate of its degradation decreased. There are two possible reasons for this behavior. First of all, the finer the dispersion the better the interfacial adhesion so the slower the enzyme diffusion from the LDPE-Starch or LDPE-TPS interfaces. Secondly, the larger starch particle can uptake more water and hence more enzyme is activated on the starch surface.

The initial degree of starch degradation seems to be faster and the rate is exhibiting a decreasing trend with time. This is because the accessible starch molecules are larger at the beginning of the test and starts to decrease as biodegradation proceeds. In some area of the blends, starch domains may be well protected with the synthetic resin, resulting in diffusion difficulties of the enzyme molecules. The similar results were also reported in other studies [124, 125].

Comparing the degradation rates of blend films with 20 TPS and 40 TPS, higher amount of glucose was evolved in the sample with 40 wt% TPS which is expected because of the higher starch content however the amount of starch removed from PE/PG/40TPS sample was lower than the twice of that evolved from PE/MA/20TPS.

This was ascribed to the better dispersion with smaller TPS particle size in the former product due to slightly better compatibilizing efficiency of PG, as previously shown in Section 4.2.5.

The positive effect of Na^+mmt on degradation rate was only apparent at data taken after 72 hours of incubation while it was seen after 24 hours for organoclay. In order to clarify the effect of clay, another nanocomposite film sample containing larger amount of organoclay (4 phr) was prepared and subjected to the biodegradation test at similar conditions. The result revealed that more starch was hydrolyzed into glycose molecule in this sample indicating the acceleration effect of organoclay in starch degradation. This behavior can be explained by the tendency of clay particles to absorb or interact with water molecules leading to the faster activation of enzyme. The presence of clay particles near TPS phase can confirm this assumption (see Figure 4.33c). The improved biodegradability of PCL and PLA nanocomposites with clay was also reported previoulsly in compost environment [97, 99]. It is expected that clay will have double effect in increasing the rate of biodegradation of LDPE/TPS blends in soil environment since it is also know to accelerate the photo-oxidative degradation of polyolefins [93-96].

Table 4.14 The degree of starch degradation in blend films after 3 days of enzyme incubation.

Sample	Degree of Starch Degradation (%)		
	24 hrs.	**48hrs.**	**72 hrs.**
PE/20 St	37.8	65.4	73.7
PE/MA/20St	27.0	31.0	34.7
PE/MA/20TPS	18.4	19.3	20.9
PE/MA/20TPS-Na^+mmt	18.2	18.8	26.4
PE/PG/40TPS	27.8	32.3	36.3
PE/PG/40TPS/Nanofil	30.6	32.4	35.2
PE/PG/40TPS/Nanofil_4 phr	39.0	41.4	42.6

SEM images of the film surfaces taken after the biodegradation test exhibited a porous structure and the pore sizes corroborates perfectly with the data given in Table 4.14. The black droplets in SEM images are pores formed by enzyme and white areas around the pores are the edge of the surrounding synthetic polymer appearing with less thickness compared to the unaffected area of polymer films (Figure 4.32 and 4.33).

The products are partially biodegradable at first due to the presence of synthetic polymer besides the biopolymer. However, in soil conditions, the presence of porous structure is suggested to enhance the accessibility of synthetic part to oxygen and microorganisms, thereby increasing the degradation rate of the synthetic part. This mechanisms is most valid at high biopolymer contents due to the formation of more surface area for oxygen permeability after biopolymer removal and also due to the possibility of the dispersed part of the biopolymer to join together forming the more continous structure, which in turn resulting in less biopolymer particles that are entrapped by synthetic resin. The highest amount of biopolymer that can be incorporated into LDPE matrix without sacrifying the other physical properties was found to be 40 wt% in this study. This biopolymer amount is high enough to create highly porous structure as seen in SEM images (Figure 4.33) and hence to make LDPE matrix much rapidly degradable.

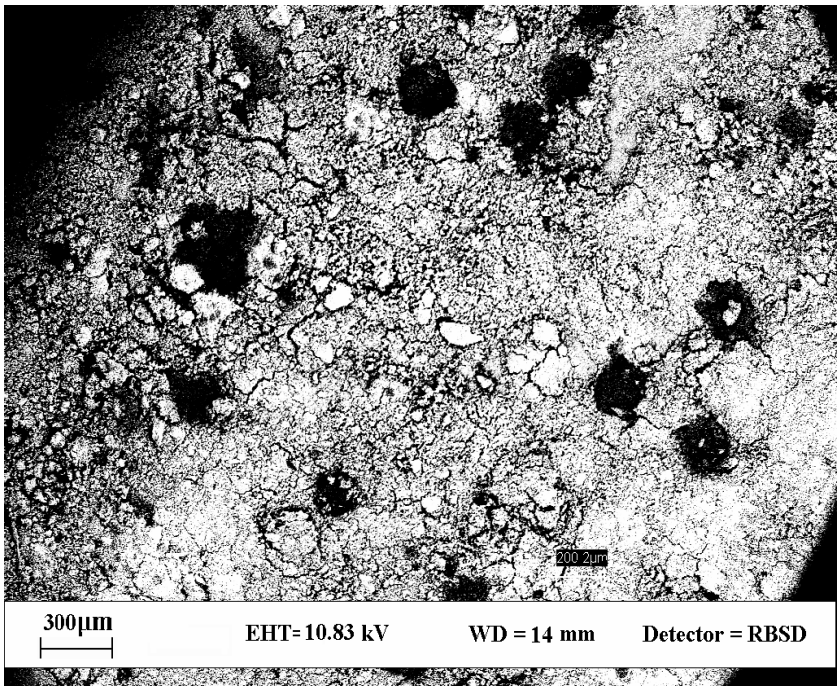
300µm
EHT= 10.83 kV
WD = 14 mm
Detector = RBSD

(a)

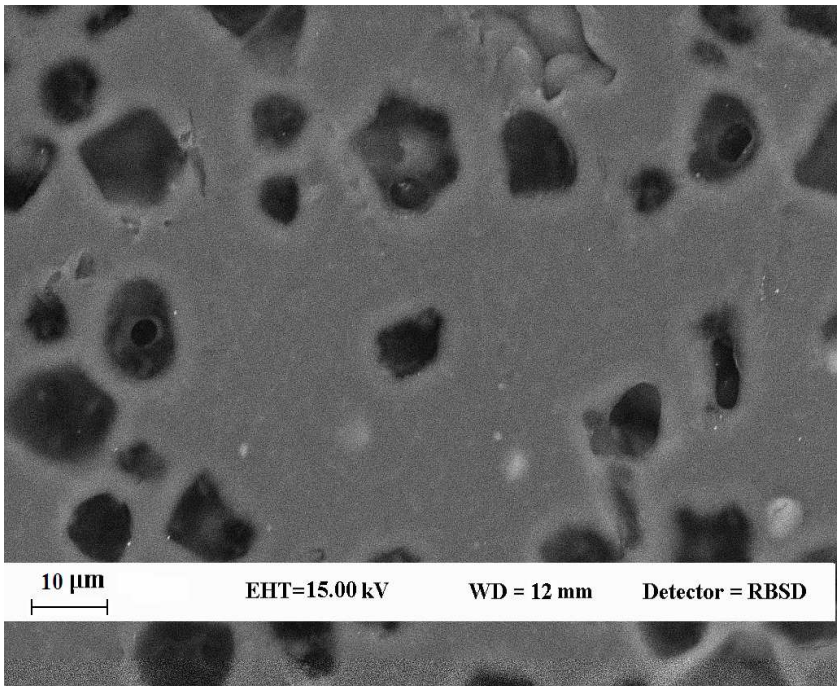
10 µm
EHT=15.00 kV
WD = 12 mm
Detector = RBSD

(b)

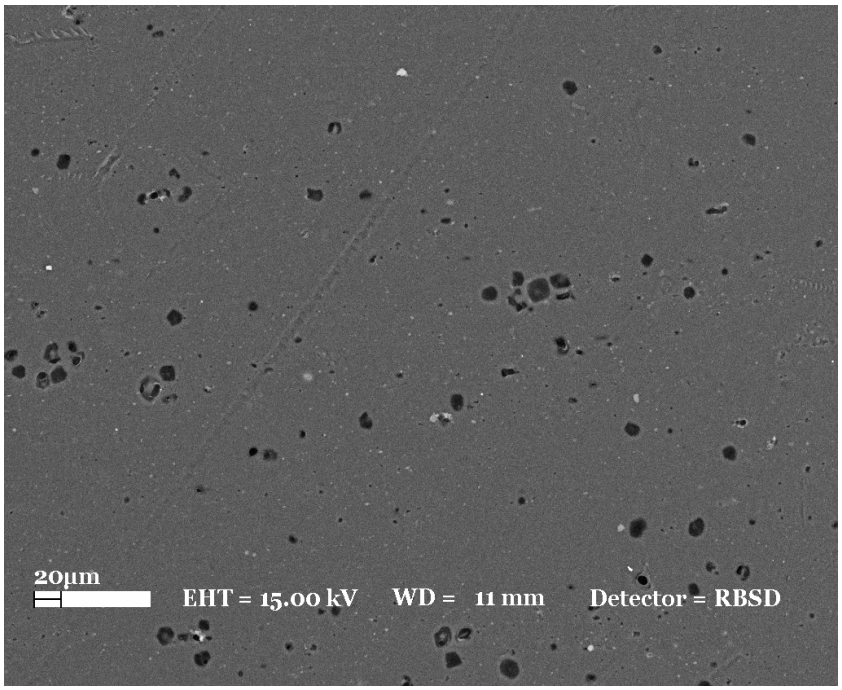

(c)

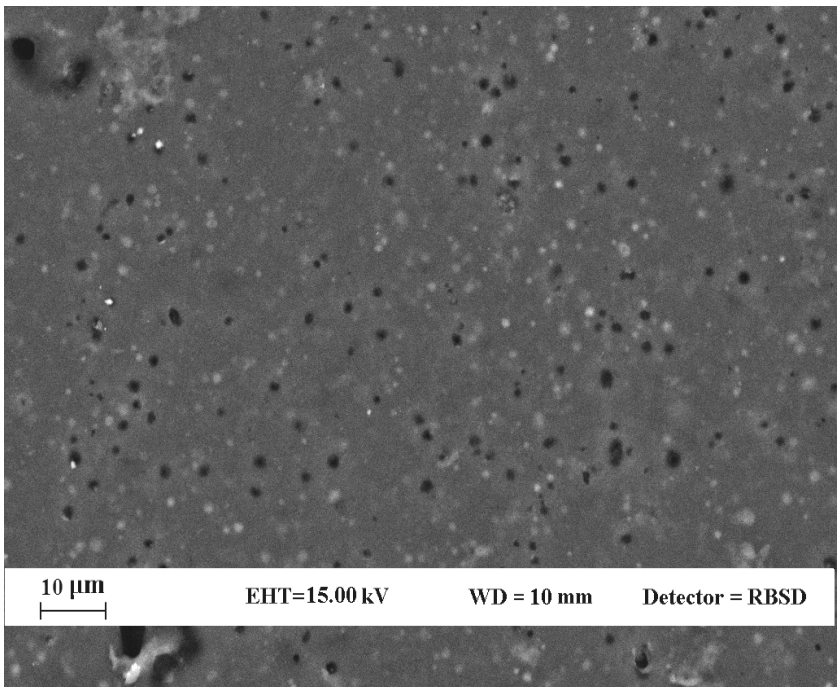

(d)

Figure 4.32 SEM images of degraded (a) PE/20St, (b) PE/MA/20St, (c) PE/MA/20TPS and (d) PE/MA/20TPS-Na^{+}mmt films after incubation in enzyme solution for 55 h.

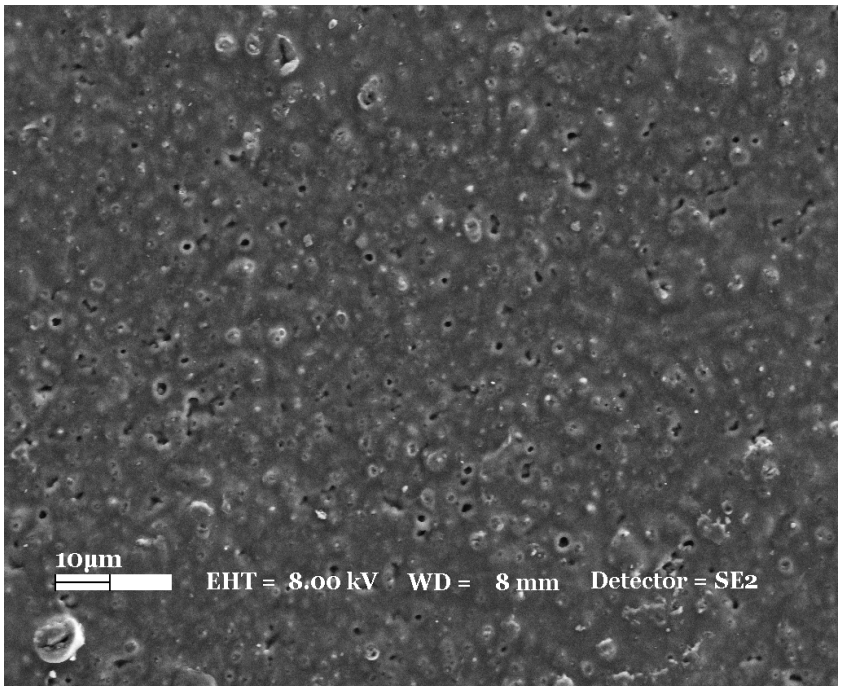
10µm
EHT = 8.00 kV
WD = 8 mm
Detector = SE2

(a)

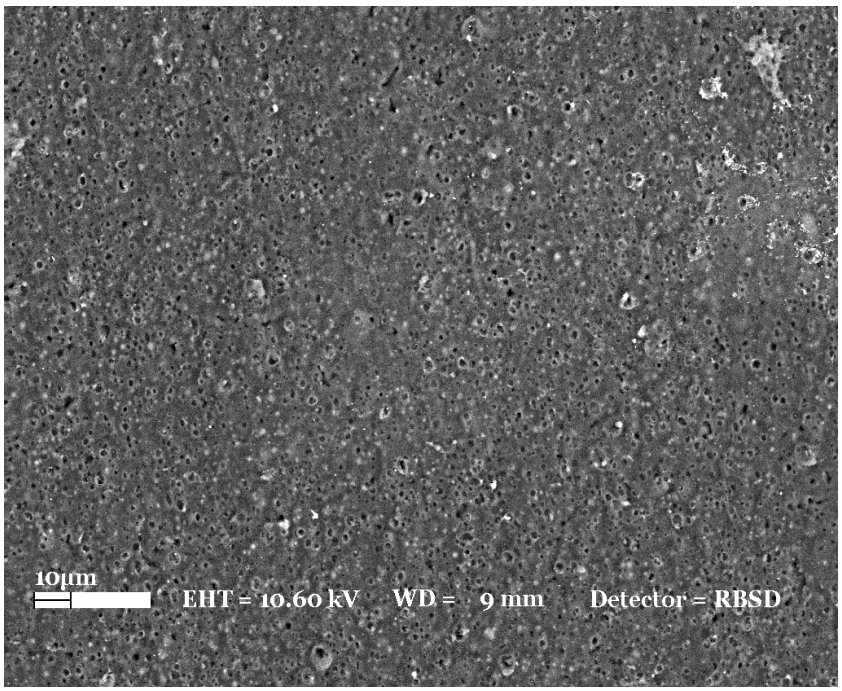
10µm
EHT = 10.60 kV
WD = 9 mm
Detector = RBSD

(b)

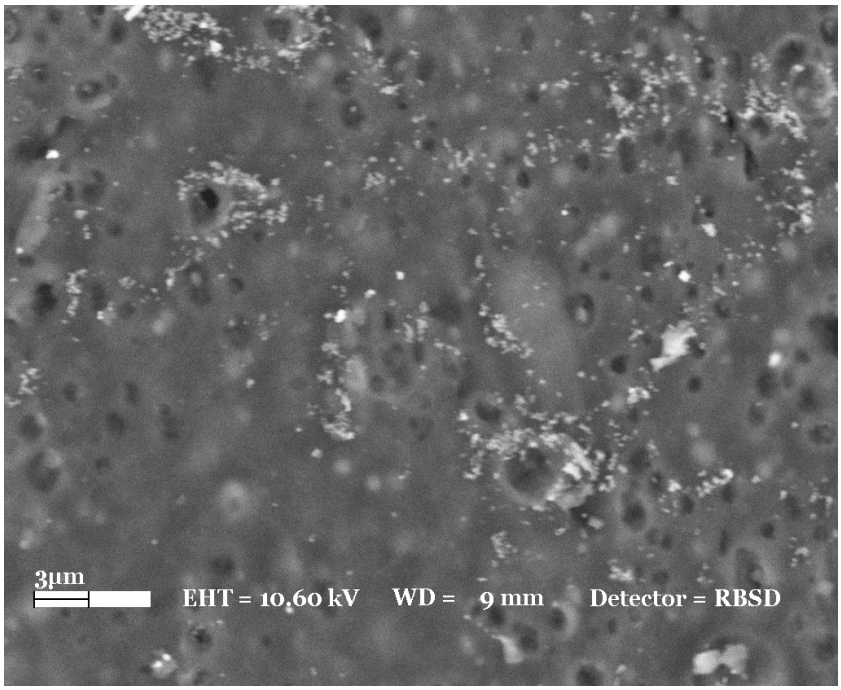

(c)

Figure 4.33 SEM images of degraded (a) PE/PG/40TPS, (b) PE/PG/40TPS/Nanofil and (c) PE/PG/40TPS/Nanofil_4 phr.

5. CONCLUSION

Increasing the degradation rate of LDPE, which is the largest tonnage used polymer type in industry especially in packaging sector, without loosing its excellent mechanical properties is a rather difficult problem. Most of the researches have been focused on the preparation of LDPE-Starch blends after Griffin suggested that incorporation of biopolymer could increase the degradation rate of thermoplastic resin by the formation of porous structure. However, a literature review on the mechanical behavior of such blends reveals that the excellent mechanical strength and the physical appearence of the synthetic polymers are deteriorated by the addition of biopolymer. Especially, in film applications of this blends, significant decrease in tensile strength, flexibility, tear and heat seal strength and moisture barrier properties limit their usage in packaging sector.

This study shows that by using proper combinations of polymeric materials, reinforcing agents and processing conditions, it is possible to produce bio-/synthetic polymer blends with an optimum combination of desirable mechanical properties as well as biodegradation performance. With this approach, LDPE/Starch blends reinforced with layered clays were successfully prepared using twin screw extruder and the products were shaped using hot press, injection molding, film-casting and film-blowing techniques. In order to find the suitable combination of the blend components, the effect of compatibilizer, starch form and its content, clay type and processing methods on the physico-mechanical properties of the blend were investigated. Results showed that using MAgPE as a compatibilizer significantly improves the starch dispersion quality in blends. This is because MAgPE provides chemical linkage between starch molecules and maleic anhydride groups through the formation of ester bonds, while it makes physical interaction with LDPE chains. It was shown that processing conditions like temperature profile and shear rate are also important factors

to provide these interactions between the polymeric components during flow inside the extruder. Similar viscosity profiles during polymer melt flow means good contact between the components and leads to obtain homogeneous blend morphology. Using TPS instead of unplasticized starch as biopolymer component is also effective in order to improve physical appearance as well as the mechanical properties. Yet, tensile properties, especially elongational properties, of the blends were poor compared to the properties of LDPE itself in hot pressed film samples. The significant improvements in mechanical performance were only achieved by melt blending LDPE with 20 wt% TPS-Na^+mmt nanocomposite, which had been prepared using solution intercalation technique. Tensile strength of the film prepared from this blend was found to be 10.6 MPa, compared to 9.7 MPa in virgin LDPE film, and the elongation at break as being %125, indicating the strenght and flexibility of the resulting composition. These improvements in tensile properties mainly result from the better dispersion of TPS phase in nanocomposite structure and the characteristic of nano-dispersed layered clays such that applied load/stress are homogeneously dispersed throughout the matrix.

In order to provide high level of biodegradability to the blend formulation, the maximum amount of TPS that can be incorporated into LDPE matrix without loosing much from its mechanical properties was investigated by examining the changes in mechanical as well as fracture behaviours of injection molded samples. It was shown that the use of TPS is limited by 40 wt% in terms of flexibility since beyond that content the fracture mechanism turns from ductile to brittle failure by the disruption of LDPE phase continuity. TPS particles act as reinforcing agents by increasing the tensile strength of LDPE in injecton molded samples. Whereas, they decrease the tensile strength of LDPE films prepared using hot-pressing, film-casting and film-blowing techniques. Different effects of TPS in different shaping process is mainly due to the more efficient stress transfer in injection molded samples through the formation of entanglements, as compared to more oriented and hence less interconnected structure in film samples. Another reason could be the size of TPS particles that were larger in film samples due to the swelling of TPS particles during the cooling process.

Two types of layered clay were employed in LDPE/40TPS blend formulations. The first one is Na^+mmt and it was first dispersed in TPS phase, as both of them has very hydrophilic characteristics by nature. The formation of intercalated nanocomposite

morphology is evident fom XRD pattern. The second clay type that was found to be most suitable for LDPE matrix is Nanofil organoclay. LDPE-Nanofil masterbatch was first prepared and it was melt blended with LDPE, MAgPE and TPS granules. It was observed that different clay types and different dispersion method results in nanocomposite structure exhibiting different performance. The presence of organoclay in LDPE matrix mainly improves the mechanical, tear and heat seal strength of the films, while the intercalation of natural Na^+-montmorillonite clay with starch molecules is more effective in enhancing the moisture barrier properties.

The reinforcing effect of clay layers depends on fracture mechanism and hence it is significantly affected by TPS content. At low biopolymer content, such as 20 wt.% based on polymeric content, the load applied during tensile test is carried by the entire structure so that clay layers are effective in stress transfer mechanism, irrespective of the phase they are mainly dispersed. As TPS content is increased to 40 wt.%, the failure occurs first at the interface between TPS and LDPE phases, so that presence of Na^+mmt on TPS phase does not have any influence but reinforcing LDPE matrix, which is the main load carrying phase, is more effective on the stress transfer mechanism. Compared with the stiffing effect of clay layers in the samples prepared by film-blowing method with film-casting one, due to different cooling process, the clay layers are mostly oriented in cross direction during blowing-up process and consequently, the improvement in elastic modulus is much significant in that direction than in machine direction. On the contrary, it is the machine direction where the elastic modulus is higher in cast-film nanocomposite samples.

In terms of transparency, LDPE/TPS blend films are less transparent compared to LDPE film due to the surface roughness created by TPS particles. The water contact angle as well as the surface energy measurements colloborates with the findings in light transmittance. In terms of biodegradability, starch degradation rate increases with TPS content, its particle size and the presence of layered clay. All the films exhibites a porous structure in enzyme solution, leaving the remaining part of the film more susceptible to oxidative and hence biotic reactions

Finally, it is noteworty to indicate that the performance properties of the newly developed biodegradable nanocomposite films are good enough to be used as a

potential material for replacing/substituting LDPE for future ‘green’ packaging materials.

6. REFERENCES

1. Ratajska, M. & Boryniec, S. Biodegradation of some natural polymers in blends with polyolefins. *Polymers for Advanced Technology* **10**, 625-633 (1999)

2. Ratner, B.D., Hoffman, A.S., Schoen, F.J. & Lemons, J.E. *Biomaterial Science*. Elsevier Science, 1996

3. Liu, W., Wang, Y.J., & Sun, Z. Effects of polyethylene-grafted maleic anhydride (PE-g-MA) on thermal properties, morphology, and tensile properties of low-density polyethylene (LDPE) and corn starch blends. *Journal of Applied Polymer Science* **88**, 2904-2911 (2003)

4. Raj, B., Annadurai, V., Somashekar, R., Raj, M. & Siddarramaiah, S. Structure–property relation in low-density polyethylene–starch immiscible blends**.** *European Polymer Journal* **37**, 943-948 (2001)

5. Raj, B., Sankar, U.K. & Sıddaramaiah, S. Low density polyethylene/starch blend films for food packaging applications. *Advences in Polymer Technology* **23**, 32-45 (2004)

6. Gonzalez, F.J.R., Ramsay, B.A. & Favis, B.D. High performance ldpe/thermoplastic starch blends: a sustainable alternative to pure polyethylene. *Polymer* **44**, 1517-1526 (2003)

7. Willett, J.L. Mechanical properties of LDPE/granular starch composites. *Journal of Applied Polymer Science* **54**, 1685-1695 (1994)

8. McGlashan, S.A. & Halley, P.J. Preparation and characterisation of biodegradable starch-based nanocomposite materials. *Polymer Intenational* **52**, 1767-1773 (2003)

9. Otey, F.H., Westhoff, R.P. & Russel, C.R. Biodegradable films from starch and ethylene-acrylic acid copolymer. *Industrial & Engineering Chemistry Product Research and Development* **16**, 305-308 (1977)

10. Wang, Y.; Andrianaivo, M.; Rakotonirainy, M. & Padua, G.W., Thermal behavior of zein-based biodegradable films. *Starch/Stärke* **55**, 25-29 (2003).

11. Lörcks, J., Properties and applications of compostable starch-based plastic material. *Polymer Degradation and Stability* **59**, 245-249 (1998)
12. Jang, B.C., Huh, S.Y., Jang, J.G. & Bae, Y.C. Mechanical properties and morphology of the modified HDPE/starch reactive blend. *Journal of Applied Polymer Science* **82**, 3313-3320 (2001)

13. Kang, B.G.; Yoon, S.H.; Lee, S.H.; Yie, J.E.; Yoon, B.S. & Suh, M.H., Studies on the physical properties of modified starch-filled HDPE film. *Journal of Applied Polymer Science* **60**, 1977-1984 (1996)

14. Evangelists, R.L., Nikolov, Z.L., Sung, W., Jane, J.L. & Gelina, R.J. Effect of compounding and starch modification on properties of. starch-filled low density polyethylene. *Industrial & Engineering Chemistry Product Research and Development* **30**, 1841-1846 (1991)

15. Averous, L., Moro, L., Dole, P. & Fringang, C. Properties of thermoplastic blends: starch–polycaprolactone. *Polymer* **41**, 4157-4167 (2000)

16. Martin, O. & Averous, L. Poly(lactic acid): plasticization and properties of biodegradable multiphase systems. *Polymer* **42**, 6209-6219 (2001)

17. Park, H.M., Li, X., Jin,C.Z., Park, C.Y., Cho, W.J. & Ha, C.S. Preparation and properties of biodegradable thermoplastic starch/clay hybrids. *Macromolecular Materials and Engineering* **287**, 553-558 (2002)

18. Wilhelm, H.M., Sierakowski, M.R., Souza, G.P. & Wypych, F. Starch films reinforced with mineral clay. *Carbohydrate Polymers* **52**, 101-110 (2003)

19. Chandra, R. & Rustgi, R. Biodegradation of maleated linear low-density polyethylene and starch blends. *Polymer Degradation and Stability* **56**, 185-202 (1997)

20. Jang, B.C., Huh, S.Y., Jang, J.G. & Bae, Y.C. Mechanical properties and morphology of the modified hdpe/starch reactive blend. *Journal of Applied Polymer Science* **82**, 3313–3320 (2001)

21. Sailaja, R. R. N. & Chanda, M. Use of maleic anhydride–grafted polyethylene as compatibilizer for hdpe–tapioca starch blends: effects on mechanical properties. *Journal of Applied Polymer Science* **80**, 863–872 (2001)

22. Pedroso, A. G. & Rosa, D. S. Effects of the compatibilizer PE-g-GMA on the mechanical, thermal and morphological properties of virgin and reprocessed LDPE/corn starch blends. *Polymers For Advanced Technologies* **16**, 310–317 (2005)

23. Ratanakamnuan, U. & Aht-Ong, D. Preparation and characterization of low-density polyethylene/banana starch films containing compatibilizer and photosensitizer *Journal of Applied Polymer Science***100**, 2717–2724 (2006)

24. Griffin, G.J.L. Biodegradable synthetic resin sheet material containing starch and a fatty material. U.S. Patent No: 4016117 (1977)

25. Griffin, G.J.L. Synthetic polymers and the living environment. *Pure and Applied Chemisty* **52**, 399-407 (1980)

26. Wool, R.P., Raghavan, D., Wagner, G.C. & Billieux, S. Biodegradation dynamics of polymer-starch composites. *Journal of Applied Polymer Science* **77**. 1643-1657 (2000)

27. Nakashima, T., Hiraku, I. & Matsuo, M. Biodegradation of high-strength and high-modulus PE-starch composite films buried in several kinds of soils. *Journal of Macromolecular Science-Physics Part B Physics* **41**, 85-98 (2002).

28. Nakashima, T., Nagasaki, S., Ito, H., Xu, C., Bin, Y. & Matsuo, M. Biodegradation of biaxially stretched polyethylene-starch composite films. *Polymer Journal* **34**, 234-241 (2002)

29. Dave, H., Rao, P.V.C. & Desai, J.D. Biodegradation of starch–polyethylene films in soil and by microbial cultures. *World Journal of Microbiology & Biotechnology* **13**, 655-658 (1997)

30. Turkiye Plastik Sektor Raporu 2004, Plastik Arastırma ve Gelistirme Vakfı (PAGEV), http://www.pagev.org.tr/Turkiye Plastik Sektör Raporu 2004.pdf

31. Stevens, E.S. Green Plastics: An Introduction to the New Science of Biodegradable Plastics, Princeton: Princeton University Press, 2002

32. Ehrenstein, G.W. Polymeric Materials: structure, properties, applications. Munich : Hanser Publishers , Cincinnati, Ohio : Hanser Gardner Publications, 2001

33. Ram, A. Fundamentals of Polymer Engineering, New York : Plenum Press, 1997

34. Scott, G. & Wiles, D.M. Programmed-life plastics from polyolefins: a new look at sustainability. *Biomacromolecules* **2**, 615-622 (2001)

35. Technical market research report: *RP-175R* Biodegradable Polymers, htpp://www.bccresearch.com

36. Malanda, L.M., Park, C. B. & Balatinecz, J. J. Characterization of microcellular foamed pvc/cellulosic-fibre composites. *Journal of Cellular Plastics* **32**, 449-469 (1996)

37. Chazeau , L., Cavaillé, J. Y. , Canova , G. , Dendievel , R. & Boutherin, B. Viscoelastic properties of plasticized PVC reinforced with cellulose whiskers. *Journal of Applied Polymer Science* **71**, 1797 – 1808 (1999)

38. Mohanty, A. K., Wibowo, A., Misra, M. & Drzal, L. T. Development of renewable resource-based celluloseacetate bioplastic: effect of process engineering on the performance of cellulosic plastics. *Polymer Engineering and Science* **43**, 1151–1161 (2003)

39. Park, H.M., Liang,X., Mohanty,A.K., Misra, M. & Drzal, L.T. Effect of compatibilizer on nanostructure of the biodegradable cellulose acetate/organoclay nanocomposites. *Macromolecules* **37***,* 9076-9082 (2004)

40. Biodegradable Coverages for Sustainable Agriculture, http://www.ictp.cnr.it/life/task1d1.html

41. Reddy, C.S.K. , Ghai, R., Rashmi, Kalia, V.C. Polyhydroxyalkanoates: an overview. *Bioresource Technology* **87,** 137–146 (2003)

42. Production of natureworks polylactide (pla) film on blown film equipment designed for producing low density polyethylene (ldpe) film, http://www.natureworksllc.com/media/files/natureworks pla on ldpe film line.pdf

43. Summary Report Biodegradable Polymers and Sustainability: Insights from Life Cycle Assessment, http://www.oakdenehollins.co.uk/pdf/biodegradable_ polymers.pdf

44. Method for the injection moulding of capsules from destructured starch. EP Patent Application No. EP-A-O 304401 (1987)

45. Bikiaris, D., Pavlidou, E., Prinos, J. ,Aburto, J., Alric, I., Borredonb, E. & Panayiotou, C. Biodegradation of octanoated starch and its blends with LDPE. *Polymer Degradation and Stability* **60**, 437-447 (1998)

46. Otey et al. Degradable starch-based agricultural mulch film. U.S. Patent No. 3,949,145 (1976)

47. Mayer, et al. Method of producing biodegradable starch-based product from unprocessed raw materials. U.S. Patent No. 5,322,866 (1994)

48. Tudorachi, N., Cascaval, C.N., Rusu, M. & Pruteanu, M. Testing of polyvinyl alcohol and starch mixtures as biodegradable polymeric materials. *Polymer Testing* **19**, 785–799 (2000)

49. Mayer, et al. Cellulose acetate and starch based biodegradable injection molded plastics compositions and methods of manufacture U.S. Patent No. 5,288,318 (1994)

50. Kotnis, M.A., O'Brien, G.S. & Willett, J.L. Processing and mechanical properties of biodegradable poly(hydroxy- butyrate-co-valerate)-starch compositions. J. Environ. Polym. Deg**. 3** 97-105 (1995)

51. Narayan, R., Krishnan, M. & DuBois, P. polysaccharides grafted with aliphatic polyesters derived from cyclic esters. U.S. Patent No: 5, 540, 929 (1996)

52. Catia, B., Vittorio, B. & Alessandro, M. Polymers of a hydrophobic nature, filled with starch complexes. EP Patent No: 1621579 (A1) (2006)

53. Hamid, S.H., Amin, M.B. & Maadhah, A.G. Handbook of polymer degradation. New York: M.Dekker (1992)

54. Yoo, S.I., Lee, T.Y., Yoon, J.S., Lee, I.M., Kım, M.N. & Lee, H.S. Interfacial adhesion reaction of polyethylene and starch blends using maleated polyethylene reactive compatibilizer. *Journal of Applied Polymer Science* **83**, 767–776 (2002)

55. Griffin, Synthetic resin sheet material. U.S. Patent No: 4,021,388 (1977)

56. George, E.R., Sullivan, T.M. & Park, E.H. Thermoplastic starch blends with a poly(ethylene-co-vinyl alcohol): Processability and physical properties. *Polymer Engineering and Science* **34**, 17-23 (1994)

57. Bikiaris, D. & Panayiotou, C. LDPE/Starch blends compatibilized with pe-g-ma copolymers. *Journal of Applied Polymer Science* **70**, 1503–1521 (1998)

58. Wang, S., Yu, J. & Yu, J. Influence of maleic anhydride on the compatibility of thermal plasticized starch and linear low-density polyethylene. *Journal of Applied Polymer Science* **93**, 686–695 (2004)

59. Girija, B. G. & Sailaja, R. R. N. Low-density polyethylene/plasticized tapioca starch blends with the low-density polyethylene functionalized with maleate ester: mechanical and thermal properties. *Journal of Applied Polymer Science* **101**, 1109–1120 (2006)

60. Winey, K.I. & Vaia R.A. Polymer nanocomposites. *MRS Bulletin* **32**, 314-322 (2007)

61. Ray, S.S. & Okamoto, M. Polymer/layered silicate nanocomposites: a review from preparation to processing. *Progress in Polymer Science* **28**, 1539–1641(2003)

62. Ferrara, G. Nanofiller-containing polyolefinic composites: from production to applications. *Nanocomposite Conference*, Bruxelles, 2006

63. Ray, S.S. & Bousmina M. Biodegradable polymers and their layered silicate nanocomposites: In greening the 21st century materials world. *Progress in Materials Science* **50**, 962–1079 (2005)

64. Blumstein, A. Polymerization of adsorbed monolayers: II. Thermal degradation of the inserted polymers. *Journal of Polym Science Part A: Polymer Chemistry* **3**, 2665–2673 (1965)

65. Theng, BKG. Formation and properties of clay–polymer complexes. Elsevier, Amsterdam, 1979

66. Fukushima, Y., Okada, A., Kawasumi, M., Kurauchi, T. & Kamigaito, O. Swelling behavior of montmorillonite by poly-6-amide. *Clay Mineral* **23**, 27-34 (1988)

67. Usuki, A., Kojima, Y., Kawasumi, M., Okada, A., Fukushima, Y., Kurauchi, T. & Kamigaito, O. Synthesis of nylon-6 clay hybrid. *Journal of Materials Research* **8** 1179-1183 (1993)

68. Chen, T.K., Tien, Y.I. & Wei, K.H. Synthesis and characterization of novel segmented polyurethane/clay nanocomposite via poly(1-caprolactone)/clay. *Journal of Polymer Science, Part A: Polymer Chemistry* **37**, 2225–2233 (1999)

69. Wang, Z. & Pinnavaia, T.J. Nanolayer reinforcement of elastomeric polyurethane. *Chemistry of Materials* **10**, 3769–71 (1998)

70. Akelah, A., & Moet, A. Polymer-clay nanocomposites: free-radical grafting of polystyrene on to organophilic montmorillonite interlayers. *Journal of Materials Science* **31**, 358-3596 (1996)

71. Doh, J.G. & Cho, I. Synthesis and properties of polystyrene-organoammonium montmorillonite hybrid. *Polymer Bulletin* **41,** 511-517 (1998)

72. Inceoglu, F., Cengiz, O.M., Unal, M. & Menceloglu, Y.Z. Effect of PS-Nanocomposite on SEBS/PP. *NanoTR-II Nanoscience and Nanotechnology Conference*, Preprint, Ankara, 2006

73. Rong, J., Jing, Z., Li, H. & Sheng, M. A polethylene nanocomposite prepared via in-situ polymerization. *Macromolecular Rapid Communications* **22**, 329-334 (2001)

74. Heinemann, J., Reochert, P., Thomann, R. & Mulhaupt, R. Polyolefin nanocomposites formed by melt compounding and transition metal catalyzed ethene homo- and copolymerization in the presence of layered silicates. *Macromolecular Rapid Communications* **20**, 423-430 (1999)

75. Ke, Y.C., Long, C.F. & Qi, Z.N. Crystallization, properties, and crystal and nanoscale morphology of PET-clay nanocomposites. *Journal of Applied Polymer Science* **71**, 1139-1146 (1999)

76. Nigam, V., Setua, D.K., Mathur,G.N. & Kar, K.K. Epoxy-montmorillonite clay nanocomposites: synthesis and characterization. *Journal of Applied Polymer Science* **93**, 2201–2210 (2004)

77. Inceoglu, F., Dalgicdir, C. & Menceloglu, Y.Z. Effect of Organoclay on the Physical Properties of UV-Curable Coatings. *232nd American Chemical Society National Meeting*: *PMSE Preprint*, San Francisco, 2006

78. Inceoglu, F., Dalgicdir, C. & Menceloglu, Y.Z. Effect of Organoclay on the Physical Properties of UV-Curable Coatings. Book Chapter submitted to *ACS Symposium Series Book,* 2007

79. Inceoglu, A.B. & Yilmazer, U. Synthesis and mechanical properties of unsaturated polyester based nanocomposites. *Polymer Engineering and Science* **43**, 661-669 (2003)

80. Ogata, N., Kawakage, S. & Ogihara, T. Poly(vinyl alcohol)-clay and poly(ethylene oxide)-clay blend prepared using water as solvent. *Journal of Applied Polymer Science* **66** 573-581 (1997)

81. Darder, M., Colilla, M. & Ruiz-Hitzky, E. Biopolymer-clay nanocomposites based on chitosan intercalated in montmorillonite. *Chemistry of Materials* **15***,* 3774-3780 (2003)

82. Alexandre, M. & Dubois, P. Polymer-layered silicate nanocomposites: preparation, properties and uses of a new class of materials. *Materials Science and Engineering* **28** 1-63 (2000)

83. Pandey, J.K. & Singh, R.P.Green nanocomposites from renewable resources: effect of plasticizer on the structure and material properties of clay-filled starch. *Starch/Stärke* **57**, 8–15 (2005)

84. Wilhelm, H.M., Sierakowski, M.R., Souza, G.P., Wypych, F. The influences of layered compounds on the properties of starch/layered compound composites. *Polymer International* **52**, 1035–44 (2003)

85. Manias, E., Touny, A., Lu, K.S., Gilman J.W. & Chung, T.C. Polypropylene/silicate nanocomposites, synthetic routes and material properties. *Polymeric Materials: Science & Engineering* **82**, 282-283 (2000)

86. Jeon, H.G., Jung, H.T., Lee, S.W. & Hudson, S.D. Morphology of polymer silicate nanocomposites. High density polyethylene and a nitrile. *Polymer Bulletin* **41**, 107-113 (1998)

87. Vaia, R.A. & Giannelis, E.P. Lattice of polymer melt intercalationin organically-modified layered silicates. *Macromolecules* **30**, 7990–7999 (1997)

88. Vaia, R.A., Jandt, K.D., Kramer, E.J. & Giannelis, E.P. Kinetics of polymer melts intercalation. *Macromolecules* **28**, 8080–8085 (1995)

89. Vaia, R.A., Ishii, H.& Giannelis, E.P. Synthesis and properties of two-dimensional nanostructures by direct intercalation of polymer melts in layered silicates. *Chemistry of Materials* **5**,1694–1696 (1993)

90. Liu, L.M. , Qi, Z.N. & Zhu, X.G. Studies on nylon-6 clay nanocomposites by melt-intercalation process, *Journal of Applied Polymer* Science **71**, 1133-1138 (1999)

91. Wang, K.H., Choi, M.H., Koo, C.M., Xu, M., Chung, I.J., Jang, M.C., Choi, S.W. & Song, H.H. Morphology and physical properties of polyethylene/silicate nanocomposite prepared by melt intercalation. *Journal of Polymer Science, Part B: Polymer Physics* **40**, 1454–1463 (2002)

92. Cho, J.W, Logsdon, J., Omachinski, S., Qian, G., Lan T., Womer T.W. & Smith W.S. Nanocomposites: A single screw mixing study of nanoclay-filled polypropylene. Technical paper, Antec 2002

93. Qin, H.L., Zhao, C.G., Zhang, S.M., Chen, G.M. & Yang, M.S. Photo-oxidative degradation of polyethylene/montmorillonite nanocomposite. *Polymer Degradation and Stability* **81**,497- 500 (2003)

94. Qin, H., Zhang, Z., Feng, M., Gong, F.L., Zhang, S.M. & Yang, M.S. The influence of interlayer cations on the photo-oxidative degradation of polyethylene/montmorillonite composites. *Journal of Polymer Science, Part B: Polymer Physics* **42**, 3006- 3012 (2004)

95. Tidjani, A., Wilkie, C.A. Photo-oxidation of polymeric-inorganic nanocomposites: chemical, thermal stability and fire retardancy investigations. *Polymer Degradation and Stability* **74**, 33- 37 (2001)

96. Qin, H., Zhanga, S., Liua, H., Xiea, S., Yanga, M. & Shen, D. Photo-oxidative degradation of polypropylene/montmorillonite nanocomposites. *Polymer* **46** 3149–3156 (2005)

97. Tetto, J.A., Steeves, D.M., Welsh, E.A. & Powell, B.E. Biodegradable poly(1-caprolactone)/clay nanocomposites. Technical paper, Antec 1999, 1628–1632

98. Lee, S.R., Park, H.M., Lim, H.L., Kang, T., Li, X., Cho, W.J. & Ha, C.S. Microstructure, tensile properties, and biodegradability of aliphatic polyester/clay nanocomposites. *Polymer* **43**, 2495–500 (2002)

99. Sinha, R.S., Yamada, K., Okamoto, M. & Ueda, K. New polylactide/layered silicate nanocomposite: a novel biodegradable material. *Nano Letters* **2**, 1093–1096 (2002)

100. Lim, S.T., Jane, J.L. , Rajagopalan, S. & Seib, P.A. Effect of starch granule size on physical properties of starch-filled polyethylene film. *Biotechnology Progress* **8**, 51-57 (1992)

101. Kwok, D. Y. & Neumann, A. W. Contact angle measurement and contact angle interpretation. *Advanced Colloid Interfaces* **81**, 167 (1999)

102. Owens, D. K. & Wendt, R. C. Estimation of the surface free energy of the polymers. *Journal of Applied Polymer Science* **13**, 1741 (1969)

103. Wu, S. *Polymer interface and Adhesion*. Basel, New York, 1982

104. Miller, G.L. Use of dinitrosalicyclic acid reagent for determination of reducing sugar. *Analytical Chemistry* **31**, 426-428 (1959)

105. Inceoglu, F., Inan, C.M. & Menceloglu, Y.Z. Preparation and Properties of Biodegradable Starch-Clay Nanocomposite, *ACS Fall Meeting: Polymer Preprint*, San Diego, 2005

106. Inceoglu F. & Menceloglu, Y.Z. Biodegradable Thermoplastic Nanocomposite Polymers, *International Patent Application No. 06404001.7*, 2006

107. Inceoglu F., Inan, C.M. & Menceloglu, Y.Z. Transparent Biodegradable Low Density Polyethylene /Starch Nanocomposite Films, submitted to *Composite Science and Engineering*, 2007

108. Mani, R.& Bhattacharya, M. Properties of injection moulded blends of starch and modifed biodegradable polyesters. *European Polymer Journal* **37**, 515-526 (2001)

109. Matzinos, P., Bikiaris, D., Kokkou, S. & Panayiotou, C. Processing and characterization of ldpe/starch products. *Journal of Applied Polymer Science* **79**, 2548–2557 (2001)

110. Dean, K., Yu, L. & Wu, D.Y. Preparation and characterization of melt-extruded thermoplastic starch/clay nanocomposites. *Composite Science and Technology* doi:10.1016 (2006)

111. Fischer HR, Fischer S. Biodegradable thermoplastic material. US Patent 6,811,599 (2004)

112. Hatakeyama, T. & Liu, Z. Handbook of Thermal Analysis. Wiley, New York (1999)

113. Tadmor, Z. & Gogos, C. G. Principles of Polymer Processing. John Wiley & Sons, New York (1979)

114. http://www.treofan.com/productscout/pdfs/121.pdf

115. Haugaard, V.K., Udsen, A.M., Mortensen, G., Høegh, L., Petersen, K. & Monahan, F. Potential food applications of biobased materials. an eu-concerted action project. *Starch/Stärke* **53** 189–200 (2001)

116. Holton, E.E., Asp, E.H. & Zottola, E.A. Corn-starch-containing polyethylene film used as food packaging. *Cereal Foods World* **39**, 237–241 (1994)

117. Petersen, K., Nielsen, P.V., Bertelsen, G. , Lawther, M. , Olsen, M.B., Nilsson, N.H. & Mortensen, G. Potential of biobased materials for food packaging. *Trends in Food Science and Technoogy* **10**, 52–68 (1999)

118. Petersen, K., Nielsen, P.V. &. Olsen, M.B. Physical and mechanical properties of biobased materials – starch, polylactate and polyhydroxybutyrate. *Starch/Stärke* **53** 356–361 (2001)

119. Arvanitoyannis, I., Biliaderis, C.G., Ogawa, H.& Kawasaki, N. Biodegradable films made from low-density polyethylene (LDPE), rice starch and potato starch for food packaging applications: Part 1. *Carbohydrate Polymers* **36***,* 89–104 (1998)

120. Psomiadou, E., Arvanitoyannis, I., Biliaderis, C.G., Ogawa, H. & Kawasaki, N. Biodegradable films made from low density polyethylene (LDPE), wheat starch and soluble starch for food packaging applications. Part 2. *Carbohydrate Polymers* **33***,* 227– 242 (1997)

121. Carvalho, A.J.F., Curvelo, A.A.S. &. Gandini, A. Surface chemical modification of thermoplastic starch: reactions with isocyanates, epoxy functions and stearoyl chloride. *Industrial Crops and Products* **21**, 331–336 (2005)

122. Langmuir, I. Constitution and fundamental properties of solids and liquids. I. Solids. *Journal of American Chemical Society* **38**, 2221 (1916)

123. Wenzel, R.N. Resistance of solid surfaces to wetting by water. *Industrial & Engineering Chemistry* **28**, 988 (1936)

124. Park, H.M., Lee, S.R., Chowdhury, S.R., Kang,T.K., Kim,H.K., Park, S.H. & Ha, C.S. Tensile properties, morphology, and biodegradability of blends of starch with various thermoplastics. *Journal of Applied Polymer Science* **86**, 2907–2915 (2002)

125. Ray, S.S. & Bousmina, M. Biodegradable polymers and their layered silicate nanocomposites: In greening the 21st century materials world. *Progress in Materials Science* **50**, 962–1079 (2005)